Fall 2013

Characterization of CAXCK31, a Bacterial Calcium/Proton Antiporter

Marc Robert Ridilla
Purdue University

Graduate School ETD Form 9
(Revised 12/07)

PURDUE UNIVERSITY
GRADUATE SCHOOL
Thesis/Dissertation Acceptance

This is to certify that the thesis/dissertation prepared

By Marc Robert Ridilla

Entitled

Characterization of CAXCK31, a Bacterial Calcium/Proton Antiporter

For the degree of Doctor of Philosophy

Is approved by the final examining committee:

Jeffrey T. Bolin
Chair

Dinesh A. Yernool

Eric L. Barker

William A. Cramer

To the best of my knowledge and as understood by the student in the *Research Integrity and Copyright Disclaimer (Graduate School Form 20)*, this thesis/dissertation adheres to the provisions of Purdue University's "Policy on Integrity in Research" and the use of copyrighted material.

Approved by Major Professor(s): Jeffrey T. Bolin

Dinesh A. Yernool

Approved by: Christine A. Hrycyna 10/10/2013
Head of the Graduate Program Date

CHARACTERIZATION OF CAX^{CK31}, A BACTERIAL CALCIUM/PROTON ANTIPORTER

A Dissertation

Submitted to the Faculty

of

Purdue University

by

Marc Robert Ridilla

In Partial Fulfillment of the

Requirements for the Degree

of

Doctor of Philosophy

December 2013

Purdue University

West Lafayette, Indiana

TABLE OF CONTENTS

Page

LIST OF TABLES

LIST OF FIGURES

Figure Page

Figure Page

LIST OF ABBREVIATIONS

C12E8 - polyoxyethylene(8)dodecyl ether

CaCA - calcium/cation antiporter

DDM - n-dodecyl β-D-maltopyranoside

FC12 - Fos-Choline-12

FRET - Förster resonance energy transfer

HEPES - 2-[4-(2-hydroxyethyl)piperazin-1-yl]ethanesulfonic acid

FSEC - fluorescence size exclusion chromatography

IMV - inverted membrane vesicle

LysoFC12 - LysoFos Choline 12

MALS - multiangle laser light scattering

PC - phosphatidylcholine

PDB - Protein Data Bank

PDC - protein−detergent complex

POPC - 1-palmitoyl-2-oleoyl-*sn*-glycero-3-phosphocholine

POPE - 1-palmitoyl-2-oleoyl-*sn*-glycero-3-phosphoethanolamine

POPS - 1-palmitoyl-2-oleoyl-sn-glycero-3-phospho-L-serine

SM - sphingomyelin

S-200 - Superdex-200

TEV - Tobacco Etch Virus

TM - transmembrane helix.

ABSTRACT

Ridilla, Marc R. Ph.D., Purdue University, December 2013. Characterization of Bacterial Calcium/Proton Antiporter CAX^{CK31}. Major Professors: Dinesh Yernool and Jeffrey Bolin.

To better understand a class of transporters known as Calcium/Cation Antiporters (CaCAs), the bacterial calcium/proton antiporter CAX^{CK31} was purified and characterized. New methods were developed for its heterologous overexpression and purification. These methods help to define stress responses to toxic membrane overproduction in *E. coli* and may be broadly applicable to studies of membrane proteins. The results from a variety of biochemical and biophysical experiments demonstrated that CAX^{CK31} exists as a dimer in the membrane and can be purified in the dimeric state. The methods used include chemical cross-linking, FRET, and SEC-MALS. In addition, various transport properties of CAX^{CK31}, including substrate selectivity, pH dependence, and transport rates, have been characterized for the first time.

CHAPTER 1. INTRODUCTION

1.1 Physiological Roles of Calcium/Cation Antiporters

Maintenance of transmembrane chemical and electrical potentials is essential to all cells. In cells that require large, rapid changes in these potentials, such as neurons and myocytes (Figure 1-1), membrane proteins facilitate efficient movement of specific ions to create or dissipate concentration gradients. One such protein is the Sodium/Calcium (Na^+/Ca^{2+}) Exchanger (NCX). Human NCX is predominantly expressed in brain, heart, and kidney, tissues whose functions rely heavily on Ca^{2+} potentials. A maximum Ca^{2+} turnover of 5000 s^{-1} makes NCX the primary Ca^{2+} transporter in cardiac myocytes (Berridge, Bootman, and Roderick 2003), compared to 100 Ca^{2+} / s for the next-fastest Ca^{2+} transporter, the plasma membrane Ca^{2+} ATPase (PMCA) (Blaustein and Lederer 1999). Indeed cardiac-specific knockout mice develop cardiac hypertrophy and suffer heart failure (Henderson et al. 2004).

A recent review (Khananshvili 2013) lists NCX involvement in the following systemic functions: excitation-contraction coupling in cardiomyocytes, vasoconstriction of smooth muscle cells, insulin secretion in β-cells, synaptic

secretion of neurotransmitters, Ca^{2+} reabsorption in the kidney, as well as in immune response of dendritic and B-cells.

CAX family exchangers in plants and yeasts are essential for toxin removal and heavy metal tolerance (Kamiya and Maeshima 2004; Edmond et al. 2009).

1.2 The Calcium/Cation Antiporter Superfamily

Members of the Calcium/Cation Antiporter (CaCA) superfamily range in size from 302-1199 amino acid residues (461-1199 in the animal kingdom alone). Eukaryotic exchangers have hydrophilic domains of 200-550 residues that are not required for ion transport but have been shown in some cases to function in regulation. All characterized CaCAs function in Ca^{2+} extrusion, although Cd^{2+}, Mg^{2+}, and Mn^{2+} can be transported by certain plant exchangers. The counter-transported cations reflect the sequence divergence that defines five families within the CaCA superfamily: the NCX and NCKX families of animal Na^{+}/Ca^{2+} exchangers; the YRBG family of bacterial and archaeal exchangers, which takes its name from the *yrbG* gene in *E. coli*; the CAX family of cation/H^{+} exchangers found in yeasts, plants, archaea, and eubacteria; and the cation/Ca^{2+} exchangers, or CCX.

The CaCA superfamily exhibits such divergence that it is not possible to identify a signature sequence applicable to all CaCAs but not to other proteins. In fact,

no residue is fully conserved in the superfamily. Nevertheless, the characteristic of two sequences approximating the motif G(S/T)SxP(D/E) predicted near opposite sides of the membrane and separated by five transmembrane alpha-helices has identified proteins ubiquitously, in animals,
plants, yeast, archaea and bacteria. These sequences are called α-repeat elements, α-repeats, or α1 and α2 repeats.

1.3 Molecular Structure of Calcium/Cation Antiporters

The currently-accepted topological model for the CaCA superfamily is depicted in Figure 1-2C. All members of the CaCA superfamily possess two “clusters” of predicted transmembrane helices, each with a conserved and essential α-repeat region (Lytton 2007). Only eukaryotic NCX (e.g. NCX1) contains the pictured cytoplasmic regulatory domains. Structures of canine and murine NCX regulatory domains have been determined (Hilge, Aelen, and Vuister 2006; Nicoll et al. 2006).

The first (and only, at the time of writing) CaCA of known structure is the NCX of *Methanocaldococcus jannaschii*, NCX_Mj (PDB ID: 3V5U), which was determined by X-ray crystallography to a resolution of 1.90 Å (Liao et al. 2012). The protein exists as a monomer in the crystal. At 302 residues, NCX_Mj is the smallest member of the CaCA superfamily, and it also exhibits greater sequence similarity between its N-terminal and C-terminal halves than other CaCAs we examined (this is exemplified by superimposable structures of these halves).

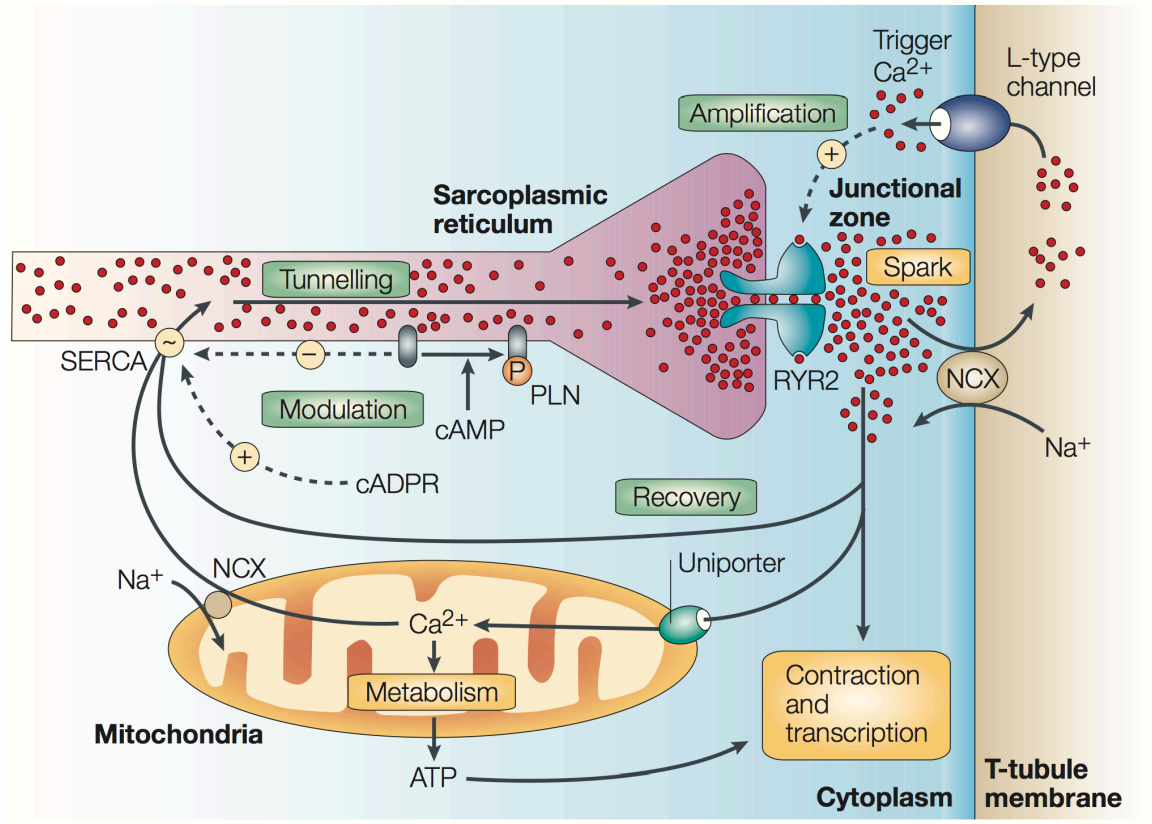

Figure 1-1. Cardiac calcium signaling.
From (Berridge, Bootman, and Roderick 2003). Signaling begins with an amplification step in the junctional zone, where the L-type channel on the T-tubule membrane responds to depolarization by introducing a small pulse of trigger Ca^{2+}, which then diffuses across the narrow gap of the junctional zone to activate ryanodine receptor 2 (RYR2) to generate a spark (Ca^{2+} is shown as red circles). Ca^{2+} from this spark diffuses out to activate contraction. Recovery occurs as Ca^{2+} is pumped out of the cell by the Na^{+}/Ca^{2+} exchanger (NCX) or is returned to the sarcoplasmic reticulum (SR) by sarco(endo)plasmic Ca^{2+}-ATPase (SERCA) pumps on the non-junctional region of the SR.

One calcium ion is observed in its translocation pathway. It is octahedrally coordinated by the side chains of glutamates E54 and E213 and backbone carbonyls of threonines T50 and T209; these pairs of residues align in the aforementioned comparison of NCX_Mj's N- and C-terminal sequences. Three sodium ion binding sites are also observed in the translocation pathway. However, despite agreement with the generally-accepted $3Na^{+}$:$1Ca^{2+}$ transport stoichiometry of cardiac NCX, no conclusions about stoichiometry should be made from the structure alone.

Remarkably, the model locates the Ca^{2+} binding site close to the protein-lipid acyl chain interface in contrast to the more centrally located, protein-enclosed ion binding sites of other secondary transporters. Furthermore, the path from the extracellular side to the Ca^{2+} binding site was proposed to be delimited by TM2C, TM6, TM7, and bulk lipids, which would expose the acyl chains to water and ions, an unfavorable condition (Figure 3-9). A dimeric assembly resolves these concerns as discussed in **Chapter 3**.

1.4 Transport Properties of Calcium/Cation Antiporters

There are several points of interest regarding transport properties of CaCAs: (1) selectivity, or which divalent cations can be transported instead of Ca^{2+}, (2) what is transported as the counterion; (2) electrogenicity and stoichiometry of transport of substrates; and (3) classical kinetic characterization to determine K_M and V_{max}.

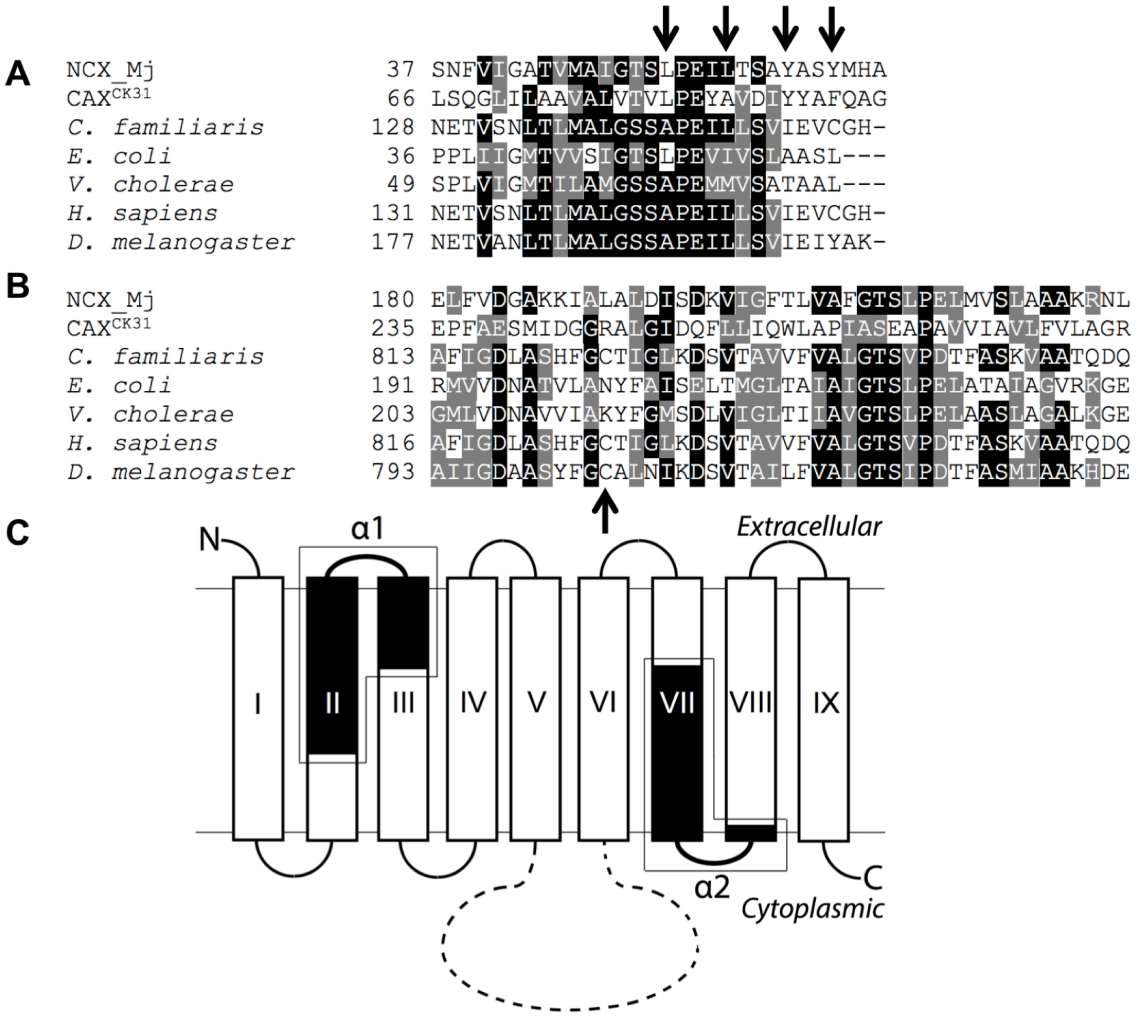

Figure 1-2. Prokaryotic CAX^{CK31} as a model for Eukaryotic NCX.
Multiple sequence alignments of the conserved α-1 (A) and α-2 (B) repeats of selected Ca^{2+}-cation exchangers. Residues conserved in 50 % of sequences are in black; similar residues are in gray. C, predicted topological model for Ca^{2+}-cation exchangers. Nine helices are labeled with roman numerals. Conserved α-1 and α-2 repeat sequences are shaded and boxed. The broken line indicates the cytoplasmic domain of eukaryotic exchangers involved in regulation, but not in transport *per se* (Hilgemann 1990; Matsuoka et al. 1995).

The most thoroughly characterized CaCA in terms of structural determinants of selectivity is the cation/H^+ exchanger from rice, OsCAX1a, in which nearly every residue of the α1 and α2 regions was mutated (Kamiya and Maeshima 2004).Yeast expressing these mutant OxCAX1a and lacking its own Ca^{2+}/H^+ exchanger and Ca^{2+}-ATPase was plated on Ca^{2+} or Mn^{2+} containing media to assay tolerance. Interestingly a T354A mutation increased tolerance to Mn^{2+}; this residue's role in transport is not clear from the NCX_Mj structure (I238). A similar scanning mutagenesis was performed for canine cardiac NCX1 expressed in Chinese hamster lung cells with functional assessment by uptake of radioactive Ca^{2+} or Co^{2+} (Shigekawa et al. 2002). Similar to the case of the rice exchanger, several residues were identified for which mutation increased Co^{2+} uptake rates (G123, H124, N125, T127) but which have no readily identified equivalents in the NCX_Mj structure (a gap is required at this position for sequence alignment).

Despite extensive investigation, the Na^+:Ca^{2+} stoichiometry in NCX transport has yet to be determined with certainty, even for the best characterized NCX1. The best model for NCX1 involves mutually-exclusive binding of one Ca^{2+} ion or three Na^+ ions, either one resulting in a change in conformation allowing release on the opposite side of the membrane (see Figure 1-3 and (Lytton 2007)). The exact exchange stoichiometry may be unique to each NCX, and it may vary depending on environment (i.e. Na^+ and/or Ca^{2+} potentials).

The kinetic parameters K_M and V_{max} have been determined for for a number of plant CAX family members. These values seem very dependent on experimental conditions (e.g. pH, presence of any membrane potential) but generally hover around a K_M of 43 μM Ca^{2+} and V_{max} of nmol Ca^{2+}/min/mg CAX (Edmond et al. 2009).

1.5 CAX^{CK31}

Caulobacter sp K31 CAX is 440 amino acid residues in length, none of which are cysteines, and is predicted to contain 11 helices, the first of which is 73.9 % likely to be a signal peptide cleaved at residue 28 (Petersen et al. 2011). Its calculated molecular weight is 46849.2 Da, its theoretical pI is 5.50, and it should have a -5 charge at physiological pH (Wilkins et al. 1999).

A construct truncated to residue 416 (22 residues beyond the final transmembrane helix), dubbed CAX^{CK31} is the subject of most of our work. It has a calculated molecular weight of 44200.3 Da, a theoretical pI of 5.55, and carries a -3 charge at physiological pH (Wilkins et al. 1999).

1.6 Specific Aims of This Research

The goals of this research were:

1. to understand and improve heterologous overexpression of toxic membrane proteins in *E. coli* by mitigation of cellular stress responses;

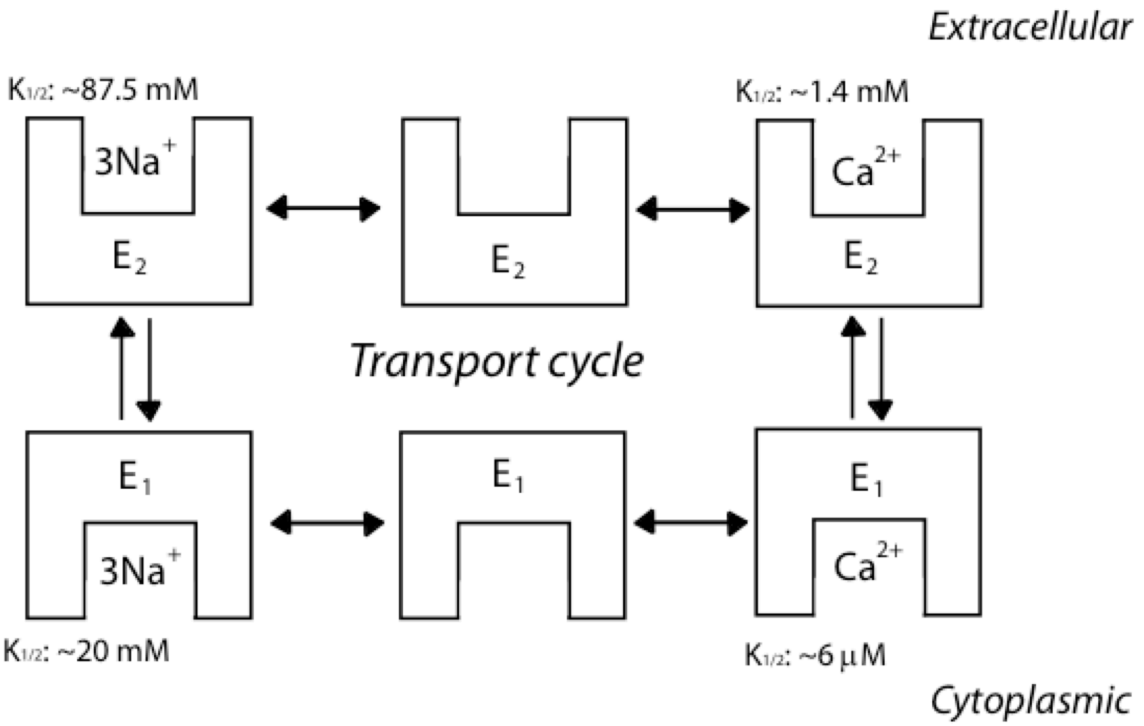

Figure 1-3. Alternating-access model proposed for transport cycle of NCX assuming $3Na^+/1Ca^{2+}$ stoichiometry.
E_1 and E_2 indicate inward-facing and outward-facing structural states of NCX; transitions between states are possible only with substrate bound. Directionality of transport is largely determined by differences in substrate affinities unique to each structural state (*i.e.* E_1 is more likely to bind Ca^{2+} than E_2). Indicted affinities reflect those determined for cardiac NCX1 (Shigekawa and Iwamoto 2001).

2. to purify and analyze structural properties of a bacterial calcium/proton antiporter;

3. to characterize the transport properties of a bacterial calcium/proton antiporter.

1.7 Organization of This Thesis

Chapter Two describes the selection, expression, and purification of CaCAs, including transcriptomic analysis of the response of *E. coli* to CAX^{CK31} overexpression.

Chapter Three establishes the existence of a dimeric oligomerization state of CAX^{CK31} and the conditions needed to purify dimeric CAX^{CK31} in detergent solution, and work identifying the dimer interface is described.

Chapter Four explains efforts to describe the transport properties of CAX^{CK31} using inverted membrane vesicles or proteoliposomes. Monovalent and divalent cations transported by CAX^{CK31} are identified, the pH sensitivity of transport activity is established, and K_M's for the transport of Ca^{2+} and Zn^{2+} are identified. Furthermore a generalized method is presented for quantification of very small amounts of protein applicable to measurement of reconstitution efficiency of proteoliposome preparations.

Chapter Five discusses ongoing work and future directions for the project, such as efforts to crystallize CAX^{CK31} monomers and dimers, including the application of surface entropy reduction, antibody fragments, and lipidic cubic phase to promote crystallogenesis. The feasibility of coupling FRET measurement with SEC (SEC-FRET) for simultaneous analysis of protein-protein interactions and

complex hydrodynamics is discussed. Lastly, the effects of lipids on the stability of CaCAs and potential strategies for their elucidation are addressed.

CHAPTER 2. EXPRESSION OF PROKARYOTIC CALCIUM/CATION ANTIPORTERS IN *E. COLI*

2.1 Introduction

This Chapter describes the selection, expression, and purification of CaCAs studied, including transcriptomic analysis of the response of *E. coli* to CAX^{CK31} overexpression.

2.2 Selection of Prokaryotic Calcium/Cation Antiporters

Heterologous expression is subject to organism-specific efficiencies in transcription and translation of different sequences, therefore it is wise to test a variety of homologous proteins from different organisms. Our screening ultimately identified three out of thirty homologs, internally designated N2, N21, and CAX^{CK31}, capable of expression and purification at levels suitable for biochemical experiments. All experiments described herein have been completed with CAX^{CK31} except where noted.

Thirty-six prokaryotic homologs of cardiac Na^+/Ca^{2+} exchanger were identified based on the following criteria: (i) ≥25% sequence identity with cardiac Na^+/Ca^{2+} exchanger, (ii) the presence of residues conserved in the family of cation/Ca^{2+} exchangers (Cai and Lytton 2004), (iii) <60% identity with any other selection (to

effectively cover sequence space), and (iv) the presence of the characteristic α-repeat sequences (Schwarz and Benzer 1997; Philipson and Nicoll 2000). Thirty of these genes were commercially-available. They were cloned into the pETCTGFPHis11 vector for expression as NCX-GFP-$(His)_{11}$ green fluorescent protein (GFP) fusion proteins. Four had detectable expression in *E. coli*.

2.3 Cloning and Expression of Prokaryotic CaCAs

Prokaryotic CaCAs N2, N21, CAX^{CK31}, and N24 differ in overall length and are predicted to differ in number of transmembrane segments, position of the C-terminus, and presence of a membrane-targeting signal peptide sequence.

The genes encoding these proteins have been cloned for expression as fusion proteins linked at the C-terminus via a Tobacco Etch Virus (TEV) Protease cleavage site to GFP and with a C-terminal His-tag. Additionally, N- and C-terminally truncated constructs of N21 and CAX^{CK31} have been prepared: Limited trypsin proteolysis experiments coupled with secondary structure prediction software led us to believe that an extended C-terminal region does not contribute to the core structure of CaCAs. N21-398, consisting of residues 31-428, N21-404, consisting of residues 1-404, N21-406, consisting of residues 1-406, and CAX^{CK31}-416, consisting of residues 1-416 and henceforth referred to simply as CAX^{CK31} (full-length CAX^{CK31} will henceforth be referred to as CAX^{CK31}-440) were generated to eliminate this unstructured C-terminal region. Truncation constructs N21-406 and CAX^{CK31} express at higher levels and are more stable

than any full-length construct. N21-406 is truncated by 22 amino acids at the C-terminus to a position 19 amino acids beyond the end of the eleventh predicted

transmembrane helix. CAX^{CK31} is truncated by 24 amino acids to a position 20 amino acids beyond the end of the eleventh predicted transmembrane helix.

To identify the best conditions for the expression of each construct, small-scale (50-mL) cultures were grown, varying *E. coli* strain, media type, inducer and inducer concentration, and temperature and duration of incubation after induction:

Expression strains: BL21-AI, BL21-C41, BL21-C43

Media: 2xYT, LB, SOB, TB

Inducer (concentration): Arabinose (0.01875 %, 0.025 %, 0.03125 %, for AI cells), IPTG (200 µM, for C41 and C43 cells))

Temperature after induction: 18 °C, 25 °C, 32 °C, 37 °C

Time after induction: 5 hours, 8 hours, 20 hours

Cultures were inoculated by dilution of overnight starter cultures to a starting OD600 of 0.05. Cultures were incubated at 37 °C until OD600 neared 0.6, (chilled, if necessary, to the desired expression temperature), induced, and then incubated at the desired expression temperature for the desired duration. Cells were harvested by centrifugation.

Expression was initially assessed by whole-cell fluorescence measurement. Nominal fluorescence intensities were used to compare relative expression of the GFP component of our fusion constructs.

Cells harvested from 1 mL liquid culture were resuspended in 200 µL of a buffer (usually 20 mM Tris pH 8.0, 300 mM NaCl) and transferred into a 96-well opaque microplate. GFP fluorescence (ex395/em507) intensities were measured and compared to evaluate relative expression levels. Fluorescence-based expression levels for selected full-length constructs and expression conditions are summarized in Table 2-1. These data indicated that N21 was the best-expressing full-length construct in AI cells, and the best condition for expression was a 25 °C incubation for 20 hours in 2xYT media after induction with 0.025 % Arabinose. After truncation to residue 416, expression of CAX^{CK31} under these conditions was much greater than for any other construct under any conditions. Expression in other *E. coli* strains was less than the AI strain under all conditions.

Expression level alone was not an exclusive criterion to choose a particular clone for further study. The stability of the protein must be evaluated. The FSEC method developed by the Gouaux lab (Kawate and Gouaux 2006) was employed for this type of analysis. By observing the SEC behavior of only the fluorescent fusion protein, its stability/monodispersity could be assessed even in an unpurified state (*i.e.* directly from cell lysate).

Cells from 1 mL liquid culture were lysed by sonication and mixed in buffer containing 20 mM DDM for two hours to extract integral membrane proteins into detergent micelles. This detergent extract was loaded directly onto a S200 SEC column for FSEC analysis.

Fluorescence chromatogram peak areas recapitulated whole-cell fluorescence measurements, and peak position, breadth, and overall shape gave information about relative size and stability of the protein observed. Figure 2-1 shows a typical set of experiments comparing N21 expressed in AI, C41, and C43 cells and CAX^{CK31}-440 expressed in AI cells. Two significant fluorescence peaks were always observed, indicating that some proteolysis had released GFP from the fusion protein. Because the C-terminal His-tag was required for purification, it was essential to choose expression conditions that minimized this proteolysis. From Figure 2-1, it is clear that N21 in AI cells had the greatest expression level of full-length constructs, the sharpest, most symmetric peak, and minimal proteolysis. After the truncations described above, N21-406 and CAX^{CK31} equally outperformed all full-length constructs. N21 and CAX^{CK31} are 62 % identical and 77 % similar, and their behavior in all experiments to be discussed was indistinguishable.

Table 2-1. Expression assessment by whole-cell GFP fluorescence. Relative fluorescence was expressed as a percentage of the best expression Nominal Fluorescence.

NCX	Strain	Media	Temperature after induction	[Arabinose] (%)	Time after induction	Nominal Fluorescence	Relative Fluorescence (%)
N21	AI	2xYT	25	0.02500	20 h	19848	100
N21	AI	SOB	25	0.02500	20 h	17442	88
N21	AI	LB	25	0.02500	20 h	13522	68
N21	AI	LB	25	0.03125	20 h	13374	67
N21	AI	LB	25	0.01875	20 h	13299	67
N21	AI	TB	25	0.02500	20 h	10552	53
N21	AI	LB	18	0.02500	20 h	9136	46
N21	AI	LB	32	0.02500	20 h	6921	35
N21	AI	LB	32	0.02500	4.5 h	5414	27
N21	AI	LB	25	0.03125	5.5 h	4668	24
N21	AI	LB	25	0.01875	5.5 h	4150	21
N21	AI	TB	25	0.02500	5.5 h	4127	21
N21	AI	LB	25	0.02500	5.5 h	3757	19
N21	AI	SOB	25	0.02500	5.5 h	2543	13
N21	AI	2xYT	25	0.02500	5.5 h	1681	8
N21	AI	LB	18	0.02500	4.5 h	277	1
N2	AI	TB	25	0.02500	20 h	1251	6
N2	AI	2xYT	25	0.02500	20 h	566	3
N2	AI	TB	25	0.02500	5.5 h	548	3
N2	AI	SOB	25	0.02500	20 h	529	3
N2	AI	SOB	25	0.02500	5.5 h	460	2
N2	AI	2xYT	25	0.02500	5.5 h	431	2
N2	AI	LB	32	0.02500	20 h	333	2
N2	AI	LB	18	0.02500	20 h	267	1
N2	AI	LB	32	0.02500	4.5 h	235	1
N2	AI	LB	25	0.02500	20 h	233	1
N2	AI	LB	25	0.02500	5.5 h	181	1
N2	AI	LB	18	0.02500	4.5 h	170	1
N22	AI	2xYT	25	0.02500	20 h	9519	48
N22	AI	SOB	25	0.02500	20 h	8861	45
N22	AI	TB	25	0.02500	20 h	8038	40
N22	AI	LB	25	0.03125	20 h	4346	22
N22	AI	2xYT	25	0.02500	5.5 h	4095	21
N22	AI	LB	25	0.01875	20 h	4032	20
N22	AI	LB	25	0.02500	20 h	3657	18
N22	AI	LB	32	0.02500	20 h	3354	17
N22	AI	LB	18	0.02500	20 h	3238	16
N22	AI	LB	25	0.03125	5.5 h	2118	11
N22	AI	LB	32	0.02500	4.5 h	2065	10
N22	AI	TB	25	0.02500	5.5 h	1950	10
N22	AI	SOB	25	0.02500	5.5 h	1895	10
N22	AI	LB	25	0.01875	5.5 h	1824	9
N22	AI	LB	25	0.02500	5.5 h	1740	9
N22	AI	LB	18	0.02500	4.5 h	174	1
N24	AI	2xYT	25	0.02500	20 h	13374	67
N24	AI	TB	25	0.02500	20 h	12075	61
N24	AI	LB	25	0.01875	20 h	5291	27
N24	AI	LB	25	0.02500	20 h	3493	18
N24	AI	LB	32	0.02500	20 h	3376	17
N24	AI	LB	18	0.02500	20 h	3200	16
N24	AI	LB	25	0.03125	20 h	2762	14
N24	AI	TB	25	0.02500	5.5 h	2709	14
N24	AI	LB	25	0.01875	5.5 h	2481	13
N24	AI	LB	25	0.02500	5.5 h	2448	12
N24	AI	LB	32	0.02500	4.5 h	2178	11
N24	AI	LB	25	0.03125	5.5 h	2059	10
N24	AI	SOB	25	0.02500	20 h	1599	8
N24	AI	2xYT	25	0.02500	5.5 h	1151	6
N24	AI	SOB	25	0.02500	5.5 h	858	4
N24	AI	LB	18	0.02500	4.5 h	298	2

2.4 The Restrained Expression Method

Note: complete details of this section have been published by *Protein Science* (Narayanan, Ridilla, and Yernool 2011). The publication's abstract and a brief summary are provided here.

"A major rate-limiting step in determining structures of membrane proteins is heterologous protein production. Toxicity often associated with rapid overexpression results in reduced biomass along with low yields of target protein. Mitigation of toxic effects was achieved using ''restrained expression,'' a controlled reduction in the frequency of transcription initiation by exploiting the infrequent transitions of Lac repressor to a free state from its complex with the lac-operator site within a T7lac promoter that occur in the absence of the inducer isopropyl β-D-1-thiogalactopyranoside (Beckwith 1967). In addition, production of the T7 RNA polymerase that drives transcription of the target is limited using the tightly regulated arabinose promoter in *Escherichia coli* strain BL21-AI (Figure 2-2). A 200-fold range of green fluorescent protein expression levels can be achieved using this approach. Application to members of a family of ion pumps results in 5- to 25-fold increases in expression over the benchmark BL21(DE3) host strain. A viral ion channel highly toxic to *E. coli* can also be overexpressed. In comparative analyses, restrained expression outperforms commonly used *E. coli* expression strategies. The mechanism underlying improved target protein yield arises from minimization of protein aggregation and

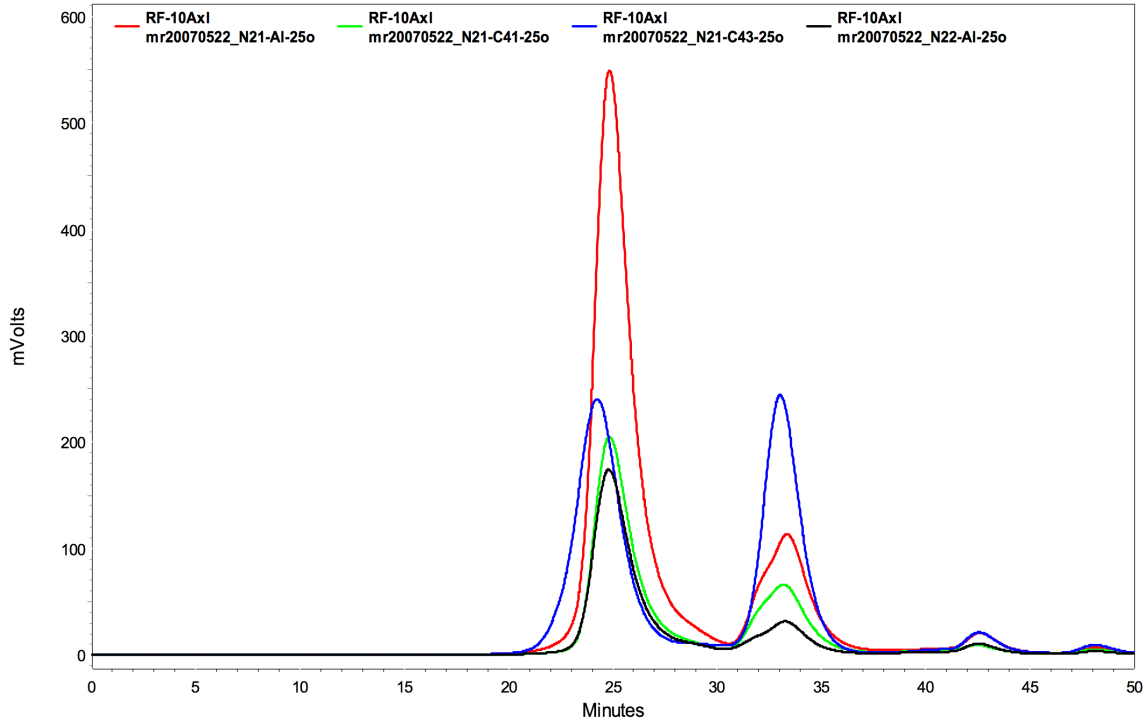

Figure 2-1. Whole-lysate detergent extract FSEC analysis of expression experiments.
Red, N21/AI cells. Green, N21/C41 cells. Blue, N21/C43 cells. Black, CAX^{CK31}/AI cells.

proteolysis that reduce membrane integrity and cell viability. This study establishes a method to overexpress toxic proteins."

Membrane protein expression yields are typically lower than those of soluble proteins, and NCX expression is toxic to *E. coli* (Narayanan, Ridilla, and Yernool 2011). Thus optimization of expression conditions was essential. Variables tested included expression vector (*i.e.* promoter), *E. coli* strain, media type (including manufacturer), flask size, culture temperature (before and after induction), inducer concentration, induction point, expression duration, and shaking intensity. The results of these studies identified key mechanisms by which expression levels were improved by 5- to 25-fold over original benchmarks.

Methodology (brief; for full details see (Narayanan, Ridilla, and Yernool 2011)): Cells were grown in 50 mL 2xYT medium [1.0% (w/v) yeast extract; 1.6% (w/v) tryptone; 0.5% (w/v) NaCl] in 250-mL baffled flasks with shaking at 37 ºC to an OD600 equal to 0.6 (measured in a BioSpec-mini spectrophotometer (Shimadzu, Kyoto, Japan)), the induction point empirically determined to produce optimal expression. After cooling cultures to 25 ºC, target gene expression was initiated by addition of inducers. Cells were collected by centrifugation (5000 × g for 15 min) and washed with 20 mM Tris, pH 8.0; 300 mM NaCl to clear media components before analysis.

Fluorescence derived from expression of GFP fusion proteins from cells representing 1 mL culture was measured with excitation and emission wavelengths of 395 nm and 509 nm, respectively.To analyze the membrane-integrated fraction of GFP-fusion proteins, prepared cell membranes (Kawate and Gouaux 2006) were solubilized using 20 mM DDM in 20 mM Tris, pH 8.0, 300 mM NaCl supplemented with protease inhibitors. Detergent extracts of membranes were analyzed by fluorescence-detection size-exclusion chromatography (FSEC) (Kawate and Gouaux 2006) in 20 mM Tris, pH 8.0, 300 mM NaCl containing 0.2 mM DDM. The elution positions of fusion proteins were identified by continuously monitoring fluorescence (excitation 395 nm, emission 510 nm) using an in-line detector.

2.5 Transcriptomic Analysis of the Restrained Expression Method

Response of *E. coli* to Overexpression of CAX^{CK31}. The mechanism of toxicity associated with overproduction of membrane proteins was investigated by comparing the effects of rapid *versus* restrained modes of expression of CAX^{CK31}. When the Restrained Expression method for the production of toxic membrane proteins in *E. coli* was introduced (Narayanan, Ridilla, and Yernool 2011), enhanced proteolytic activity was reported in cells overexpressing membrane proteins by unrestrained methods, and it was hypothesized that mitigation of this and other stress responses underlie the effectiveness of Restrained Expression. Analysis showed that during rapid expression an accumulation of aggregated protein in the cytosol elicited a stress response that included enhanced

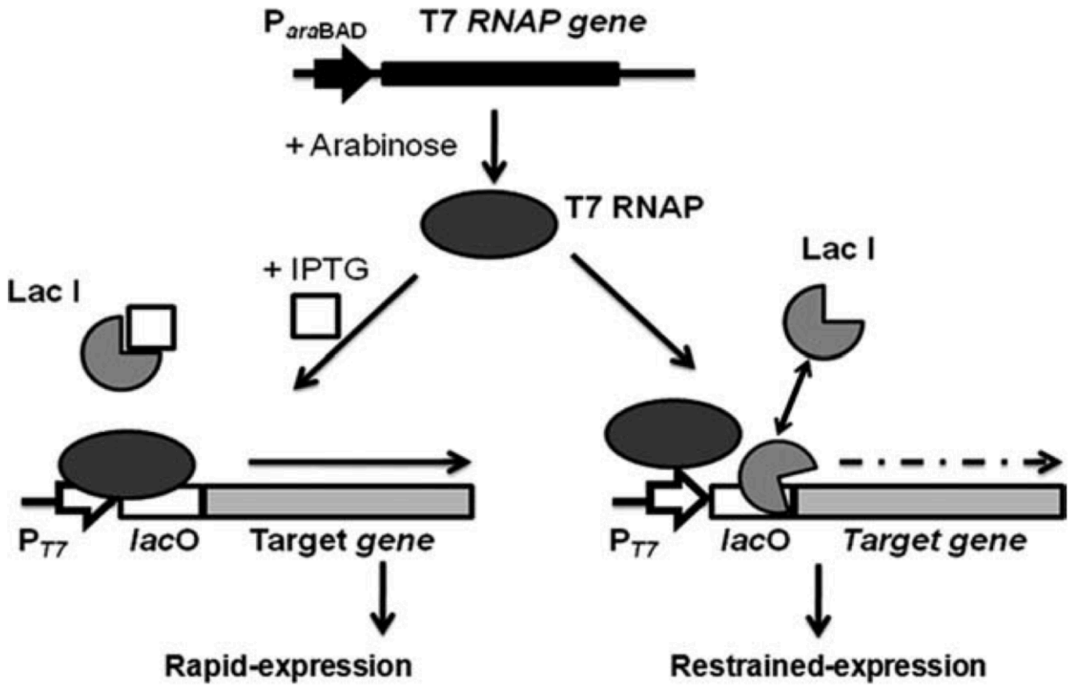

Figure 2-2. A model to achieve stringent control over expression.
IPTG and arabinose induce expression of target and T7 RNA polymerase (T7 RNAP) genes under control of hybrid P_{T7lac} and arabinose-inducible P_{araBAD} promoters, respectively. Two potential modes of induction, restrained, and rapid expression, involve addition of arabinose and arabinose plus IPTG, respectively. In restrained expression, sporadic transcription of the target gene (dashed line) occurs because of the equilibrium between free and lacO-bound states of lac repressor (LacI) in the absence of IPTG. Reproduced with permission from (Narayanan, Ridilla, and Yernool 2011).

proteolysis, decreased membrane integrity, and loss of ability to generate and sustain electrochemical potential necessary for energy generation leadingultimately to cell death.

Application of the restrained mode of expression to the same target protein significantly reduced the various stress responses, resulting in increased viability of host cells and accumulation of the target protein. The dissimilar cellular responses to production of the same target protein by rapid *vs.* restrained modes opened up a new avenue of investigation: detailed observation of the cellular responses at the transcriptomic/regulatory level *via* whole-transcriptome profiling by RNA-seq (Wang, Gerstein, and Snyder 2009). Sequencing has been completed for mRNA isolated from *E. coli* overexpressing toxic and non-toxic proteins by both rapid and restrained modes. The data consisted of roughly 37 million sequence reads *per* sample representing nearly 4,000 genes or 93 % of the *E. coli* genome. The data identified 22 *E. coli* genes with greater than 20-fold increases in transcription resulting from rapid overexpression of CAX^{CK31} as compared to overexpression of the soluble, non-toxic protein GFP (and 81 genes with greater than 10-fold increases in transcription), all of whose transcription levels differ less between CAX^{CK31} and GFP when the Restrained Expression methodology is utilized (Table 2-1). This clearly demonstrated the stress mitigation of the Restrained Expression method, resulting in *E. coli* able to express toxic proteins at levels closer to those of non-toxic proteins. Key molecular components of stress response contributing to the global physiological

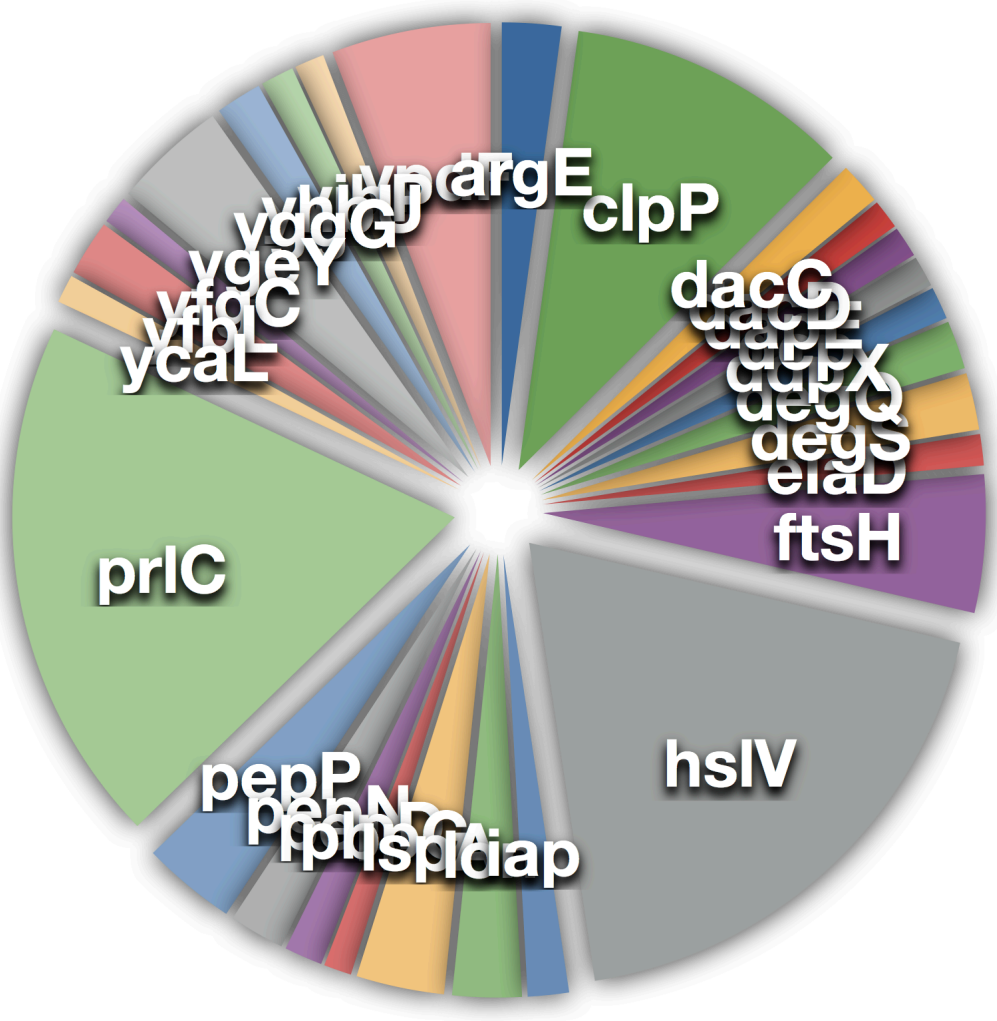

Figure 2-3. Relative changes in abundance of the 28 detected transcripts associated with the Gene Ontology Biological Process "Proteolysis" (GO:0006508) when comparing overexpression of CAX^{CK31} and GFP.
Only clpP, hslV, and prlC transcripts were stimulated by more than 10-fold suggesting that these were the major molecular components contributing to the difference in proteolytic activity observed to result from overexpression of toxic membrane proteins as opposed to non-toxic soluble proteins. Genes whose transctiption changed less than 10-fold were lon, ftsH, argE, dacC, ddpX, dapE, pepD, ygeY, pepP, ypdF, elaD, pepN, dacD, dcp, degQ, degS, iap, lspA, pbpG, ycaL, yfbL, yfgC, yggG, yhbU, and yibP.

effects observed could then be identified, *e.g.* enhanced proteolytic activity arose primarily from increased expression of three proteases, PrlC, HslV, and ClpP (Figure 2-3).

RNA-seq was performed to evaluate transcriptional responses to expression of a toxic membrane protein. Responses to rapid expression and restrained expression were compared; GFP expression under identical conditions was compared as a (non-toxic, soluble protein) control.

Introduction:

Protein expression begins with gene transcription and proceeds through translation and folding steps; this is sufficient for cytoplasmic proteins, however membrane proteins require trafficking to membrane and insertion. The protein biogenesis pathway can be challenged at any step.

Heterologous overexpression of proteins in *E. coli* has been shown to influence key pathways (Hoffmann and Rinas 2004; Gill, Valdes, and Bentley 2000; Wagner et al. 2007). Responses to CAX^{CK31} expression included cytoplasmic protein aggregation, increased proteolysis, loss of membrane integrity, and growth arrest. Restrained expression mitigated these effects and enhanced expressability (Narayanan, Ridilla, and Yernool 2011).

Table 2-2. Differential gene transcription in *E. coli* responding to overexpression of CAX^{CK31} vs. GFP.

	Fold Increase in Transcription (CAXCK31/GFP)	
Gene	Rapid Expression	Restrained Expression
small heat shock protein ibpB	177.68	66.71
DNA-binding transcriptional dual regulator soxS	116.01	52.10
small heat shock protein ibpA	92.15	35.99
superoxide dismutase sodA	91.12	-1.41
stress-induced protein yhcN	67.32	7.55
glycerol-3-phosphate dehydrogenase glpD	59.14	17.10
pyruvate-flavodoxin oxidoreductase ydbK	39.75	6.91
protein disaggregation chaperone clpB	38.89	22.80
conserved protein ybeD	32.12	6.18
molecular chaperone htpG	31.12	9.67
Hsp33-like chaperonin hslO	30.48	3.47
magnesium-transporting ATPase mgtA	29.51	1.75
DNA-binding transcriptional repressor lldR	28.28	5.15
phosphopentomutase deoB	28.27	13.08
phage shock protein G (pspG)	27.88	3.56
L-lactate dehydrogenase lldD	25.58	8.57
ribonucleotide reductase stimulatory protein nrdI	24.51	2.49
regulatory protein for the phage shock protein operon pspA	24.42	5.19
molecular chaperone dnaK	24.01	8.57
heat shock protein Hsp15 involved in ribosome recycling (hslR)	23.83	3.33
heat shock protein hspQ	20.62	8.68
periplasmic repressor cpxP	20.31	5.61

E. coli cultures expressing CAX^{CK31}-GFP (samples designated witn a “N”) or GFP (samples designated with a “G”) were grown at 37 °C to OD600=0.6, chilled to 25 °C, induced for either restrained (0.1 % arabinose; samples designated with “RE”) or rapid (0.01 % arabinose and 0.5 mM IPTG; samples designated with “RA”) expression, and incubated for an additional 3 hours before harvesting. Total RNA was isolated using the RNeasy Protect Bacteria Kit (QIAGEN), and mRNA was subsequently enriched using the MICROBExpress Kit (Ambion). RNA-seq data was collected at the Purdue Genomics Core. Data analysis proceeded as follows: transcript counts (FPKM) for each gene of each biological sample were compared with those of the appropriate other biological sample by division to give fold-change in regulation (inverse-reciprocals were taken for quotients less than 1 so that they appeared as negative fold-change).

Four pairwise comparisons were made among four biological variations: CAX^{CK31} Rapid (NRA) / GFP Rapid (GRA), CAX^{CK31} Restrained (NRE) / NRA, GFP Restrained (GRE) / GRA, and NRE / GRE. Primary focus was given to the 25 most upregulated and 25 most downregulated genes in each comparison.

CAX^{CK31} Rapid (NRA) / GFP Rapid (GRA).

First it was useful to examine the differences between overexpression of a toxic membrane protein and a nontoxic soluble protein using standard, rapid expression methods. This identifed the regulatory responses directly resulting from CAX^{CK31}’s toxicity rather than heterologous overexpression alone. Of the

top 25 upregulated genes (Table 2-2), 13 were members of the σ70 “housekeeping” regulon, 11 were members of the σ32 “heat shock” regulon, 5 were members of the σ54 “nitrogen-limitation” regulon, 1 was a member of the σ28 “flagellar” regulon, and 1 was a member of the σ38 “starvation/stationary phase” regulon.

The most upregulated gene was inclusion body associated protein ibpB (+177.68; numbers in parentheses indicate fold change in expression), which, when accompanied by ibpA (+92.15) binds to aggregated proteins (Laskowska, Wawrzynów, and Taylor 1996) and forms a functional triad of heat-shock-induced chaperones with clpB (+38.89) and dnaK (+24.01) (Mogk et al. 2003). HSP90 family molecular chaperone htpG (+31.12), molecular chaperone Hsp33 (hslO, +30.48), and extracytoplasmic stress resistance chaperone cpxP (+20.31) were also upregulated (cpxP is also induced by high pH (Danese and Silhavy 1998) and/or biofilm formation (Beloin et al. 2004)). Chaperone upregulation was a consequence of the increased protein aggregation demonstrated with rapid CAX^{CK31}, as was the upregulation of ribosome recycling heat shock protein Hsp15 (hslR, +23.83), hemimethylated DNA-binding heat shock protein hspQ (+20.62), protease/chaperone hslU (+19.66), and the broad specificity cytoplasmic protease oligopeptidase A (prlC, +19.75). The second most upregulated gene was transcriptional activator soxS (+116.01), which participates in the removal of superoxide and nitric oxide by upregulating superoxide dismutase sodA (+91.12), which dismutes superoxide into oxygen and hydrogen

Table 2-3. Top 25 genes upregulated in NRA *vs.* GRA.

Gene	NRA/GRA	Sigma Regulon	Regulon Condition
clpB	38.89	70, 32	housekeeping, heat shock
cpxP	20.31	70	housekeeping
deoB	28.27	70	housekeeping
dnaK	24.01	32	heat shock
glpD	59.14	70	housekeeping
hslO	30.48	54, 32, 28	nitrogen-limitation, heat shock, flagellar
hslR	23.83	32	heat shock
hslU	19.66	32	heat shock
hspQ	20.62	32	heat shock
htpG	31.12	54, 32	nitrogen-limitation, heat shock
ibpA	92.15	32	heat shock
ibpB	177.68	54, 32	nitrogen-limitation, heat shock
lldD	25.58	70	housekeeping
lldR	28.28	70	housekeeping
mgtA	29.51	70	housekeeping
nrdI	24.51	70	housekeeping
prlC	19.75	32	heat shock
pspA	24.42	54	nitrogen-limitation
pspG	27.88	54	nitrogen-limitation
sodA	91.12	70	housekeeping
soxS	116.01	70	housekeeping
ybeD	32.12	70, 32	housekeeping, heat shock
ydbK	39.75	70	housekeeping
yhcN	67.32	70	housekeeping
ymgA	19.73	38	starvation/stationary phase

peroxide; hydrogen peroxide (J. Lee et al. 2010) and cytoplasmic pH (Kannan et al. 2008) stress upregulate yhcN (+67.32). Oxidative stress was also likely to cause the upregulation of pyruvate:flavodoxin oxidoreductase ydbK (+39.75) and flavodoxin nrdI (+24.51), which stimulates ribonucleotide reductase. Upregulation of glycerol-3-phosphate dehydrogenase gene glpD (+59.14) enhances utilization of glycerol-3-phosphate or its precursors, glycerol and glycerophosphodiesters, for biosynthesis of phospholipids. Predicted regulator of amino acid or nucleoside metabolism ybeD (+32.12) was upregulated. Magnesium transporter mgtA (+29.51) may have been upregulated to compensate for compromised divalent cation homeostasis resulting from CAX^{CK31} overexpression, as the switch to the restrained expression method resulted in its significant downregulation (-12.55 in NRE/NRA). Lactate regulator transcription factor lldR (+28.28) is induced upon biofilm formation (Beloin et al. 2004) as well as controlling expression of genes involved in transport and catabolism of L-lactate, such as lactate dehydrogenase lldD (+25.58). Upregulation of ymgA (+19.73) should decrease biofilm formation. Phosphopentomutase deoB (+28.17) involved in purine metabolism was upregulated. Phage shock protein operon regulatory protein pspA (+24.42) is induced by energy depletion-related stress and induces phage shock protein G (pspG, +27.88), which appears to affect motility.

Of the top 25 downregulated genes (Table 2-3), 12 were members of the σ70 “housekeeping” regulon, 3 were members of the σ32 “heat shock” regulon, 2

were members of the σ28 “flagellar” regulon, 2 were members of the σ38 “starvation/stationary phase” regulon, 1 was a member of the σ24 “extracytoplasmic/extreme heat stress” regulon, and 1 was a member of the σ54 “nitrogen-limitation” regulon (8 have not had their regulons identified).

The most downregulated gene was the maltose/maltodextrin ABC transporter ATP binding subunit malK (-14.56). The next most downregulated gene was biofilm stress and motility protein bsmA (-13.13), which likely resulted in compromised acid and peroxide stress resistance (M. M. Weber et al. 2010). Reduction in transcriptional regulator dicC (-10.28) should have resulted in cell division inhibition *via* increased dicB expression (no data). yphF (-10.16) is a periplasmic binding component of a predicted ATP-dependent sugar transporter; araF (-10.09) is the periplasmic binding component of the arabinose ABC transporter (arabinose was still present in both NRA and GRA). Downregulation of fucose isomerase fucI (-8.93) results in decreased degradation of both L-fucose and D-arabinose. Prepilin peptidase dependent genes ppdA (-9.86) and ppdB (-7.24) were downregulated, however previous studies suggested that their over- or under-expression does not affect chemotaxis or flagellar motility (Park et al. 2001). Downregulation of transcriptional activator tdcA (-9.57) results in downregulation of the complete tdc operon involved in transport and metabolism of threonine and serine. Another downregulated regulator was sgrT (-9.16), which regulates the activity of PtsG involved in the glucose-phosphate stress

Table 2-4. Top 25 genes downregulated in NRA *vs.* GRA.

Gene	NRA/GRA	Sigma Regulon	Regulon Condition
araF	-10.09	38, 70	starvation/stationary phase, housekeeping
bsmA	-13.13	?	?
dicC	-10.28	?	?
fryB	-10.38	?	?
ftnA	-8.73	70	housekeeping
fucI	-8.93	70	housekeeping
malK	-14.56	70	housekeeping
melA	-8.93	70	housekeeping
melB	-8.29	70	housekeeping
ppdA	-9.86	28	flagellar
ppdB	-7.24	28	flagellar
sgrT	-9.16	38, 70	starvation/stationary phase, housekeeping
ssnA	-7.31	54	nitrogen-limitation
tdcA	-9.57	?	?
ybaV	-9.91	70	housekeeping
ybiA	-8.33	32	heat shock
yehK	-7.70	70	housekeeping
yeiA	-8.67	70	housekeeping
yeiT	-7.57	70	housekeeping
yfbM	-12.28	?	?
ygeW	-7.54	32, 24	heat shock, extracytoplasmic/extreme heat stress
ygfM	-7.88	?	?
ykgE	-10.34	32, 70	heat shock, housekeeping
yncI	-9.96	?	?
yphF	-10.16	?	?

response. Downregulation of melibiose transporter melB (-8.29) and [alpha]-galactosidase melA (-8.93), both members of the melibiose metabolic pathway, suggested a decreased need for the utilization of [alpha]-galactosides as nutrients. Downregulation of ferritin ftnA (-8.73) indicated a decreased need for iron storage. Downregulation of yeiA (-8.67) and yeiT (-7.57) is associated with growth in liquid culture rather than biofilm formation as they are required for swarming motility; their sequences suggested they are dihydropyrimidine dehydrogenases or glutamate synthases. Downregulation of ybiA (-8.33) is also expected to impair swarming motility. The structure of ygeW (-7.54) resembled that of a transcarbamoylase, suggesting a role in *de novo* pyrimidine synthesis. Downregulation of predicted hydrolase ssnA (-7.31) is associated with increased viability at the beginning of stationary phase (Yamada, Talukder, and Nitta 1999). Many downregulated genes were poorly characterized. The third most downregulated gene, yfbM (-12.28) has not been characterized, nor has any protein of similar sequence or structure (PDB:1RYL). The situation is similar for fryB (-10.38), although its sequence suggested a role in phosphotransfer, yncI (-9.96), whose sequence suggested it is a transposase, ybaV (-9.91), whose sequence suggested it is a competence protein, or yehK (-7.70). Downregulated ykgE (-10.34) is a predicted oxidoreductase, but it is not associated with a particular pathway; ygfM (-7.88) is a predicted selenate oxidoreductase involved in purine salvage.

CAX^{CK31} Restrained (NRE) / CAX^{CK31} Rapid (NRA).

Next cells expressing CAX^{CK31} under the restrained expression regimen were compared to cells expressing CAX^{CK31} under the rapid expression regimen. Prior studies demonstrated that enhanced expression of CAX^{CK31} was accompanied by decreased accumulation of cytoplasmic aggregates, decreased general proteome activity, increased membrane integrity, etc. (Narayanan, Ridilla, and Yernool 2011). What regulatory pathways are affected by the treatment to support these findings? The answer may suggest ways to further improve upon expression methodologies. Of the top 25 upregulated genes (Table 2-4), 18 were members of the σ70 “housekeeping” regulon, 3 were members of the σ38 “starvation/stationary phase” regulon, 2 were members of the σ24 “extracytoplasmic/extreme heat stress” regulon, 2 were members of the σ32 “heat shock” regulon, and 2 were members of the σ54 “nitrogen-limitation” regulon (6 have not had their regulons identified).

Many of the most upregulated genes suggested cells desperate for carbon. The most upregulated gene was putative glucarate MFS transporter garP (+73.41), which was accompanied by galactarate dehydratase garD (+61.76), glycerate kinase garK (+31.07), glucarate aldolase garL (+62.77), and tartronate semialdehyde reductase garR (+46.53) genes involved in utilization of glucarate, galactarate, or glycerate as carbon sources, as well as ytfQ (+34.56), the periplasmic binding component of the galactose ABC transporter. The periplasmic binding protein of the arabinose ABC transporter, araF (+20.47), was

Table 2-5. Top 25 genes upregulated in NRE *vs.* NRA.

Gene	NRE/NRA	Sigma Regulon	Regulon Condition
araF	20.47	38, 70	starvation/stationary phase, housekeeping
astA	17.84	38, 54, 70	starvation/stationary phase, nitrogen-limitation, housekeeping
astC	20.86	38, 54, 70	starvation/stationary phase, nitrogen-limitation, housekeeping
cdaR	21.36	?	?
fadB	17.19	70	housekeeping
garD	61.76	?	?
garK	31.07	70	housekeeping
garL	62.77	70	housekeeping
garP	73.41	70	housekeeping
garR	46.53	70	housekeeping
melB	18.47	70	housekeeping
nanA	38.84	70	housekeeping
nanE	21.46	70	housekeeping
nanK	17.46	70	housekeeping
nanT	26.28	70	housekeeping
tdcB	20.34	?	?
tdcC	15.27	?	?
tnaA	61.81	70	housekeeping
tnaB	42.57	70	housekeeping
ydcH	23.84	?	?
ydeN	49.97	70	housekeeping
yhcH	16.29	32, 70	heat shock, housekeeping
yjhC	18.40	24, 70, 32	extracytoplasmic/extreme heat stress, housekeeping, heat shock
yphF	16.25	?	?
ytfQ	34.56	24	extracytoplasmic/extreme heat stress

highly upregulated, but this was unsurprising given the utilization of arabinose for induction of expression in these cultures. Also upregulated was another predicted periplasmic binding protein of another predicted sugar transporter, yphF (+16.25). The carbohydrate diacid regulator cdaR (+21.36) that regulates genes involved in the uptake and metabolism of galactarate and glucarate was also highly upregulated. The cells also upregulate several amino acid metabolic pathways. For tryptophan as a carbon source, tryptophan transporter tnaB (+42.57) and tryptophanase tnaA (+61.81) were both highly upregulated; and for threonine, catabolic threonine dehydratase tdcB (+20.34) and threonine/serine transporter tdcC (+15.27). The sialic acid metabolic pathway was also highly upregulated, with lyase nanA (+38.84), epimerase nanE (+21.46), kinase nanK (+17.46), transporter nanT (+26.28), and predicted oxidoreductase yjhC (+18.40) all among the 25 most upregulated genes. The uncharacterized yhcH (+16.29) also seems to be a member of the sialic acid catabolic operon. Two genes involved in the ammonia-producing arginine catabolic pathway, arginine succinyltransferase astA (+17.84) and succinylornithine transaminase astC (+20.86), were upregulated. The melibiose transporter melB (+18.47) that was downregulated in NRA/GRA was highly upregulated moving to restrained expression; melA (+15.09) expression followed suit. fadB (+17.19) is the [alpha] subunit of the fatty acid oxidation complex. Uncharacterized highly upregulated genes included predicted sulfatase ydeN (+49.97) and ydcH (+23.84).

Of the top 25 downregulated genes (Table 2-5), 18 were members of the σ70 “housekeeping” regulon, 2 were members of the σ24 “extracytoplasmic/extreme heat stress” regulon, and 1 was a member of the σ38 “starvation/stationary phase” regulon (7 have not had their regulons identified).

The most downregulated gene was major cold shock protein cspA (-20.48), which was accompanied by cspG (-11.90). A number of downregulated genes play a role in the cells’ nucleic acid management. Downregulation of RNA helicase deaD (-18.86) should have hindered assembly of the large ribosomal subunit, although decreased RNAse P (rnpA, -12.10) may have ultimately counteracted effects on translation efficiency; downregulation of tRNA dihydrouridine synthase dusB (-8.33) decreased 5,6-dihydrouridine modification in cellular tRNA. The electron-donating thioredoxin nrdH (-7.77) for ribonucleotide reductase was downregulated, potentially reducing DNA synthesis. The large reduction of fis (-15.96) suggested huge changes to nucleoid structure, as its role in nucleoid structure organization and maintenance involves not only direct binding but also regulation of many genes of similar purpose such as gyrase and topoisomerase I; fis modulates transcription of 21% of the *E. coli* genome (Cho et al. 2008). Surprisingly fis expression changed little in the other three comparisons, so this effect must have been a direct consequence of the change in CAX^{CK31} expression. Transporters were another group strongly represented in the downregulated genes of this comparison. Downregulated fepA (-14.87) and fepD (-17.03) encode the outer membrane porin and inner

membrane ABC transporter, respectively, involved with transport of enterobactin-iron. Downregulation of magnesium transporter mgtA (-12.55) was likely a consequence of decreased disruption of divalent cation homeostasis resulting from decreased CAX^{CK31} overexpression at the time of sampling (Figure 2-1). The reduction in σ38 stabilizer iraM (-9.38) also indicated reduced Mg^{2+} starvation; this should decrease expression of that sigma factor's regulon of "starvation/stationary phase" genes. Downregulation of bhsA (-12.29) should increase the permeability of the outer membrane to copper; it is also suggestive of decreased biofilm formation. Downregulation of "multiple antibiotic resistance" repressor marR (-9.59) suggested a generally increased stress response (including multidrug efflux and resistance to antibiotics, oxidative stress, organic solvents and heavy metals), *via* the marRAB operon. A hydroxylated, aromatic carboxylic acid efflux transporter, aaeA (-8.16), and a hexose 6-phosphate MFS transporter, uhpT (-7.88), were also downregulated. Lac operon members β-galactoside transacetylase lacA (-83.23), β-galactoside permease lacY (-82.42), and β-galactosidase lacZ (-80.33) were likely among the most downregulated genes in this comparison due to the elimination of IPTG induction. Mitigation of the oxidative stress resulting from rapid expression of CAX^{CK31} suggested by upregulated genes in NRA/GRA was evidenced by downregulation of superoxide dismutase sodA (-7.48), however its regulator soxS (-2.74) and downstream hydrogen peroxide responsive gene yhcN (-4.27) were much less affected. Reduced pH stress was also evidenced by the downregulation of glutamic acid decarboxylase transcriptional activator gadE (-7.00). The third most

Table 2-6. Top 25 genes downregulated in NRE *vs.* NRA.

Gene	NRE/NRA	Sigma Regulon	Regulon Condition
aaeA	-8.16	?	?
azuC	-11.16	70	housekeeping
bhsA	-12.29	70, 24	housekeeping, extracytoplasmic/extreme heat stress
cspA	-20.48	70	housekeeping
cspG	-11.90	?	?
deaD	-18.86	70, 24	housekeeping, extracytoplasmic/extreme heat stress
dusB	-8.33	70	housekeeping
fepA	-14.87	70	housekeeping
fepD	-17.03	70	housekeeping
fis	-15.96	70	housekeeping
gadE	-7.00	70, 38	housekeeping, starvation/stationary phase
iraM	-9.38	70	housekeeping
lacA	-8.30	70	housekeeping
lacY	-9.88	70	housekeeping
lacZ	-16.12	70	housekeeping
marR	-9.59	70	housekeeping
mgtA	-12.55	70	housekeeping
nrdH	-7.77	70	housekeeping
rnpA	-12.10	?	?
sodA	-7.48	70	housekeeping
suhB	-10.81	?	?
uhpT	-7.88	70	housekeeping
yebO	-7.94	?	?
yjcB	-9.17	?	?
yneG	-17.34	?	?

downregulated gene, yneG (-17.34) is completely uncharacterized and was also highly downregulated in the NRE/GRE comparison. azuC (-11.16) partitions to the inner membrane (Fontaine, Fuchs, and Storz 2011), but its function is unknown; yjcB (-9.17) and yebO (-7.94) are predicted inner membrane proteins. The physiological role of inositol monophosphatase suhB (-10.81) is unknown; it is a suppressor of secY (Shiba, Ito, and Yura 1984), rpoH (Yano et al. 1990), and dnaB (S. F. Chang et al. 1991) mutants.

GFP Restrained (GRE) / GFP Rapid (GRA).

The restrained expression method was compared to the rapid expression method for the expression of GFP to identify differences between the methods not specifically resulting from the toxicity of CAX^{CK31}. Consistent with the hypothesis that differences here would be minimal as there was less stress to mitigate, changes in gene transcription were generally of a lesser magnitude than those seen in all of our other comparisons.

Of the top 25 upregulated genes (Table 2-6), 20 were members of the σ70 “housekeeping” regulon, 3 were members of the σ38 “starvation/stationary phase” regulon, 3 were members of the σ54 “nitrogen-limitation” regulon, 2 were members of the σ24 “extracytoplasmic/extreme heat stress” regulon, 1 was a member of the σ28 “flagellar” regulon, and 1 was a member of the σ32 “heat shock” regulon (2 have not had their regulons identified).

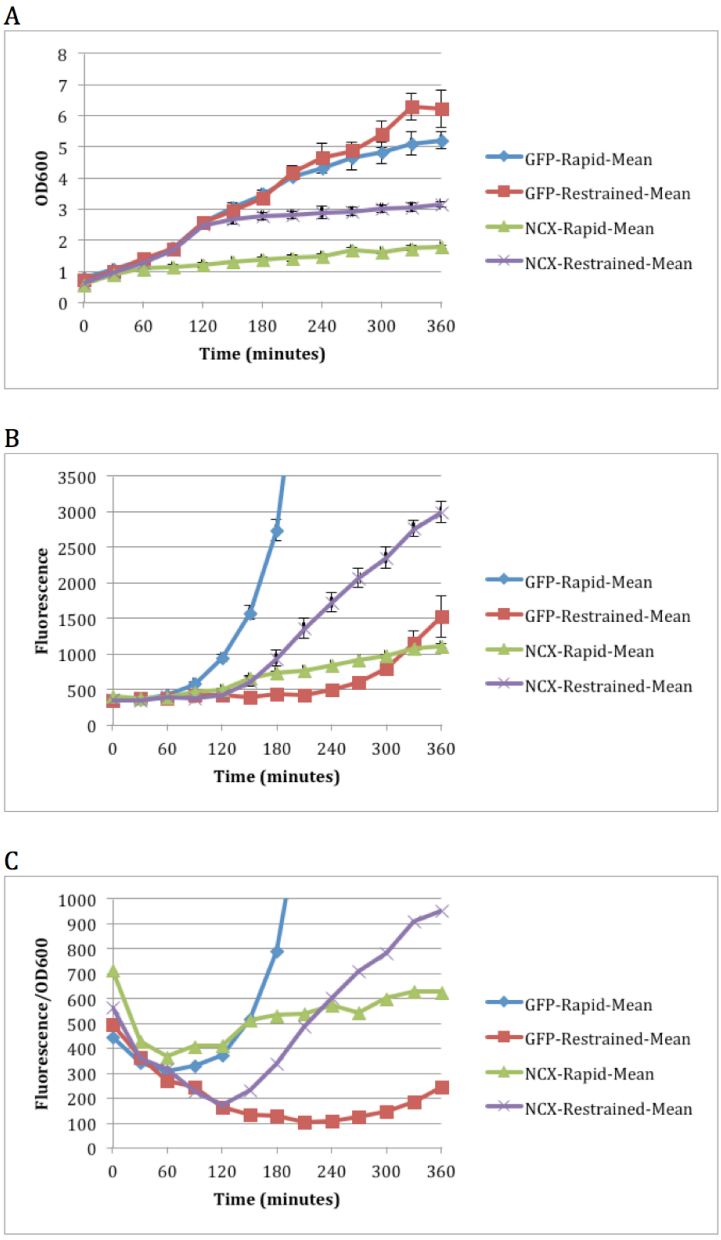

Figure 2-4. Heterologous overexpression of CAX^{CK31}-GFP or GFP in *E. coli* by restrained or rapid expression.
A, cell growth monitored by optical density at 600 nm (OD600) shows growth arrest resulting from CAX^{CK31} toxicity was mitigated by restrained expression. B, GFP fluorescence per mL culture showing enhanced total production of CAX^{CK31}-GFP by restrained expression. C, GFP fluorescence normalized by cell density exemplified differences in overexpressed protein levels per cell (*e.g.* at the time of sampling (3 hours post-induction, NRA cells contained more CAX^{CK31}-GFP than NRE cells).

Again carbon sourcing genes were among the most upregulated. The most upregulated gene was garR (+20.61), accompanied by garD (+18.43), garK (+18.00), and garL (+16.08) of the glucarate/galactarate/glycerate metabolic pathway; garP was surprisingly absent from the top 25 upregulated genes but was slightly upregulated (+5.07). Many more of the genes most upregulated in the NRE/NRA comparison were present here as well: ammonia-producing arginine catabolic pathway genes astA (+8.80) and astC (+15.35), fatty acid oxidation complex [alpha] subunit gene fadB (+9.35), and sialic acid catabolism operon genes nanA (+14.73), nanE (+7.27), nanK (+6.81), nanT (+7.96), and yhcH (+7.11). All of the above, however, were upregulated to a much lesser extent by the switch from rapid to restrained expression of GFP than the switch from rapid to restrained expression of CAX^{CK31}. Other highly upregulated transporters included the [alpha]-ketoglutarate MFS transporter kgtP (+8.35) essential for growth on [alpha]-ketoglutarate and the sodium/proline symporter (that can also transport propionate (Reed et al. 2006)) putP (+7.04). The problem of oxidative stress seemed to increase by the switch from rapid to restrained expression, as sodA (+17.24) is upregulated despite lower GFP expression, however the upregulation was much less than that seen in NRA/GRA. Biotin carboxylase accC (+6.71) is involved in protein and lipid metabolism and prevents buildup of organic acids that could trigger iron-mediated oxidative stress (Bruno-Bárcena, Azcárate-Peril, and Hassan 2010). Upregulation of ycdO (+8.74), the periplasmic component of the ferrous iron transporter, was an indication of iron limitation, low pH, or zinc stress. Nucleotide diphosphate

kinase ndk (+7.07) is implicated in the stringent response to amino acid starvation as the kinase converting GDP to GTP. Glycerol kinase glpK (+6.47) was also upregulated. The transcriptional activator mhpR (+9.81) of several genes involved in the degradation of phenylproprionate was upregulated. Induction of ATP-binding helicase phoH (+9.35) was an indication of phosphate starvation. Upregulation of ymgC (+8.84) has been associated with acid shock and should decrease biofilm formation and motility. ydeM (+6.71) is predicted to participate in the maturation of an anaerobic sulfatase. yfeY (+6.31) is a predicted outer membrane lipoprotein induced by extracytoplasmic stress. Periplasmic protease/chaperone degP (+6.15), rounded out the top 25 upregulated genes.

Of the top 25 downregulated genes (Table 2-7), 11 were members of the σ70 “housekeeping” regulon, 2 were members of the σ24 “extracytoplasmic/extreme heat stress” regulon, 2 were members of the σ54 “starvation/stationary phase” regulon, 1 was a member of the σ28 “flagellar” regulon, and 1 was a member of the σ32 “heat shock” regulon (10 have not had their regulons identified).

The most downregulated gene was β-galactoside transacetylase lacA (-83.23), which was again joined by other lac operon members β-galactoside permease lacY (-82.42) and β-galactosidase lacZ (-80.33) as well as the lac repressor lacI (-7.16). The next most downregulated genes were trimethylamine oxide (TMAO)

Table 2-7. Top 25 genes upregulated in GRE *vs.* GRA.

Gene	GRE/GRA	Sigma Regulon	Regulon Condition
accC	6.71	70	housekeeping
astA	8.80	38, 54, 70	starvation/stationary phase, nitrogen-limitation, housekeeping
astC	15.35	38, 54, 70	starvation/stationary phase, nitrogen-limitation, housekeeping
degP	6.15	24	extracytoplasmic/extreme heat stress
fadB	9.35	70	housekeeping
garD	18.43	?	?
garK	18.00	70	housekeeping
garL	16.08	70	housekeeping
garR	20.61	70	housekeeping
glpK	6.47	70	housekeeping
kgtP	8.35	28, 70	flagellar, housekeeping
mhpR	9.81	70	housekeeping
nanA	14.73	70	housekeeping
nanE	7.27	70	housekeeping
nanK	6.81	70	housekeeping
nanT	7.96	70	housekeeping
ndk	7.07	70	housekeeping
phoH	9.35	70	housekeeping
putP	7.04	70	housekeeping
sodA	17.24	70	housekeeping
ycdO	8.74	54, 70	nitrogen-limitation, housekeeping
ydeM	6.71	?	?
yfeY	6.31	24	extracytoplasmic/extreme heat stress
yhcH	7.11	32, 70	heat shock, housekeeping
ymgC	8.84	38	starvation/stationary phase

anaerobic respiration operon members TMAO reductase cytochrome c-type subunit torC (-44.10), TorA private chaperone torD (-38.75), and TorD catalytic subunit torA (-35.49). TMAO reductase appears to have coevolved with molybdoprotein partners (Ilbert, Méjean, and Iobbi-Nivol 2004) of which putative selenate reductase genes xdhD (-6.86) and ygfK (-6.47) were also downregulated. Three proteins involved in the synthesis of the biofilm adhesin PGA, PGA transporter pgaA (-8.72), PGA N-deacetylase pgaB (-14.72), and polysaccharide polymerase pgaC (-9.59), were downregulated. A component of the MdtJI spermidine transporter, mdtI (-11.28) was highly downregulated (mdtJ is only -2.16). Sulfur metabolism seemed to be reduced *via* several genes: two components of the sulfate/thiosulfate ABC transporter, periplasmic binding protein cysP (-6.77) and membrane subunit cysU (-6.34), were downregulated, and so was thiS (-6.39), the sulfur source for the thiazole moiety in thiamin biosynthesis. Predicted transcarbamylase ygeW (-9.00) was downregulated to a greater extent than in NRA/GRA. Prepilin peptidase dependent gene ppdD (-7.68) was downregulated. The predicted hydrolase ssnA (-6.96) highly downregulated in NRA/GRA was also here among the most downregulated genes, promoting viability at the beginning of stationary phase. Uncharacterized highly downregulated genes included predicted sialic acid transporter ycgI (-24.23), which seemed to conflict with the number of upregulated sialic acid metabolism genes (including a transporter, nanT) in this comparison, ybfA (-14.33), yfbM (-8.11; also downregulated in NRA/GRA), predicted membrane

Table 2-8. Top 25 genes downregulated in GRE *vs.* GRA.

Gene	GRE/GRA	Sigma Regulon	Regulon Condition
cysP	-6.77	70	housekeeping
cysU	-6.34	70	housekeeping
lacA	-83.23	70	housekeeping
lacI	-7.16	70	housekeeping
lacY	-82.42	70	housekeeping
lacZ	-80.33	70	housekeeping
mdtI	-11.28	?	?
pgaA	-8.72	?	?
pgaB	-14.27	?	?
pgaC	-9.59	?	?
ppdD	-7.68	70	housekeeping
ssnA	-6.96	54	nitrogen-limitation
thiS	-6.39	?	?
torA	-35.49	70	housekeeping
torC	-44.10	70	housekeeping
torD	-38.75	70	housekeeping
xdhD	-6.86	?	?
ybfA	-14.33	28, 24	flagellar, extracytoplasmic/extreme heat stress
ycgI	-24.23	?	?
yehK	-7.30	70	housekeeping
yfbM	-8.11	?	?
ygeW	-9.00	32, 24	heat shock, extracytoplasmic/extreme heat stress
ygfK	-6.47	54	nitrogen-limitation
yghG	-6.27	?	?
yjhE	-7.46	?	?

protein yjhE (-7.46; upregulated in NRE/GRE), yehK (-7.30; also downregulated in NRA/GRA), and predicted lipoprotein yghG (-6.27).

CAX^{CK31} Restrained (NRE) / GFP Restrained (GRE).

The differences between overexpression of CAX^{CK31} and GFP using restrained expression methods well demonstrated the method's success in mitigating the deleterious responses of cells to rapid expression of the toxic CAX^{CK31} identified above in NRA/GRA. Of the top 25 upregulated genes (Table 2-8), 12 were members of the σ32 "heat shock" regulon, 12 were members of the σ70 "housekeeping" regulon, 2 were members of the σ54 "nitrogen-limitation" regulon, and 1 was a member of the σ38 "starvation/stationary phase" regulon (4 have not had their regulons identified).

As in NRA/GRA, among the most upregulated genes were still ibpB (+66.71), ibpA (+35.99), clpB (+22.80), and dnaK (+8.57). Also still upregulated were deoB (+13.08), glpD (+17.10), hslU (+11.00), hspQ (+8.68), htpG (+9.67), lldD (+8.57), and soxS (+52.10), but all were upregulated to a lesser extent than in NRA/GRA, demonstrating the mitigation of the toxic responses to rapid CAX^{CK31} overexpression. The aerobic glycerol-3-phosphate dehydrogenase also upregulated in NRA/GRA was now joined by anaerobic glycerol-3-phosphate dehydrogenase, composed of large subunit glpA (+11.41), membrane anchor subunit glpB (+11.46), and small subunit glpC (+11.58). In this comparison, regulator of biofilm formation (contradictory reports exist as to whether bssS

increases (Beloin et al. 2004) or decreases (Domka, Lee, and Wood 2006) biofilm formation) bssS (+17.73) joined the list of most upregulated genes; remember that downregulation of biofilm stress and motility protein bsmA in NRA/GRA likely resulted in compromised acid and peroxide stress resistance. Sulfur metabolism again changed significantly, this time via upregulation of thiamin biosynthesis sulfur source thiS (+14.33). Upregulation of glmZ (+10.82) was an indication of decreased intracellular glucosamine concentration (Kalamorz et al. 2007). Upregulation of the universal stress protein uspG (+9.94) could have been triggered by carbon or phosphate starvation (Bochkareva, Girshovich, and Bibi 2002). The sodium/proton antiporter nhaA (+9.21) was upregulated, typically resulting from increased extracellular Na^+ or Li^+. Upregulation of formamidopyrimidine DNA glycosylase mutM (+8.55) indicated a need to repair free radical induced DNA lesions. Upregulation of zntR (+8.04), the transcriptional regulator of zntA (+3.48) was a response to a need for lead, cadmium, or zinc efflux. Uncharacterized highly upregulated genes included predicted membrane proteins yjhE (+12.59; downregulated in GRE/GRA), yqaE (+10.87), and ycjF (+9.65), and predicted nucleotide binding protein ycjX (+9.17).

Of the top 25 downregulated genes (Table 2-9), 15 were members of the σ70 “housekeeping” regulon, 2 were members of the σ38 “starvation/stationary phase” regulon, 1 was a member of the σ24 “extracytoplasmic/extreme heat stress” regulon, and 1 was a member of the σ32 “heat shock” regulon (9 have not had their regulons identified).

Table 2-9. Top 25 genes upregulated in NRE *vs.* GRE.

Gene	NRE/GRE	Sigma Regulon	Regulon Condition
bssS	17.73	70, 32	housekeeping, heat shock
clpB	22.80	70, 32	housekeeping, heat shock
deoB	13.08	70	housekeeping
dnaK	8.57	32	heat shock
glmZ	10.82	70	housekeeping
glpA	11.41	70	housekeeping
glpB	11.46	70	housekeeping
glpC	11.58	70	housekeeping
glpD	17.10	70	housekeeping
hslU	11.00	32	heat shock
hspQ	8.68	32	heat shock
htpG	9.67	54, 32	nitrogen-limitation, heat shock
ibpA	35.99	32	heat shock
ibpB	66.71	54, 32	nitrogen-limitation, heat shock
lldD	8.57	70	housekeeping
mutM	8.55	32	heat shock
nhaA	9.21	38, 70	starvation/stationary phase, housekeeping
soxS	52.10	70	housekeeping
thiS	14.33	?	?
uspG	9.94	?	?
ycjF	9.65	32	heat shock
ycjX	9.17	32	heat shock
yjhE	12.59	?	?
yqaE	10.87	?	?
zntR	8.04	70, 32	housekeeping, heat shock

The most downregulated gene, yeeD (-11.47) was completely uncharacterized but is 96 % identical to tRNA 2-thiouridine synthesizing protein SirA, and so possibly demonstrated the decreased transcription that was the basis of the restrained expression technique; downregulation of transcription elongation factor greA (-4.55) suggested a reduction in stalled RNA polymerases (or simply RNA polymerization in general). There was also downregulation of one 50S ribosomal subunit, rpmH (-4.37), and reduced levels of [beta]-methylthiolated 30S ribosomal subunit protein S12 will result from downregulation of ycaO (-3.42). Meanwhile, downregulation of purine salvage protein adenine phosphoribosyltransferase apt (-3.56) may indicate a decreased need for purines (or thymine). The second most downregulated gene was phosphoadenosine-phosphosulfate (PAPS) reductase cysH (-10.56), which was accompanied by sulfate adenylyl transferase components cysD (-4.18) and cysN (-4.10), and sulfite reductase cysI (-4.84). σ38 stabilizer iraM (-8.50) again appeared on a list of most-downregulated genes, indicating a reduction in Mg^{2+} starvation; meanwhile downregulation of predicted lipoprotein and Mg^{2+} stimulon member (Minagawa et al. 2003) borD (-4.69) suggested decreased external Mg^{2+} availability. Together these results may have suggested that the overexpressed CAX^{CK31} is importing a lot of Mg^{2+}. Another highly downregulated gene shared between NRE/NRA and NRE/GRE was the glutamic acid decarboxylase transcriptional activator gadE (-7.14), demonstrating reduced pH stress resulting from the switch from GFP to CAX^{CK31}; could the proton-transporting capability of CAX^{CK31} have been alleviating pH stress caused by heterologous expression in

Table 2-10. Top 25 genes downregulated in NRE *vs.* GRE.

Gene	NRE/GRE	Sigma Regulon	Regulon Condition
accB	-4.13	70	housekeeping
accC	-4.35	70	housekeeping
apt	-3.56	70	housekeeping
borD	-4.69	?	?
cysD	-4.18	70	housekeeping
cysH	-10.56	70	housekeeping
cysI	-4.84	70	housekeeping
cysN	-4.10	70	housekeeping
fabA	-4.38	70	housekeeping
gadE	-7.14	70, 38	housekeeping, starvation/stationary phase
greA	-4.55	70, 24	housekeeping, extracytoplasmic/extreme heat stress
iraM	-8.50	70	housekeeping
malK	-3.93	?	?
ndk	-3.80	70	housekeeping
proV	-3.65	38, 70	starvation/stationary phase, housekeeping
rpmH	-4.37	?	?
tfaR	-4.89	?	?
ycaM	-3.41	70	housekeeping
ycaO	-3.42	?	?
ycgF	-3.56	70	housekeeping
yeeD	-11.47	?	?
yfeY	-5.70	24	extracytoplasmic/extreme heat stress
yjhD	-5.06	?	?
yncI	-6.04	?	?
yneG	-7.35	?	?

general? Three downregulated genes are involved in fatty acid biosynthetic pathways: the biotin carboxylase accC (-4.35) that was upregulated in GRE/GRA was downregulated here along with biotin carboxyl carrier protein accB (-4.13) and fabA (-4.38), a 3-hydroxydecanoyl-[acp] dehydrase involved in type II fatty acid synthesis. Maltose/maltodextrin ABC transporter subunit malK (-3.93) was much less downregulated than it was in NRA/GRA; it was joined in downregulation by the glycine betaine/proline ABC transporter's ATP binding subunit proV (-3.65). Nucleotide diphosphate kinase ndk (-3.80) suggested decreased amino acid starvation with its downregulation in this comparison (it was upregulated in GRE/GRA). The downregulation of blue light-responsive regulator ycgF (-3.56) was mysterious, but it leads to increased activity of transcriptional repressor ycgE (+1.70), which represses biofilm production. Other uncharacterized genes highly downregulated included yneG (-7.35; also downregulated in NRE/NRA), putative transposase yncI (-6.04; also downregulated in NRA/GRA), predicted outer membrane lipoprotein yfeY (-5.70; upregulated in GRE/GRA), yjhD (-5.06), predicted tail fiber assembly protein tfaR (-4.89), and predicted amino acid transporter ycaM (-3.41).

Discussion:

Stress induced by recombinant protein production in *E. coli* can be classified into three categories: (1) the metabolic consequences arising from the energy and precursor demands of increased transcription and translation, (2) effects on DNA replication, chromosomal and plasmid, and (3) responses to perceived stresses

via regulatory networks (furthering the aforementioned metabolic burden). Growth inhibition can be attributed to the metabolic burdens of plasmid maintenance (minimal) and recombinant protein synthesis rate (major). Growth ceases when recombinant protein is 30 % of total cell protein (Dong, Nilsson, and Kurland 1995). Energy demand induces respiration for ATP synthesis. Substrate level phosphorylation leads to accumulation of acetate and pyruvate excretion (George et al. 1992). Glucokinase synthesis increases upon recombinant protein production (Arora and Pedersen 1995; Oh and Liao 2000) as the need for glucose-6-phosphate exceeds the capacity of the glucose phosphotransferase system. Surplus NADPH can lead to downregulation of the oxidative branch of the pentose phosphate pathway (J. Weber, Hoffmann, and Rinas 2002), leading to the non-oxidative branch functioning as a pentose supply and all glucose being funneled to the TCA cycle. "Housekeeping" protein production is affected by competition among ribosome binding sites (Vind et al. 1993); note that this is unrelated to protein accumulation, but rather to synthesis rate. "Housekeeping" sigma factor σ70 (rpoD) is associated with most genes in growing cells; its upregulation by 19.50-fold in NRA/GRA demonstrates the cells' struggle to maintain adequate levels of their essential proteins despite the described burdens of also overproducing CAX^{CK31}. Increased translational activity induces rRNA and ribosomal protein transcription, but even ribosomal protein mRNA competes for ribosomes and thus production is ultimately decreased (Laffend and Shuler 1994). The stringent response (*i.e.* to amino acid

starvation) results in ribosomal disassembly (Gallant 1979; Dong, Nilsson, and Kurland 1995).

Chromosomal replication is impaired, and chromosome packing density is decreased (Merten 2001; Teich et al. 1998). *E. coli* may have evolved a mechanism to relocate DNA encoding membrane proteins to the membrane for increased "transertion" efficiency (Libby, Roggiani, and Goulian 2012; Woldringh 2002); expression of nucleoid reorganization genes decreased significantly when transitioning from NRA to NRE, suggesting a key role of this process in the increased efficiency of the restrained expression method.

Induced stress response categories include the heat-shock response, the stringent response, and the SOS response. Additionally, oxidative damage protection and starvation and osmotic stress responsive genes tend to be included to varying degrees depending on the protein overproduced (Gill, Valdes, and Bentley 2000). The heat-shock response is meant to combat the unfolding of proteins and changes of mRNA secondary structure caused by sudden rises in temperature; proteins involved include both folding chaperones and proteases for aggregates beyond repair. In *E. coli*, expression of heat shock genes is mediated by the heat shock sigma factor σ32 (rpoH); in our experiments, transcription of the gene encoding σ32 was increased 5.51-fold in NRA/GRA, demonstrating an increase in misfolded/aggregated proteins, then decreased 2.87-fold in NRE/NRA as the reduction in CAX^{CK31} transcription led to increased

efficiencies of translation and membrane insertion/folding. The so-called stringent response describes the effects of amino acid starvation, specifically the lack of amino-acylated tRNA. Responses typically include downregulation of transcription and translation machinery as well as amino acid biosynthesis (however our data showed upregulation of histidine and arginine biosynthesis) (D.-E. Chang, Smalley, and Conway 2002). Supplementation of media with amino acids may mitigate stress (Harcum and Bentley 1993). The SOS response is induced by the presence of single-stranded DNA typically resulting from DNA damage or hindrance of DNA replication, but it is not clear how to link these events to recombinant protein production.

Genes appearing on multiple lists revealed responses more broadly applicable to understand the differences between our proteins or our expression regimens. Upregulation in both NRA/GRA and NRE/GRE indicated genes responding to the transition from GFP to CAX^{CK31} irrespective of the expression regimen used. clpB, deoB, dnaK, glpD, hslU, hspQ, htpG, ibpA, ibpB, lldD, and soxS were upregulated in both NRA/GRA and NRE/GRE. Upregulation in NRA/GRA and downregulation in NRE/NRA indicated genes responding to rapid expression of CAX^{CK31} but whose response was mitigated by the transition to restrained expression. mgtA and sodA were upregulated in NRA/GRA and downregulated in NRE/NRA. sodA was upregulated in both NRA/GRA, as well as GRE/GRA, but downregulated in NRE/NRA. Downregulation in NRA/GRA and upregulation in NRE/NRA, like upregulation in NRA/GRA and downregulation in NRE/NRA,

also indicated genes responding to rapid expression of CAX^{CK31} but whose response was mitigated by the transition to restrained expression. araF, melB, and yphF were downregulated in NRA/GRA and upregulated in NRE/NRA. Downregulation in both NRA/GRA and NRE/GRE, like upregulation in both NRA/GRA and NRE/GRE, indicated genes responding to the transition from GFP to CAX^{CK31} irrespective of the expression regimen used. malK and yncI were downregulated in both NRA/GRA and NRE/GRE. Downregulation in both NRA/GRA and GRE/GRA indicated genes responding to a reduction in GFP expression. ssnA, yehK, yfbM, and ygeW were downregulated in both NRA/GRA and GRE/GRA. Upregulation in both NRE/NRA and GRE/GRA indicated genes responding to the transition from rapid to restrained expression irrespective of the protein overexpressed. astA, astC, fadB, garD, garK, garL, garR, nanA, nanE, nanK, nanT, and yhcH were upregulated in both NRE/NRA and GRE/GRA. Downregulation in both NRE/NRA and NRE/GRE probably indicated genes responding to increased successful CAX^{CK31} overexpression. gadE, iraM, and yneG are downregulated in both NRE/NRA and NRE/GRE. Downregulation in both NRE/NRA and GRE/GRA, like upregulation in both NRE/NRA and GRE/GRA, indicated genes responding to the transition from rapid to restrained expression irrespective of the protein overexpressed. lacA, lacY, and lacZ were downregulated in both NRE/NRA and GRE/GRA. sodA was downregulated in NRE/NRA and upregulated in GRE/GRA. accC, ndk, and yfeY were upregulated in GRE/GRA and downregulated in NRE/GRE. thiS and yjhE were downregulated in GRE/GRA and upregulated in NRE/GRE.

Inspired by the report that trigger factor KO increased deltarhodopsin expression (Nannenga and Baneyx 2011), we sought to determine whether expression was improved in cells lacking genes whose downregulation correlated with increased CAX^{CK31} expression. Keio collection knockout clones (Baba et al. 2006) were transformed with a plasmid expressing CAX^{CK31}-GFP under the control of the tet promoter. Clones selected were aceA (isocitrate lyase; glyoxylate cycle; NRE/NRA=7.79), aceK (isocitrate dehydrogenase kinase; TCA cycle/glyoxylate cycle; NRE/NRA=3.02), fis (nucleoid structure organization and maintenance; NRE/NRA=-15.96), icd (isocitrate dehydrogenase; TCA cycle; NRE/NRA=1.9), and marR (multiple antibiotic resistance repressor; NRE/NRA=-9.59). The changes in expression of each of these genes in the NRE/NRA comparison revealed a pathway contributing to the differences between expression regimens. Unfortunately, none of these knockouts significantly improved expression of CAX^{CK31}.

One limitation of transcriptomic analysis is that it cannot actually reveal which proteins' activities may change, nor can it guarantee that gene expression levels actually change to the same degrees as their transcription. Proteomics tools (e.g. 2DGE, mass-spectrometry) may accomplish the latter but also suffer from the former limitation. Despite these limitations, RNA-seq typically provides far better coverage of the genome (93 % in our case) at a lower cost, so it can be considered very effective as a hypothesis-generation tool.

These data will help to characterize the biology and stress responses of *E. coli* at the cellular level, however the primary goal of this analysis is the identification of specific pathways involved in membrane protein overexpression stress and insights into its molecular mechanism of toxicity. These data will help in development of both avenues for intervention to improve protein production and in design of more robust *E. coli* strains better able to handle stress arising from protein overproduction. A better understanding of not only genes but pathways affected by the stress of toxic membrane protein overproduction will guide these intervention efforts. Stimulation or suppression of key pathways identified by these efforts using inexpensive additives to the bacterial culture resulting in improved expression levels or cell health would be considered a major success. Likewise, pathways could be suppressed by removing genes of interest from the *E. coli* genome; and the Keio collection of single-gene deletion mutants with each nonessential *E. coli* gene removed (Baba et al. 2006) has been procured for these tests.

2.6 Purification of Calcium/Proton Antiporters from *E. coli*

Several biochemical and biophysical analyses require pure protein. Our clones were engineered with a His-tag for affinity purification and a Tobacco Etch Virus (TEV) protease cleavage recognition site between the CAX^{CK31} and GFP-His for removal of fluorescence and affinity tags. Purified protein migrated as a single band at monomer MW in SDS-PAGE and a single, Gaussian peak in SEC (Figure 3-2). Circular dichroism spectroscopic analysis revealed that purified

CAX^{CK31} contains secondary structure matching predictions from sequence analysis (74 % α / 3 % β) (Figure 3-2). Preservation of protein function through purification was confirmed by liposome reconstitution of purified protein and a Ca^{2+}-transport assay involving reporting of Ca^{2+} transport into liposomes loaded with the Ca^{2+}-sensitive dye Fura-2 (Figure 3-2; more functional assay details below).

CAX^{CK31}-GFP fusion protein was purified from detergent extracts of membranes prepared as above by immobilized cobalt affinity chromatography. While the protein was immobilized, buffer detergent changes could be accomplished by washing. Fluorescence and affinity tags could be removed by treatment with TEV protease. Protein was further purified by SEC and, when digested, treated with additional cobalt resin to clear remaining tagged protein.

Detergent Screening for Extraction of CAX^{CK31} from Membranes and Further Purification

For the purification of integral membrane proteins, detergents are required for not only solubilization of expression cell membranes but also subsequent stabilization of the protein of interest throughout purification and analysis. The same detergent(s) may not be suitable for both purposes, necessitating screening of detergents representing a variety of head-groups and chain lengths at multiple stages of purification. DDM was identified as the optimal detergent for CAX^{CK31} extraction from membranes. However, DDM proved insufficient for

stabilization of purified CAX^{CK31}, as protein precipitated from solution and was lost during IMAC, suggesting that a lipid from the *E. coli* membrane incorporated into a mixed-micelle with DDM during solubilization may have been stabilizing CAX^{CK31}, and whose removal during washing of the immobilized CAX^{CK31} destabilized it. Screening of detergents for further purification proceeded for the steps beginning with IMAC wash and identified a choline head group in addition to the dodecyl tail as essential to maintain maximal CAX^{CK31} stability in solution (Figure 3-1); 1 × CMC FC12 (1.5 mM) was identified as the optimal detergent for maintaining stability of purified CAX^{CK31}. However, as FC12 was not efficient for extraction of CAX^{CK31} from membranes, a two-step process was adopted with DDM used for extraction and FC12 used for purification. As the relative harshness of FC12 was suspected to destabilize the expected CAX^{CK31} dimer (Ridilla et al. 2012), additional detergent screening was done by reducing [FC12] to 0.5 × CMC (0.75 mM) and adding other detergents. The effect of adding 2 × CMC C12E8 (0.01 % (w/v)) exhibited as a shift to earlier elution in SEC (Figure 3-7), suggesting that it maintained the oligomerization state of CAX^{CK31}, later determined to be a dimer.

The FSEC method (Kawate and Gouaux 2006) was used to identify detergents capable of extracting protein from membrane and maintaining it in stable form. Briefly, 0.5 mL of 0.1 g/mL suspension of membrane in 20 mM Tris, pH 8.0, 300 mM NaCl was solubilized using 100 × CMC of the following detergents: DDM, FC12, β-OG. After two hours of extraction at 4 °C, the samples were clarified by

centrifugation, and supernatants were subjected to FSEC analysis with a S200 column pre-equilibrated in the same detergent solution at 1 × CMC detergent. Qualitative analysis of peaks was conducted, and detergents providing Gaussian peaks were considered for further analysis. In addition to individual detergents, detergent mixtures were also used to determine the optimal detergent combination to solubilize and purify the protein.

While the general protocol of "*E. coli* membrane isolation, resuspension, and detergent extraction → affinity chromatography purification of His-Tagged fusion protein by Talon Cobalt Resin → digestion of fusion protein by TEV Protease → SEC" has remained, much fine-tuning has been done. Several of the parameters that have been optimized were as follows:

i. His-Tag length: The initial N21 construct was cloned with eight histidines at the C-terminus. Purifications using this construct always suffered significant losses in the Talon flow-thru. The tag was increased to nine histidines; Talon yields increased by 23 %. Addition of two additional histidines increased Talon yields by another 50 %. Current losses in the Talon flow-thru with 11-His-Tagged constructs are around 10 %.

ii. Detergent(s) used for extraction and purification: As FSEC was used to assess stability of impure protein, SEC with spectrophotometric detection (280-nm UV light absorbance) was used to assess stability (as well as purity) of partially- or fully-purified protein. This tool was used to evaluate the relative

stability of purified protein in various detergents. Figure 2-5 is an example of such an analysis.

iii. Removal of GFP and uncleaved fusion protein: Because the elution points of N21-GFP fusion protein and pure N21 from the S200 SEC column were similar, they could not be completely separated by this step alone. Initially an anion-exchange chromatography step was included after TEV Protease digestion, but significant losses occurred in this step. Substituting another Cobalt affinity purification after cleavage, in which the untagged CAX^{CK31} does not bind the resin, for the anion exchange enabled us to avoid these losses (and remove unwanted proteins that happen to bind Talon resin), but this required buffer exchange to remove the Imidazole present from the elution of fusion protein from Talon resin. By attaching a small nickel affinity column in tandem after our S200 SEC column, buffer exchange and ultimate purification were accomplished in one step, saving time and minimizing loss.

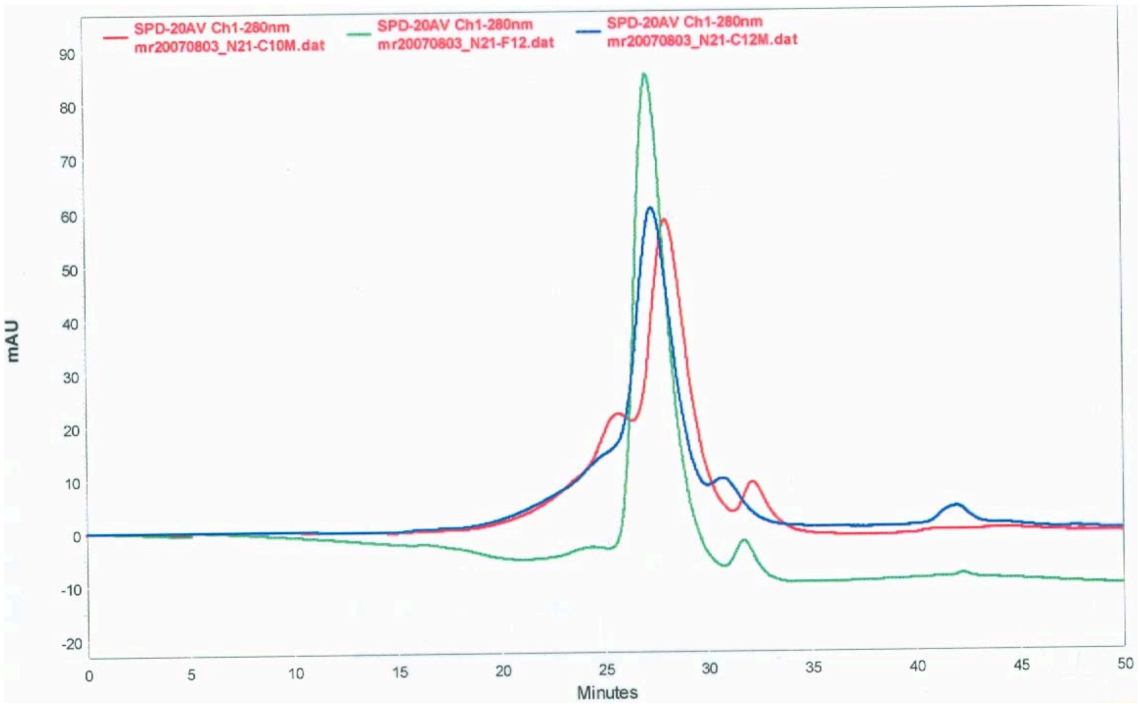

Figure 2-5. N21 detergent-stability assessment by SEC.
Red, n-Decyl-β-D-Maltopyranoside (DM). Green, FC12. Blue, DDM.

Other parameters optimized include concentration of the initial membrane resuspension and concentrations of Imidazole used in Talon binding, washing, and elution buffers.

Final yields of purified CaCAs were approximately 1.5 mg per liter of *E. coli* culture.

CAX^{CK31} Oligomerization State Determination Using Secondary FRET

Fab fragments from CAX^{CK31} antibodies have been labeled with one of several FRET-capable dyes. Association of these with CAX^{CK31} oligomers should produce detectable FRET between proximal Fabs. This assay should allow us to detect differences in CAX^{CK31} oligomerization state in detergent solution or vesicles, or in the presence of any substrates or inhibitors. It has been demonstrated that the labeling does not interfere with binding of Fabs to CAX^{CK31}.

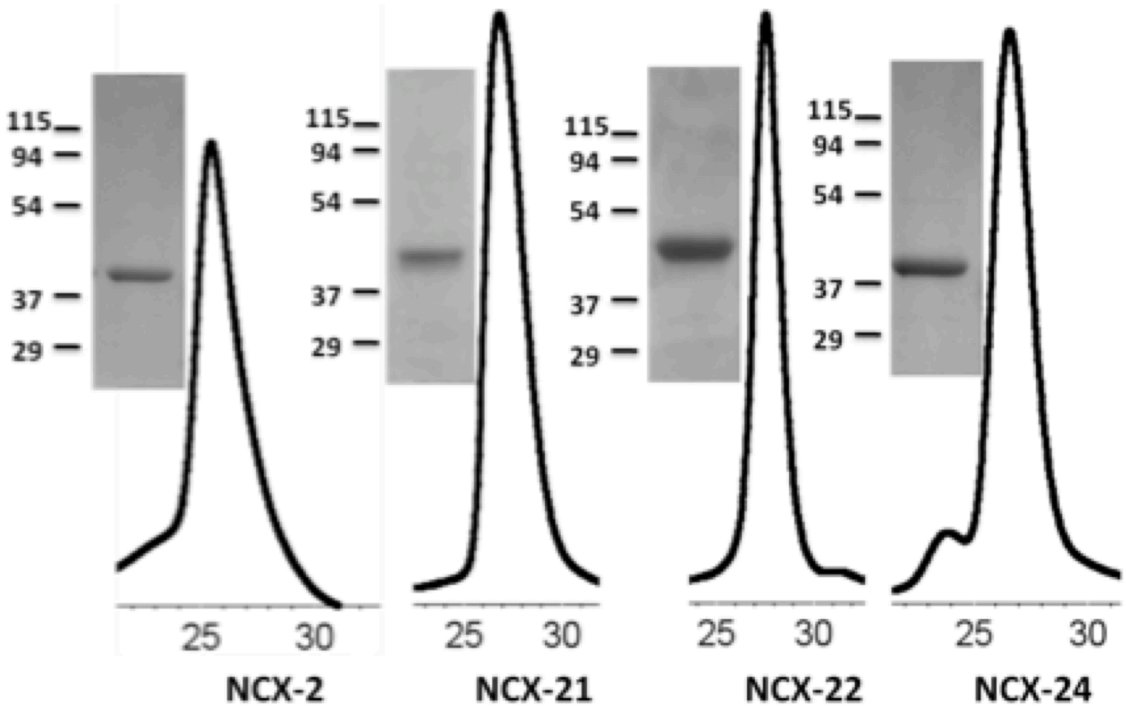

Figure 2-6. Purified calcium cation antiporters NCX-2, NCX-21, NCX-22, and NCX-24.

CHAPTER 3. IDENTIFICATION OF THE DIMER INTERFACE OF A BACTERIAL CA^{2+}/H^{+} ANTIPORTER

Note: the contents of this Chapter have been published by *Biochemistry* (Ridilla et al. 2012) and are presented below without change.

3.1 Abstract

"Members of the calcium/cation antiporter superfamily, including the cardiac sodium/calcium exchangers, are secondary active transporters that play an essential role in cellular Ca^{2+} homeostasis. A notable feature of this group of transporters is the high levels of sequence similarity in relatively short sequences constituting the functionally important α-1 and α-2 regions in contrast to relatively lower degrees of similarity in the extended adjoining sequences. This suggests a similar structure and function of core transport machinery but possible differences in topology and/or oligomerization, a topic that has not been adequately addressed. Here we present the first example of purification of a bacterial member of this superfamily (CAX^{CK31}) and analyze its quaternary structure. Purification of CAX^{CK31} required the presence of a choline headgroup-containing detergent or lipid to yield stable preparations of the monomeric transporter. H^{+}-driven Ca^{2+} transport was demonstrated by reconstituting purified

CAX^{CK31} into liposomes. Dimeric CAX^{CK31} could be isolated by manipulation of detergent micelles. Dimer formation was shown to be dependent on micelle composition as well as protein concentration. Furthermore, we establish that CAX^{CK31} forms dimers in the membrane by analysis of cross-linked proteins. Using a dimeric homology model derived from the monomeric structure of the archaeal NCX homologue (Protein Data Bank entry 3V5U), we introduced cysteine residues and through cross-linking experiments established the role of transmembrane helices 2 and 6 in the putative dimer interface."

3.2 Introduction

"The calcium/cation antiporter (CaCA) superfamily comprises five families (Cai and Lytton 2004): the NCX and NCKX families of animal Na^+/Ca^{2+} exchangers; the YRBG family of bacterial and archaeal exchangers, which takes its name from the yrbG gene in *Escherichia coli*; the CAX family of Ca^{2+}/H^+ exchangers found in yeasts, plants, archaea, and eubacteria; and the cation/Ca^{2+} exchangers, or CCX. Transporters belonging to the CaCA superfamily catalyze the following generalized transport equilibrium: $Ca^{2+}_{(in)} + [nH^+ \text{ or } nNa^+]_{(out)} \rightleftharpoons Ca^{2+}_{(out)} + [nH^+ \text{ or } nNa^+]_{(in)}$ (Saier, Tran, and Barabote 2006). Other divalent cations are transported by various members of the superfamily (Saier Jr. et al. 1999). The NCX family of transporters has been more extensively studied than any other family. Its members play a vital role in Ca^{2+} transport in excitable cells, namely, cardiac myocytes and neurons, where NCX malfunction has been implicated in various

pathologies (Blaustein and Lederer 1999; Craner et al. 2004; Jeon et al. 2003; Pott, Goldhaber, and Philipson 2004).

On the basis of sequence analysis, it was predicted that CaCA superfamily members have a core transmembrane domain that includes at least nine transmembrane helices (Table 3-1), and many members probably have additional transmembrane helices decorating the central core (Cai and Lytton 2004). The placement of the N- and C-termini with respect to the membrane is proposed to vary among families. Common to all members are two loops, designated α-1 and α-2, each containing a conserved G(S/T)SxP(D/E) motif. The level of conservation is generally greater in α-1 than in α-2 (Shigaki et al. 2006). The level of sequence conservation outside of these signature motifs is rather low within families and essentially nonexistent between families (Table 3-1). Given these large variations in sequence and topology between various families in the CaCA superfamily, an interesting question is whether quaternary structure is conserved within the superfamily.

A YRBG family transporter from *M. jannaschii* (NCX_Mj) was recently crystallized as a monomer (Liao et al. 2012); however, the apparent sufficiency of the crystallographic monomer to potentially meet the requirements for transport does not preclude an oligomeric native state (Veenhoff, Heuberger, and Poolman 2002). For example, the crystal structures of NhaA (Hunte et al. 2005; Herz et al. 2009), the H^+/Cl^- exchange transporter (Dutzler et al. 2002), and TrkH

Table 3-1. Sequence similarity among various eukaryotic, prokaryotic, and archaeal CaCAs.
Amino acid sequences representing either full-length protein or the α-1 or α-2 repeat from each were compared to that of NCX_Mj using ClustalW2. Numbers of transmembrane helices (TMs) were predicted using the program PHDhtm.

	% Identity (% Similarity) to NCX_Mj	% Identity (% Similarity) to NCX_Mj in α-1	% Identity (% Similarity) to NCX_Mj in α-2	Predicted number of TMs
M. jannaschii (NCX_Mj)	100	100	100	9*
Caulobacter Sp. K31 (CAX^{CK31})	5 (17)	16 (35)	15 (33)	11
C. familiaris	2 (17)	35 (48)	28 (41)	10
E. coli	9 (25)	45 (58)	37 (52)	10
V. cholerae	8 (22)	42 (52)	50 (57)	10
H. sapiens	2 (15)	35 (48)	28 (41)	9
D. melanogaster	3 (24)	35 (52)	37 (46)	11

* The crystal structure of NCX_Mj (PDB: 3V5U) shows 10 TMs.

(Cao et al. 2011) reveal ion pathways in each monomer, but the transporters exist as physiological dimers that, in many cases, provide additional functions (Gärtner et al. 2011; Rimon, Tzubery, and Padan 2007; Robertson, Kolmakova-Partensky, and Miller 2010). Conflicting results have kept the true oligomerization state of glucose transporter GLUT1 in question for many years (Zottola et al. 1995; Boulter and Wang 2001; Carruthers et al. 2009). Moreover, the ADP/ATP carrier has been crystallized in both monomeric (Pebay-Peyroula et al. 2003) and native dimeric (Nury et al. 2005) states from protein purified by identical methods.

This study presents the first overexpression and purification of a member of the CAX family, demonstrates H^+-driven Ca^{2+} transport, demonstrates the presence of dimers in membranes, identifies a detergent mixture that yields concentration-dependent dimerization in solution after purification, and identifies the dimer interface through model-directed mutagenesis and chemical cross-linking."

3.3 Experimental Procedures

3.3.1 Cloning and Expression

"A CAX family gene from *Caulobacter* sp. K31 (accession number ZP-01418997), herein termed CAX^{CK31}, was selected from our previous large-scale screen to identify prokaryotic CaCA that can be overexpressed in *E. coli* (Narayanan, Ridilla, and Yernool 2011). DNA encoding residues 1−416 was amplified *via* polymerase chain reaction (PCR) and cloned into vector pETCTGFP (Narayanan,

Ridilla, and Yernool 2011). The resulting clone was capable of producing a CAX^{CK31}-GFP-His_{11} fusion protein containing C-terminal green fluorescent protein and an undecahistidine tag. For Förster resonance energy transfer (FRET) experiments, GFP was replaced with monomeric cherry-red fluorescent protein (mCherry), which forms a FRET pair with GFP-fused CAX^{CK31} protein. Cysteine residues were introduced by site-directed mutagenesis using the overlap PCR method; wild-type CAX^{CK31} contains no cysteine residues.

The restrained-expression method was used to produce fusion proteins (Narayanan, Ridilla, and Yernool 2011). Briefly, cultures grown at 37 °C to an optical density of 0.6 at 600 nm were cooled to 25 °C, and target gene expression was initiated by addition of 0.01% (w/v) arabinose. Expression continued for 20 h at 25 °C. Cells were harvested by centrifugation for 15 min at 5250g."

3.3.2 Isolation of *E. coli* Membranes

"Cell pellets were resuspended in buffer A [20 mM Tris-HCl (pH 8.0) and 300 mM NaCl] and lysed using an Emulsiflex-C3 (Avestin Inc.) with a homogenizing valve pressure of 15000−20000 lb/in.^{2}. Large debris was removed from the lysate by centrifugation for 30 min at 5000g, and the resulting supernatant was centrifuged for 60 min at 180000g to sediment the membrane fraction."

3.3.3 Detergent Screening

"The fluorescence size exclusion chromatography (FSEC) method (Kawate and Gouaux 2006) was used to identify detergents capable of extracting protein from membrane and maintaining it in stable form. Briefly, 0.5 mL of a 0.1 g/mL suspension of membrane in buffer A was solubilized using 100 × CMC detergents with a variety of headgroups and acyl chain lengths. After being extracted at 4 °C for 2 h, the samples were clarified by centrifugation, and supernatants were analyzed by FSEC using a Superdex-200 (S-200, GE Healthcare) column pre-equilibrated in the same detergent solution at 1 × CMC detergent. Detergents producing qualitatively Gaussian peaks were considered for purification and further analysis. In addition to individual detergents, detergent mixtures were also used to determine the optimal conditions for solubilization and purification of the protein. All results were reproduced at least three times; chromatograms shown are representative examples."

3.3.4 Purification

"The isolated membranes were resuspended in buffer A at 0.1 g/mL, and protein was extracted with 100 × CMC *n*-dodecyl *β*-D-maltopyranoside (DDM) at 4 °C for 2 h. Extracts were clarified by centrifugation at 180000g, and His-tagged protein was incubated with 10% (v/v) TALON Co^{2+} affinity resin (BD Bioscience Inc.). The resin was packed into a column and washed with 4 column volumes of buffer B [buffer A with 1.5 mM Fos-Choline-12 (FC12)] or buffer C [buffer A with 0.75 mM FC12 and 0.01% (w/v) polyoxyethylene(8)-dodecyl ether ($C_{12}E_8$)] containing

10 mM imidazole, and then 4 column volumes of buffer B or C containing 25 mM imidazole. Protein was eluted from the resin with buffer B or C containing 300 mM imidazole. CAX^{CK31} was cleaved from GFP-His_{11} by incubation with 10% (w/w) TEV protease for 16 h at 4 °C, and cleavage products were separated by size-exclusion chromatography on a 10 mm × 300 mm S-200 column in buffer B or C."

3.3.5 Circular Dichroism Spectroscopy

"Purified CAX^{CK31} (lacking tags) at 1.0 mg/mL (22.6 μM) was used in buffer B. Spectra were collected with a Chirascan CD spectrometer (Applied Photophysics) at 20 °C from 250 to 190 nm using a quartz cuvette with a 0.1 mm optical path, a 0.5 nm step size, a 2 nm bandwidth, and a 2 s averaging time. Each spectrum was the average of five scans. The secondary structure was calculated with K2D3 (Perez-Iratxeta and Andrade-Navarro 2008) and compared with that predicted from sequence by PROFsec (Rost, Yachdav, and Liu 2004)."

3.3.6 Reconstitution and Ca^{2+} Transport Assay

"Proteoliposome preparation proceeded primarily by the protocols published by Gaillard *et al.* (Gaillard et al. 1996). Briefly, a 6:6:3:3:1 mixture of chloroform solutions of POPC, POPE, POPS, SM, and PI (1-palmitoyl-2-oleoyl-*sn*-glycero-3-phosphocholine, 1-palmitoyl-2-oleoyl-*sn*-glycero-3-phosphoethanolamine, 1-palmitoyl-2-oleoyl-*sn*-glycero-3-phospho-L-serine, sphingomyelin, and L-α-phosphatidylinositol, respectively) was dried by rotary evaporation for 16 h and

then resuspended in a 10 mM HEPES/Tris mixture (pH 7.0) and 140 mM choline chloride. The suspension was repeatedly (10 times) flash-frozen in liquid nitrogen and thawed and then extruded through a 0.2 μm filter 10 times. Purified CAX^{CK31} was added at a 1% (w/w) ratio of protein to lipid, and lipid vesicles were destabilized with 3:16 (w/w) FC12 to allow protein incorporation. FC12 was removed by three 2 h treatments with 80 mg/mL Bio-Beads (Bio-Rad, Hercules, CA) followed by centrifugation and resuspension in the appropriate internal buffer [10 mM HEPES/Tris mixture (varying pH), 140 mM choline chloride (or NaCl), and 100 μM Fura-2]. Proteoliposomes were again flash-frozen and thawed to allow penetration of internal buffer, extruded through a 0.2 μm filter 10 times, and harvested by centrifugation. Transport of Ca^{2+} was analyzed by addition of 100 μM $CaCl_2$ to a liposome suspension at 25 °C in a UVT acrylic cuvette (Evergreen Scientific), and the changes in the emission of Fura-2 at 510 nm upon excitation at 340 and 380 nm were continuously monitored using a FluoroMax-3 spectrofluorometer (HORIBA Jobin Yvon). The ratio of emission intensities at the two excitation wavelengths was computed and converted to Ca^{2+} concentration using a standard curve. The range between a baseline defined before addition of $CaCl_2$ and a systemic equilibrium obtained at the end of each assay by disrupting the liposomes with 0.003% (v/v) Triton X-100 represents the range from 0 to 100 μM Ca^{2+}. Liposomes prepared without CAX^{CK31} served as a negative control."

3.3.7 Glutaraldehyde Cross-Linking

"Glutaraldehyde cross-linking was conducted in buffer C with HEPES substituted for Tris, as glutaraldehyde reacts with Tris. Purified CAX^{CK31} at 1.0 mg/mL (22.6 μM) was incubated with 1.0−2.5 mM glutaraldehyde for 5 min at room temperature, and the reaction was terminated by the addition of 100 mM Tris-HCl (pH 8.0)."

3.3.8 Copper Phenanthroline Cross-Linking

"Purified CAX^{CK31}-F92C or CAX^{CK31}-F92C/R246C at 1.0 mg/mL (22.6 μM) or 0.1 g/mL suspensions of membranes [in 20 mM Tris (pH 8.0) and 300 mM NaCl] isolated from *E. coli* were incubated with 3 mM copper phenanthroline for 30 min at room temperature to catalyze disulfide bond formation between cysteines (Ren et al. 2008). After cross-linking in membranes, CAX^{CK31}-GFP was extracted with 1.5% (w/v) FC12 before sodium dodecyl sulfate−polyacrylamide gel electrophoresis (SDS−PAGE)."

3.3.9 Analysis of Cross-Linked Samples

"Cross-linked samples were analyzed by SDS−PAGE and MALDI-TOF mass spectrometry. Unpurified membrane samples analyzed by SDS−PAGE were visualized by Western blotting using a pentahistidine primary antibody and an AlexaFluor683-conjugated secondary antibody. Purified samples were visualized by Coommassie Blue staining. All blots were repeated several times to ensure reproducibility, and representative examples are shown."

3.3.10 FRET

"For FRET experiments, purified fusion proteins CAX^{CK31}-GFP and CAX^{CK31}-mCherry were mixed at various ratios and concentrations in buffer C. To correct for the background of CAX^{CK31}-GFP homodimers and CAX^{CK31}-mCherry homodimers, the methods described by Scheu *et al.* (Scheu et al. 2010) were employed. Briefly, mixtures of CAX^{CK31}-GFP and CAX^{CK31}-mCherry were prepared in various ratios, and fluorescence spectra corresponding to donor fluorescence (GFP; ex395/em509), acceptor fluorescence (mCherry; ex585/em610), and FRET (ex395/em610) were recorded for each mixture. Calculated FRET efficiencies (Scheu et al. 2010) should be inversely and linearly proportional to the donor fraction if true FRET occurs. Measurements were taken using 0.1 mg/mL (2.3 μM), 5.0 mg/ mL (113.1 μM), and 10.0 mg/mL (226.2 μM) CAX^{CK31} (total concentrations) to evaluate the concentration dependence of CAX^{CK31} dimerization."

3.3.11 SEC-MALS

"Multiangle laser light scattering (MALS) data were collected during elution of purified CAX^{CK31} from an S-200 SEC column in buffer C. The UV (280 nm) absorbance, static multiangle laser light scattering, and differential refractive index were monitored by an in-line spectrophotometer (Agilent Technologies), miniDAWN TREOS (Wyatt Technology Corp.), and Optilab T-rEX (Wyatt Technology Corp.), respectively, and data were collected using ASTRA. Weight-average molecular masses for the polypeptide and detergent components of

protein−detergent complexes were calculated by the previously described “three-detector method” (Hayashi, Matsui, and Takagi 1989; Folta-Stogniew and Williams 1999; Wen, Arakawa, and Philo 1996; Yernool et al. 2003) from data collected at the CAX^{CK31} elution peak. SEC−MALS was analyzed at multiple CAX^{CK31} concentrations ranging from 0.1 mg/mL (2.3 μM) to 10.0 mg/mL (226.2 μM) to demonstrate the concentration dependence of dimerization. Data presented are from single runs with CAX^{CK31}; error estimates arise from internal controls used in the three-detector method calculations (Hayashi, Matsui, and Takagi 1989; Folta-Stogniew and Williams 1999; Wen, Arakawa, and Philo 1996; Yernool et al. 2003).”

3.3.12 Hypothetical Model of Dimeric CAX^{CK31}

“A TM-COFFEE (J.-M. Chang et al. 2012) sequence alignment of CAX^{CK31} and NCX_Mj was supplied to MODELLER (Sali and Blundell 1993) along with the structure of NCX_Mj (PDB entry 3V5U (Liao et al. 2012)) to create a molecular model of the CAX^{CK31} monomer. The model was checked to ensure that it obeys the *cis*-positive rule (von Heijne and Gavel 1988). Two monomers were then manipulated assuming 2-fold molecular symmetry about an axis perpendicular to the plane of the membrane until a visually reasonable fit was achieved. The dimer model was then subjected to 1000 rounds of structure idealization using REFMAC5 (Vagin et al. 2004) in the CCP4 software suite (Winn et al. 2011).”

3.4 Results

3.4.1 Surfactants and Lipids Containing the Choline Head-group Stabilize Purified CAX^{CK31}-GFP-His_{11}

"Identification and optimization of expression of CAX^{CK31} were described previously (Narayanan, Ridilla, and Yernool 2011). Multiple detergents and mixtures were screened to identify candidates that would (i) effectively solubilize the protein of interest from membranes and (ii) stabilize the protein in solution in the absence of bulk lipids. Screening identified DDM as the most effective detergent for extracting the CAX^{CK31}-GFP-His^{11} fusion protein from membranes (data not shown). Although a Gaussian SEC profile was observed immediately after extraction with DDM, storage after extraction and purification resulted in aggregation of the fusion protein (Figure 3-1A). To stabilize the protein, various types of lipids (at 0.01 mg/mL) were added to DDM-containing buffers. The fusion protein was more stable in the presence of phosphatidylcholine (PC) than in other lipid/DDM mixtures (Figure 3-1B). To explore this observation, we used DDM-containing buffer supplemented with choline chloride salt. The SEC profile changed from an aggregated protein eluting at the void volume in DDM to a peak centered at 27 min when augmented with choline chloride, suggesting that the choline moiety plays some role in stabilizing the protein (Figure 3-1C). However, the SEC peak width at half-maximum was broader than in a DDM/PC mixture, suggesting the acyl chain may also play a role. Therefore, SEC analysis was conducted in buffers containing lipidlike detergents Fos-Choline-12 and LysoFos

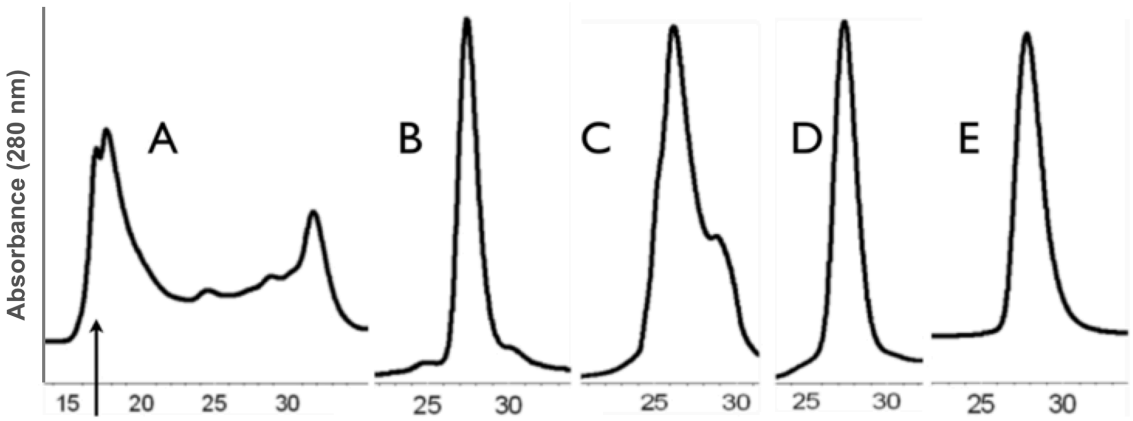

Figure 3-1. Effect of surfactants on stability of CAX^{CK31} in solution.
CAX^{CK31} was purified and analyzed by SEC in a selection of detergents or detergent/lipid mixtures (A, DDM; B, DDM + phosphatidylcholine; C, DDM + choline chloride; D, Fos-Choline-12; E, LysoFos Choline 12). The X-axes and Y-axes represent elution volume in mL and protein elution monitored by A_{280}, respectively. Peak heights have been normalized for clarity of presentation. CAX^{CK31} aggregates in DDM (A) as indicated by elution at void volume of the column indicated by an arrow at 17 mL. In contrast, the protein elutes in choline-containing detergents as a single, Gaussian peak revealing a stable preparation (D and E). Supplementing DDM with either the choline-containing lipid phosphatidylcholine (B) or the salt choline chloride (C) produces a qualitatively superior (i.e. lack of aggregation, fewer peaks, and decreased peak width at half-height) SEC profile compared to DDM alone.

Choline 12 (LysoFC12). Both detergents exhibited symmetric peaks in SEC analysis, suggesting the fusion protein was stable in these detergents (Figure 3-1D,E). Nevertheless, the ability of choline-containing detergents to extract the protein from membranes was poor. A combination of extraction with DDM (100 × CMC) and subsequent replacement with FC12 (1.5 × CMC) proved to be best for the extraction, purification, and stabilization of the fusion protein. Purified CAX^{CK31} lacking tags migrates as a single band at the expected monomer mass of 44.2 kDa via SDS−PAGE (Figure 3-2A, inset) and produces a single, Gaussian peak *via* SEC (Figure 3-2A), suggestive of a monodisperse preparation. Circular dichroism spectra (Figure 3-2B) revealed that purified CAX^{CK31} in FC12 contains secondary structure matching predictions from sequence analysis (74% α and 3% β)."

3.4.2 Purified CAX^{CK31} Retains Transport Function

"The functional integrity of purified CAX^{CK31} was established by reconstitution into liposomes and Ca^{2+} transport analysis. Proteoliposomes accumulated more Ca^{2+} than control liposomes lacking protein (Figure 3-2C). Ca^{2+}/H^{+} exchange in the absence of Na^{+} is demonstrated by the greater level of accumulation of Ca^{2+} in the lumen of liposomes with an outward-directed proton gradient than in liposomes having the same pH on both sides (*i.e.*, lower pH inside increased Ca^{2+} influx). Furthermore, an outward-directed Na^{+} gradient (under symmetrical pH conditions at pH 8.0) does not lead to an increased rate of Ca^{2+} transport over liposomes in the absence of Na^{+} under the same pH conditions,

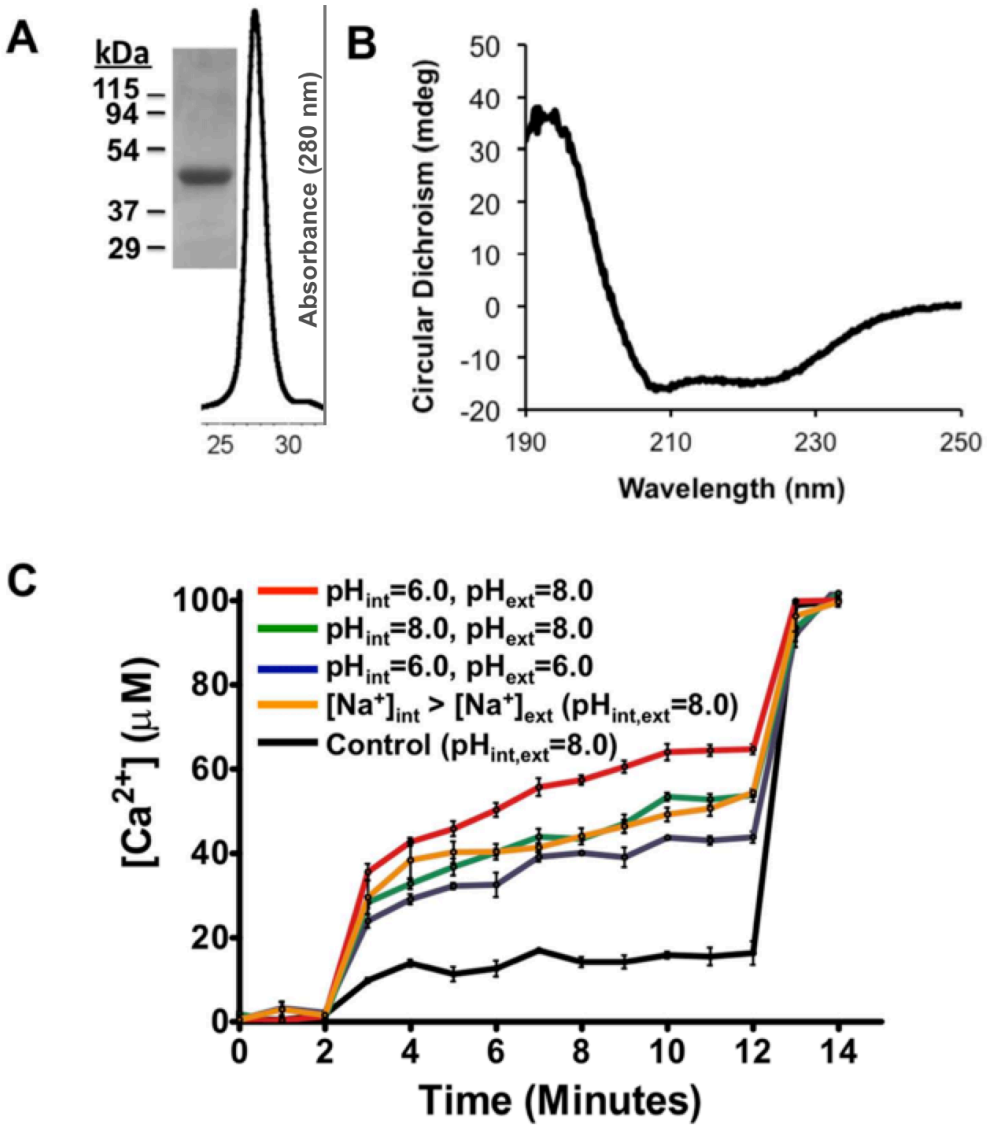

Figure 3-2. Characterization of purified CAX^{CK31}.
A: Purified CAX^{CK31} analyzed by SEC in FC12 containing buffer; inset: SDS-PAGE analysis. B: Circular Dichroism spectrum of purified CAX^{CK31}. C: Proton-driven, pH-dependent Ca^{2+} transport by reconstituted CAX^{CK31}. Transport of Ca^{2+} into liposomes loaded with Fura-2 by CAX^{CK31} (colored lines) was monitored via changes in Fura-2 fluorescence after addition of Ca^{2+} to bulk solution at 2 minutes. Systemic equilibrium was obtained at the end of each assay by disrupting the liposomes with Triton X-100 at 12 minutes. The pH inside and outside liposomes was as indicated by pH_{int} and pH_{ext}, respectively. The orange trace shows no stimulation of Ca^{2+} import by an outward-directed Na^+ gradient. Ca^{2+} entry into control liposomes lacking protein at pH 8.0 is shown in black. Data shown are means and SEM of three replicate experiments.

demonstrating that Na^+ has no effect on Ca^{2+} transport. These data suggest that CAX^{CK31} is not a Na^+/Ca^{2+} exchanger but a H^+-driven Ca^{2+} transporter. In the absence of a proton gradient (*i.e.*, the same pH on both sides of the membrane), alkaline pH stimulated Ca^{2+} transport, a behavior that is similar to the pH-dependent activation of cardiac NCX (Doering and Lederer 1993), indicating similarities in transport characteristics between the two proteins in addition to similarities in primary sequence. The SEC profile and transport activities remained the same as those of the fresh protein after storage for at least 1 week at 4 °C, indicating the preparation is stable in FC12 detergent. SEC analysis of CAX^{CK31} at protein concentrations of >5.0 mg/mL (113.1 μM) showed a small peak with a larger hydrodynamic radius suggestive of oligomerization (data not shown)."

3.4.3 CAX^{CK31} Is a Dimer in Membranes

"To analyze the oligomeric state of CAX^{CK31} in lipid bilayers, we mutated residues F92 and R246 to introduce cysteines into the previously cysteine-free protein; these positions were chosen on the basis of a previous study of oligomerization of cardiac NCX (Ren et al. 2008). *E. coli* membranes containing the CAX^{CK31}-F92C/R246C-GFP double mutant treated with copper phenanthroline were analyzed by Western blotting. The three distinct species observed match the pattern reported by Ren *et al.* (2008) and were likewise interpreted as an intermolecularly cross-linked dimer, a non-crosslinked-monomer, and an intramolecularly cross-linked monomer (Figure 3-3). Increased mobility of

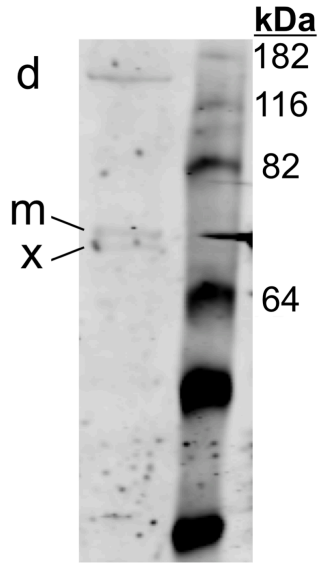

Figure 3-3. Cross-linking of CAX^{CK31} in membranes via introduced cysteine residues.
Western blots of copper-phenanthroline treated *E. coli* membranes expressing CAX^{CK31}-F92C/R246C-GFP (left lane). The abbreviations d, m, and x represent intermolecularly-crosslinked dimer, non-crosslinked monomer, and intramolecularly-crosslinked monomer, respectively. The right lane contains a mixture of proteins of known mobilitiy. Note: *E. coli* membrane sample concentrations were purposefully kept low to avoid overlap of the “m” and “x” bands, resulting in low signal-to-noise.

intramolecularly cross-linked species in nonreducing SDS−PAGE is generally attributed to either compaction of the molecule by the covalent bond between introduced cysteine side chains well-separated in primary sequence (Cumming et al. 2004) or incomplete unfolding in SDS also due to the bond (Santacruz-Toloza et al. 2000). This pattern of disulfide cross-linking is maintained in a detergent solution for the purified CAX^{CK31}-F92C/R246C double mutant lacking the GFP tags (Figure 3-4). The CAX^{CK31}-R246C single mutant could not be overexpressed at sufficient levels and therefore was not used in this analysis. Cross-linking of the F92C single mutant produced exclusively intermolecular cross-links (Figure 3-4). Disulfide-linked CAX^{CK31}-F92C was also analyzed by MALDI-TOF mass spectrometry, which revealed two major peaks at m/z values consistent with singly ionized dimeric and monomeric CAX^{CK31} (data not shown). These results show that CAX^{CK31} assembles into dimers in membranes, and the dimeric state can be stabilized in solution by cysteine cross-links."

3.4.4 The Conserved α-1 and α-2 Regions Are Close to the Dimer Interface

"Residues F92 and R246 of CAX^{CK31} are within the conserved α-1 and α-2 repeats, respectively (Figure 3-5). Equivalent residues map to the carboxyl-terminal ends of transmembrane helices 2 (TM2) and 6 (TM6) at the extracellular face of the monomeric structure of the archaeal NCX_Mj structure with the side chains pointing away from the protein core (Liao et al. 2012). Inter- and intramolecular cross-linking in the F92C/R246C double mutant of CAX^{CK31} suggests that α-repeats are close both to each other within the monomer and to

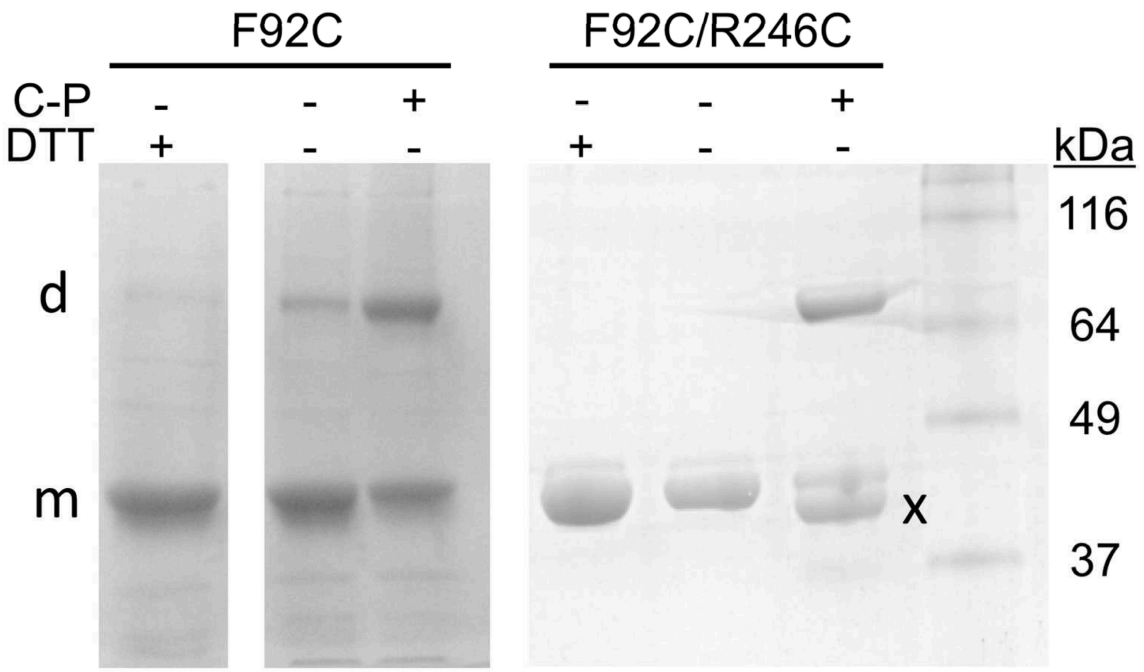

Figure 3-4. Cross-linking of CAX^{CK31} in solution via introduced cysteine residues. SDS-PAGE analysis of purified CAX^{CK31}-F92C and CAX^{CK31}-F92C/R246C treated with 3 mM copper-phenanthroline. The abbreviations d, m, and x represent intermolecularly-crosslinked dimer, non-crosslinked monomer, and intramolecularly-crosslinked monomer, respectively.

the dimer interface and is in agreement with the studies of cardiac NCX by Ren *et al.* (Ren et al. 2008). To further explore this putative dimer interface, we generated a hypothetical model of the NCX dimer (Figure 3-6A−C) and selected a series of residues near the symmetry axis and spanning the membrane for replacement with cysteines. Residues L81C, A85C, and Y89C map onto TM2C of the model, whereas K209C and V229C are on TM6. Each of five single mutants can be cross-linked with copper phenanthroline, whereas a cysteine introduced on the opposite side of the protein (L338C) does not form intermolecular cross-links (Figure 3-6D). The summation of disulfide cross-linking results strongly suggests that TM2 and TM6 form the dimer interface that extends from the extracellular side to the cytoplasmic surface."

3.4.5 Dimeric CAX^{CK31} Can Be Purified by Manipulating the Detergent Micelles

"Dimeric CAX^{CK31} in membranes is converted into a monomer during purification in FC12. We screened various reagents that alter the FC12 detergent micelles to produce CAX^{CK31} with its native quaternary structure preserved. A mixture of 0.75 mM FC12 and 0.01% (w/v) $C_{12}E_8$ detergent was identified that yielded a mixture of monomer and dimer upon glutaraldehyde cross-linking at moderate protein concentrations (1.0 mg/mL, 22.6 μM) (Figure 3-7A). This suggested that the protein may be in monomer−dimer equilibrium. However, glutaraldehyde treatment at higher protein concentrations was deemed inadvisible because of the possibility of nonspecific cross-linking. Therefore, further assessment of dimerization was conducted by SEC at 10.0 mg/mL (226.2 μM), which yielded a

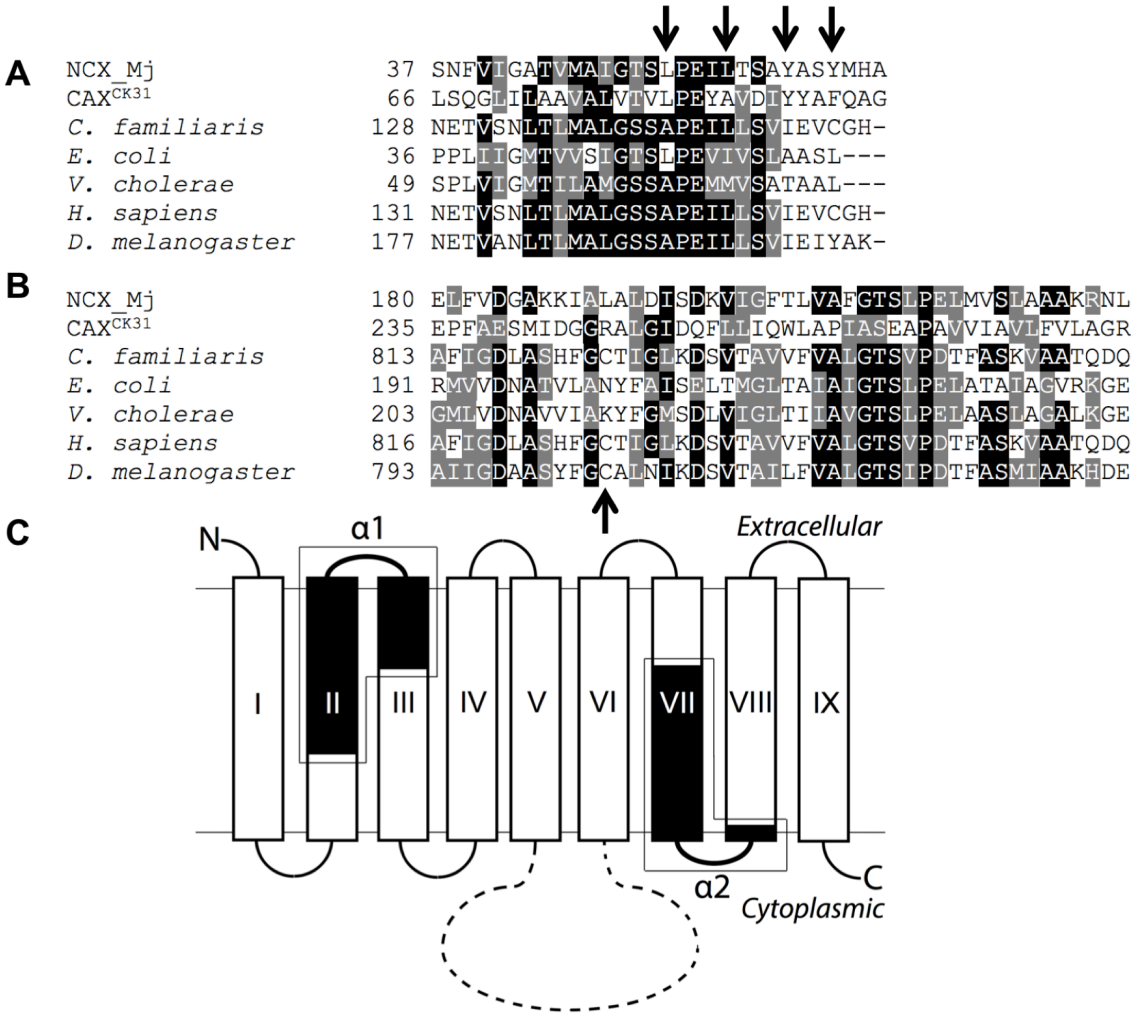

Figure 3-5. Prokaryotic CAX^{CK31} as a model for Eukaryotic NCX.
Multiple sequence alignments of the conserved α-1 (A) and α-2 (B) repeats of selected Ca^{2+}-cation exchangers. Residues conserved in 50 % of sequences are in black; similar residues are in gray. C, predicted topological model for Ca^{2+}-cation exchangers. Nine helices are labeled with roman numerals. Conserved α-1 and α-2 repeat sequences are shaded and boxed. The broken line indicates the cytoplasmic domain of eukaryotic exchangers involved in regulation, but not in transport *per se* (Hilgemann 1990; Matsuoka et al. 1995).

single peak with a species with a larger hydrodynamic radius (Figure 3-7B). The larger species could be due to protein oligomerization or formation of mixed micelles of unknown mass. To resolve this ambiguity, we conducted FRET analysis. For FRET experiments, we employed purified CAX^{CK31}-GFP and CAX^{CK31}- mCherry as the donor and acceptor, respectively (Förster radius of 51 Å), and used the methods outlined by Scheu *et al.* (Scheu et al. 2010) to detect protein homodimers: homooligomerization is validated when the FRET efficiency increases linearly with an increase in the acceptor:donor ratio. As we had previously failed to detect any effect of the presence of a GFP tag on the behavior of NCX in SEC or calcium transport assays, we did not expect the presence of the tag to affect oligomerization in a detergent solution. At the lowest concentration tested (0.1 mg/mL, 2.3 μM), the FRET efficiency increased with an increase in acceptor fraction (Figure 3-8A), indicating formation of oligomers. The FRET efficiencies were significantly greater at higher protein concentrations [5.0 mg/mL (113.1 μM) and 10.0 mg/mL (226.2 μM)], indicating that oligomerization in detergent solutions is concentration-dependent.

To characterize the dimerization of CAX^{CK31} in the absence of GFP or mCherry tags, we employed SEC−MALS. The three-detector method (Hayashi, Matsui, and Takagi 1989; Folta-Stogniew and Williams 1999; Wen, Arakawa, and Philo 1996; Yernool et al. 2003) allows estimation of the molecular mass of the polypeptide and detergent components of protein−detergent complexes (PDCs) from SEC−MALS data. We applied this method to analyze CAX^{CK31} at multiple

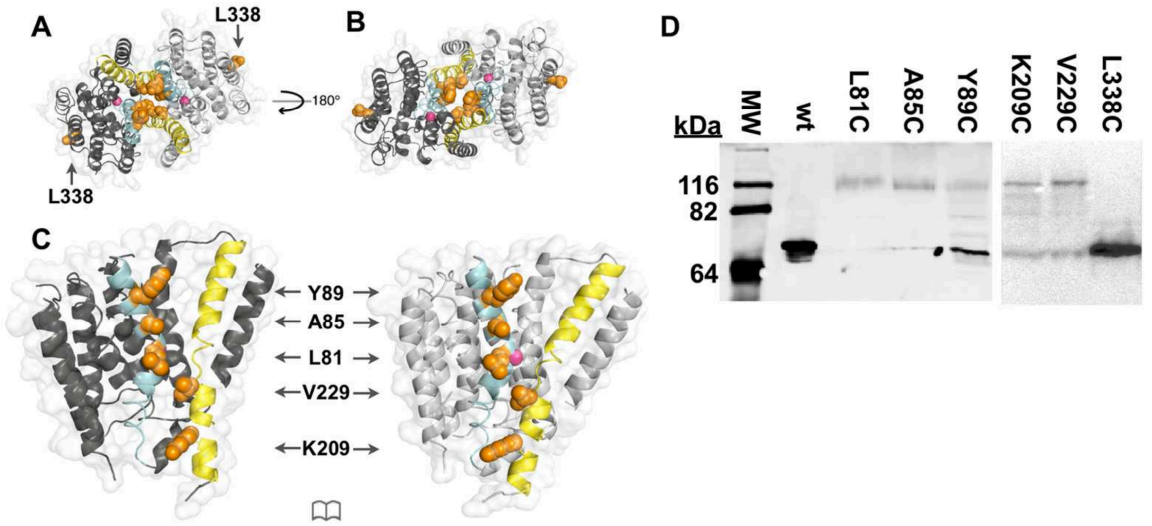

Figure 3-6. CAX^{CK31} Dimer Interface.
A. Hypothetical model of CAX^{CK31} dimer viewed from the extracellular side. A homology model of CAX^{CK31} was generated using the structure of *M. jannaschii* NCX (PDB: 3V5U), and two monomers were positioned with the proposed dimer interface made of TM2 (blue) and TM6 (yellow). Locations of Ca^{2+} are shown in magenta, and positions of Cys mutations are highlighted in orange. The L338C mutation was not expected to form intermolecular cross-links due to its distance from the proposed interface. B. View from cytoplasm. C. Open book representation of dimer model. D. Cross-linking of single cysteine mutants of CAX^{CK31} in *E. coli* membranes. Isolated membranes from *E. coli* expressing CAX^{CK31}-GFP, CAX^{CK31}-L81C-GFP, CAX^{CK31}-A85C-GFP, CAX^{CK31}-Y89C-GFP, CAX^{CK31}-K209C-GFP, CAX^{CK31}-V229C-GFP, or CAX^{CK31}-L338C-GFP were treated with copper-phenanthroline to promote disulfide bond formation. The Western Blot of treated membranes reveals the characteristic intermolecular cross-links seen with purified CAX^{CK31}.

concentrations (Figure 3-8B). As the CAX^{CK31} concentration was increased from 0.1 mg/mL (2.3 μM) to 10 mg/mL (226.2 μM), the weight-average molecular mass of the eluting species increased from 44.2 kDa (monomer) to 88.4 kDa (dimer) (Table 3-2). This is also evident from the shift in the time of elution from 29 to 26.5 min. Although neither FRET nor SEC−MALS can identify the exact fraction of CAX^{CK31} present in monomeric and dimeric forms, the weight-average molecular masses determined by SEC−MALS at the lowest and highest measurable CAX^{CK31} concentrations were approximately those expected for a CAX^{CK31} monomer and dimer, respectively, suggesting that the sample was almost completely monomeric or completely dimeric at those concentrations. The detergent:protein mass ratio in the CAX^{CK31}−FC12−$C_{12}E_8$ PDC was roughly 1:1, an expected value for integral membrane proteins, and slightly decreased in the dimer (0.84:1)."

3.5 Discussion

"Many membrane proteins exist as homooligomeric and heterooligomeric complexes (Dalbey, Wang, and Kuhn 2011). Defining their oligomerization state and maintaining that oligomeric state postpurification are nontrivial tasks, as illustrated by our studies of CAX^{CK31}. Extraction and post-extraction stabilization of CAX^{CK31} required the use of DDM and FC12/LysoFC12, nonionic and zwitterionic surfactants, respectively. Although the use of a combination of detergents is not unusual, our additional studies are revealing. The extraction of CAX^{CK31} with DDM creates a unique constraint, a requirement for a choline-like

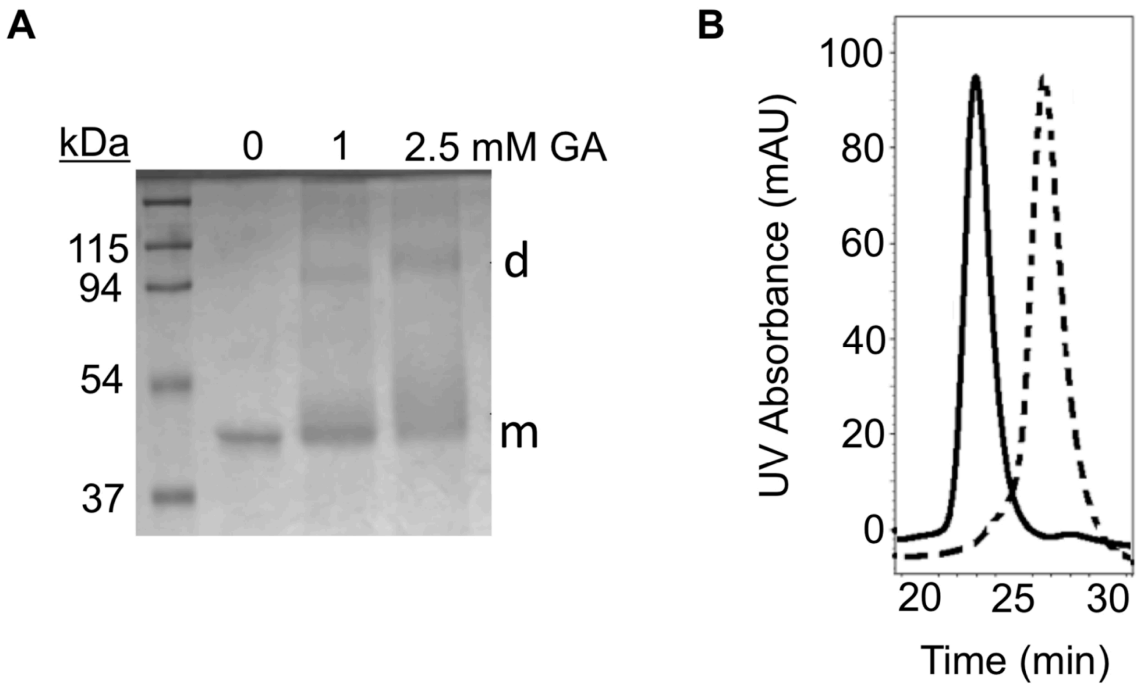

Figure 3-7. Dimerization of CAX^{CK31} purified in FC12/$C_{12}E_8$ mixture.
A: SDS-PAGE analysis of CAX^{CK31} cross-linked (at 1 mg/mL) with 1.0 or 2.5 mM glutaraldehyde. Monomeric and dimeric species are indicated by "m" and "d", respectively. B: SEC elution chromatographs of 10 mg/mL CAX^{CK31} purified in FC12 (broken line) and FC12 + $C_{12}E_8$ (solid line). Earlier elution of the $C_{12}E_8$-containing protein-detergent complex was attributed to dimerization.

moiety to maintain protein stability (Figure 3-1). Among the various lipids screened as supplements to DDM, only phosphatidylcholine was able to prevent protein aggregation. Although phosphatidylcholines are common lipids in eukaryotic cells, they are rarely present in bacteria and have not been reported in *E. coli*, our protein expression host (Sohlenkamp, López-Lara, and Geiger 2003).

FC12 and the related lysolecithin-like detergent LysoFC12 are lipidlike detergents with single 12-carbon acyl chains connected to phosphocholine headgroups. They were developed to address the loss of stabilizing effects of lipids on membrane protein structure caused by solubilization in classical detergents (Weltzien, Richter, and Ferber 1979; Garavito, Picot, and Loll 1996). Both of these detergents proved to be good replacements for mixed micelles of phosphatidylcholine and DDM during purification, resulting in significantly improved CAX^{CK31} stability, yielding monodisperse preparations. Furthermore, we demonstrate the importance of the surfactant headgroup in protein stability by using DDM supplemented with choline chloride salt (Figure 3-1). The requirement for the choline moiety holds only under conditions of detergent solubilization, as the protein was active in inverted vesicles made from *E. coli* membranes expressing CAX^{CK31} (Narayanan, Ridilla, and Yernool 2011). These data suggest that DDM extraction changes the protein, creating a putative binding site for a choline-like molecule. The generality of requirements for specific moieties after detergent extraction remains unknown. However, the Fos-Cholines were notably the most successful detergents in stabilizing a variety of

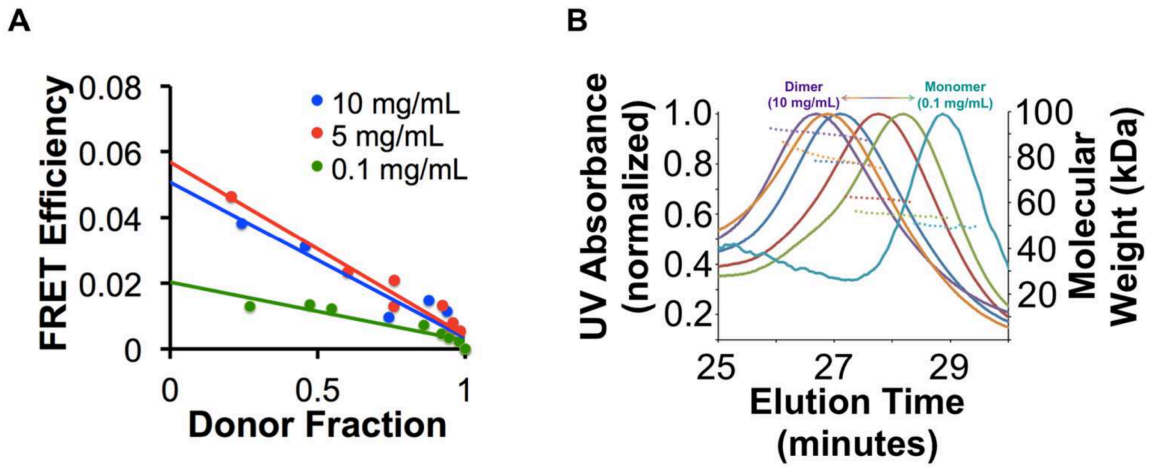

Figure 3-8. Dependence of oligomer formation on protein concentration.
A. FRET analysis of CAX^{CK31} oligomer formation in solution. FRET efficiencies for mixtures of CAX^{CK31}-GFP and CAX^{CK31}-mCherry were determined at various donor:acceptor ratios and different total CAX^{CK31} concentrations. FRET due to dimerization is confirmed by the linear relationship between FRET efficiency and donor fraction. Concentration-dependence of CAX^{CK31} dimerization is demonstrated by increased efficiencies at greater CAX^{CK31} concentrations. B. Analysis of concentration-dependence of CAX^{CK31} oligomerization by SEC-MALS. CAX^{CK31} was analyzed at 10.0 (purple), 8.0 (orange), 5.0 (blue), 2.0 (red), 1.0 (green) and 0.1 (teal) mg/mL. The change in elution time demonstrates a change in the weight-average MW of the concentration-dependent CAX^{CK31} monomer-dimer equilibrium mixture. Solid lines represent normalized UV absorbance (280 nm) of eluting CAX^{CK31}; broken lines represent weight-average molecular weights (right axis) calculated at each time point during CAX^{CK31} elution using a combination of UV absorbance, laser light scattering, and differential refractive index measurements.

membrane proteins in large-scale expression studies (Carpenter et al. 2008; Hammon et al. 2009; Lewinson, Lee, and Rees 2008).

Stabilization of CAX^{CK31} by FC12 comes at a price: it yields a monomer, a non-native state with respect to its quaternary structure in the membrane. A search for conditions that produce CAX^{CK31} dimers resulted in the identification of a mixture of FC12 and $C_{12}E_8$. The latter is a nonionic detergent with a large polyoxyethylene headgroup. The dependence on this specific detergent mixture and protein concentration to retain the dimeric state was demonstrated by FRET using CAX^{CK31}-GFP and CAX^{CK31}-mCherry. SEC−MALS confirmed that concentration-dependent dimer formation was mediated by the transporter by using protein lacking fusion tags and by a change in the detergent:protein mass ratio from 1.05 to 0.84 (Table 4.2) as the transporter concentration increased from 0.1 to 10 mg/mL, where they exist as monomer and dimer, respectively. The decrease in the detergent:protein ratio is expected when transporter molecules interact laterally *via* their transmembrane segments to displace detergent molecules. Broadly, the potential benefit of manipulation of detergent micelles to preserve the native oligomerization state of proteins is demonstrated by our studies.

CAX^{CK31} is the first bacterial member of the CaCA superfamily to be purified as monomers and dimers in solution. Recently, two archaeal homologues of the YRBG family were purified (Liao et al. 2012; Mercado Besserer et al. 2012). One

of these proteins had more than one aggregation state in solution; however, the aggregation states were not experimentally determined (Liao et al. 2012). Previously, it was established that mammalian NCX and NCKX are dimers in membranes (Ren et al. 2008; John et al. 2011; Schwarzer et al. 1997). Both mammalian and archaeal NCX use Na^+ gradients to drive Ca^{2+} transport, whereas we show CAX^{CK31} to be a H^+/Ca^{2+} transporter. As for CAX^{CK31}, weakened function at acidic pH is also seen for cardiac NCX (Boyman et al. 2011), although the mechanism of proton sensing must be different as CAX^{CK31} does not possess the eukaryotic counterpart's cytoplasmic Ca^{2+}-binding domains. The altered specificity for the monovalent cation is consistent with the idea that the H^+ gradient is the major energy source for coupled transport in bacteria (Harold and Maloney 1996). Despite the differences in substrate specificity, the central function of divalent/monovalent antiport activity is conserved in the CaCA superfamily.

The dimeric quaternary structure of CAX^{CK31} in membranes was established by cross-linking cysteines introduced at positions F92 and R246 of CAX^{CK31}, recapitulating studies of corresponding residues of cardiac NCX (Ren et al. 2008). Despite the low overall level of sequence identity, this implied that (i) the relative positions of residues in the α-1 and α-2 regions of dog NCX and CAX^{CK31} are similar and (ii) these residues are close to the dimer interface. This analysis was extended by exploiting the recently determined archaeal NCX structure (Liao et al. 2012). By modeling, we identified five additional residues on TM2 and TM6

Table 3-2. Molecular weights calculated from SEC-MALS data for the protein CAX^{CK31} and the CAX^{CK31}/FC12/$C_{12}E_8$ protein-detergent complex (PDC).

CAX^{CK31} Conc. (mg/mL)	CAX^{CK31} MW (kDa)	PDC MW (kDa)	Detergent:Protein Mass Ratio
0.1	49.8 ± 4.0	102.3 ± 8.2	1.05
1.0	54.6 ± 4.4	107.9 ± 8.6	0.98
2.0	61.6 ± 4.9	120.0 ± 9.6	0.95
5.0	77.5 ± 6.2	144.9 ± 11.6	0.87
8.0	79.7 ± 6.4	154.4 ± 12.3	0.94
10.0	90.1 ± 7.2	166.0 ± 13.3	0.84

near the symmetry axis of a putative dimer. The intermolecular disulfide cross-linking of introduced cysteines establishes the proximity of TM2 and TM6 to the intermolecular interface and suggests direct participation in dimer formation.

The determination of the crystal structure of the archaeal NCX was both a major feat and an advance in understanding the mechanism of transport (Liao et al. 2012). Our identification of TM2 and TM6 as the dimer interface has impact on our understanding of the structure and function of these transporters. Three CAX^{CK31} residues that cross-link when mutated to cysteines, L81, A85, and Y89, map to TM2C of NCX_Mj where the equivalent residues are L52, L56, and Y60, respectively (Figure 3-5 and 3-9). These NCX_Mj residues, components of the conserved α-1 repeat, are neighbors of E54 that plays a central role in ion binding and transport. E54, which is situated on the opposite side of L52 and L56 within the same helical turn, coordinates the transported Ca^{2+} ion with two oxygens (Liao et al. 2012). This places the Ca^{2+} binding site close to the protein−lipid acyl chain interface, a remarkable condition considering the more centrally located, protein-enclosed ion binding sites of other secondary transporters. Furthermore, the path from the extracellular side to the Ca^{2+} binding site was proposed to be delimited by TM2C, TM6, TM7, and bulk lipids, which would expose the acyl chains to water and ions, an unfavorable condition (Figure 3-9). These concerns can be resolved by considering our data of dimer formation with TM2 and TM6 at the interface. Such a dimer would have Ca^{2+} ions in each protomer and the ion permeation pathway leading to these ion

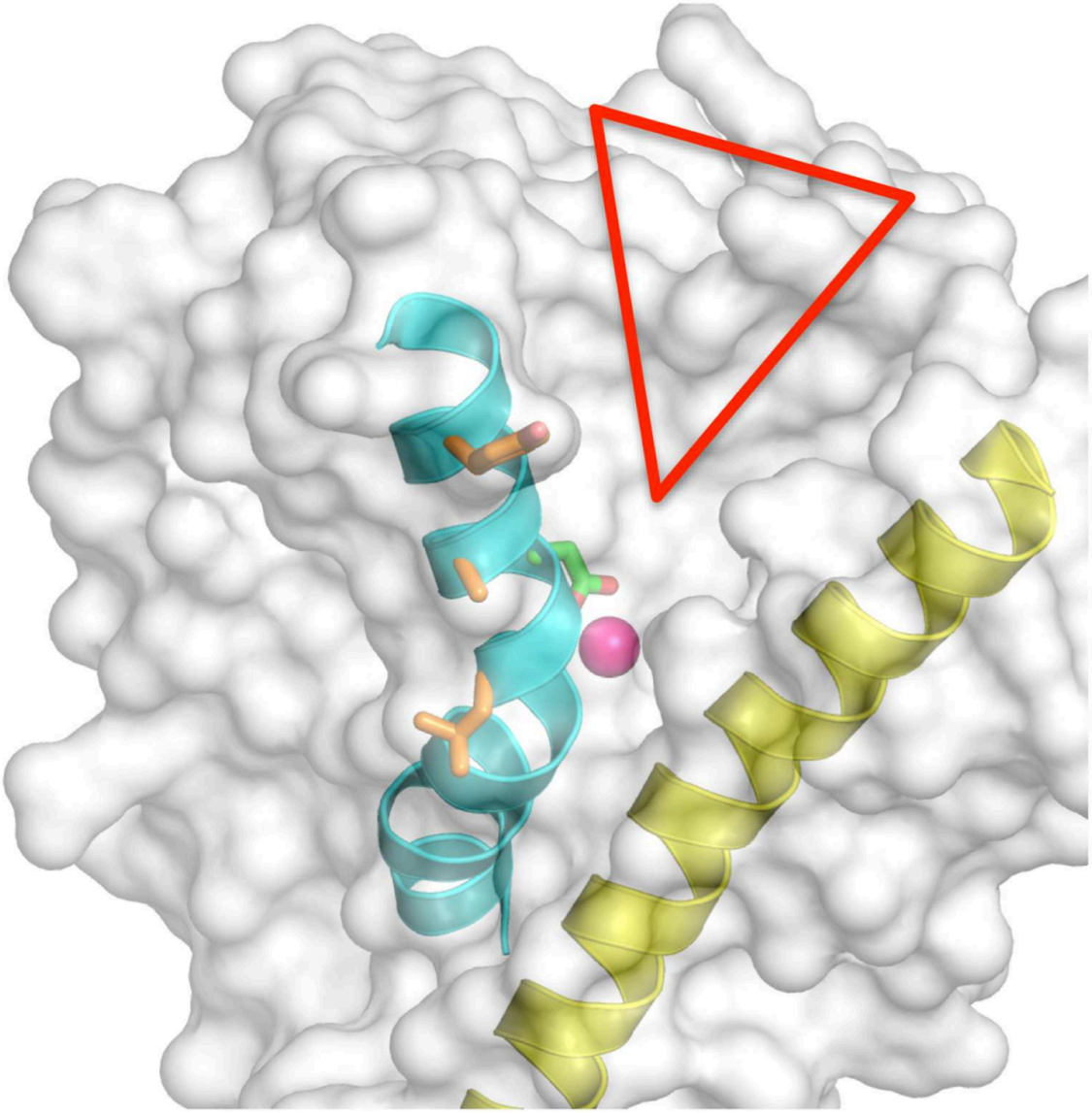

Figure 3-9. Relationship between putative dimer interface, Ca^{2+} binding site, and Ca^{2+} permeation pathway.
The structure of NCX_Mj (PDB: 3V5U) is shown in surface representation with TM2 and TM6 colored cyan and yellow, respectively. Ca^{2+} is in magenta and the Ca^{2+} coordinating residue E54 is shown in green. The interfacial residues L81, A85, and Y89 of CAX^{CK31} we identified are mapped onto equivalent positions in the NCX_Mj structure and are colored orange. The proposed Ca^{2+} entry passageway is indicated with a red triangle.

binding sites surrounded by a protein core instead of bulk lipids. This implies that a common ion permeation pathway starts at the dimer interface on the extracellular side and bifurcates to reach the Ca^{2+} binding sites. Confirmation of this model awaits determination of a crystal structure of CAX^{CK31} in dimeric form. Purification of monomeric and dimeric versions of the bacterial Ca^{2+}/H^{+} antiporter emphasizes the role of detergent micelle manipulation in isolating membrane proteins in their native quaternary structures. The growing body of evidence of CaCA dimerization suggests that quaternary structure is indeed conserved in the superfamily despite the low overall level of sequence similarity. Our analysis also shows that Ca^{2+}/H^{+} antiporters use the conserved α-repeats to support transport and oligomerization."

CHAPTER 4. CHARACTERIZATION OF TRANSPORT PROPERTIES OF CAX^{CK31}

4.1 Introduction

This Chapter explains efforts to describe the transport properties of CAX^{CK31} using inverted membrane vesicles or proteoliposomes. Monovalent and divalent cations transported by CAX^{CK31} are identified, pH sensitivity of transport activity is described, and K_M's for the transport of Ca^{2+} and Zn^{2+} are identified. Furthermore a generalized method is presented for quantification of very small amounts of protein applicable to measure reconstitution efficiency of proteoliposome preparations.

4.2 Divalent Cation Binding Analysis of CaCAs by Intrinsic Tryptophan Fluorescence.

N21 contains twelve tryptophan residues, four of which are near the highly-conserved and functionally-significant α-repeat regions (Figure 3-5C); CAX^{CK31} contains thirteen tryptophan residues, also four of which are near the α-repeat regions. Tryptophan residues are evenly distributed throughout the length of each polypeptide, falling in both transmembrane and extramembrane (predicted) regions. We were able to detect increases in tryptophan fluorescence (indicating a shift of tryptophan residues to more hydrophobic environment) upon titration

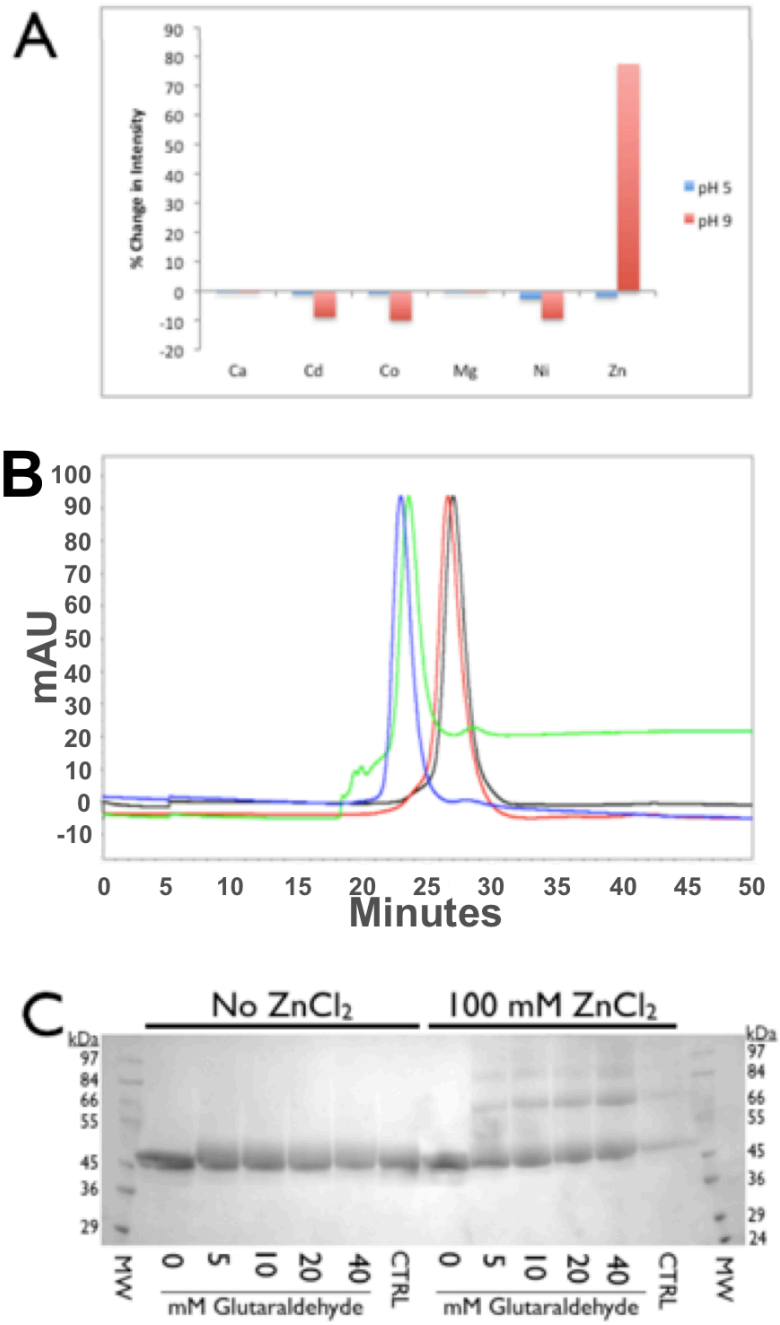

Figure 4-1. Effects of various cations on CAX^{CK31} structure.
A. Change in CAX^{CK31} tryptophan fluorescence intensity resulting from addition of 30 mM various salts at pH 5 and pH 9. B. Shift in elution time of CAX^{CK31} from Superdex-200 SEC column in the presence of $ZnCl_2$. Black: 0 mM $ZnCl_2$, Red: 10 mM $ZnCl_2$, Green: 50 mM $ZnCl_2$, Blue: 100 mM $ZnCl_2$. C. SDS-PAGE of CAX^{CK31} cross-linked with glutaraldehyde in the absence (left) and presence (right) of 100 mM $ZnCl_2$. CTRL samples denatured in 1 % SDS before reaction with 40 mM glutaraldehyde.

with zinc chloride, but no other divalent cation, and only in the presence of HEPES buffer beginning at neutral or basic pH (Figure 4-1A). (We have also shown Zn^{2+} caused a peak shift during SEC (Figure 4-1B) and an increase in glutaraldehyde cross-linking efficiency (Figure 4-1C), indicating the possibility of oligomer assembly in addition to simple structural rearrangement.) A K_d for Zn^{2+} as low as 11 mM has been identified (Figure 4-2). It is hypothesized that binding of calcium or other Group 2 elements is very weak due to the need of CaCAs to transport calcium ions efficiently and that either the greater electronegativity or lesser atomic radius of Zn^{2+} forces N21 to remain in its divalent-bound state, however cadmium does not promote oligomerization.

Neither the SEC profile nor tryptophan fluorescence intensity of N21 was affected by pH, so the observed changes must have been due to interactions between N21 and Zn^{2+}. Nevertheless the diminished response at neutral to low pH suggested some unobserved pH effect, such as a stabilization of the Na^{+}-bound state of N21 (Figure 4-1). Confusion arose due to the high acidity of $ZnCl_2$ solution and Zn^{2+}'s insolubility at basic pH. Titration of acidic $ZnCl_2$ solution into high-pH buffers lowers the solution pH (enabling solubility of Zn^{2+}), whereas low-pH buffers maintain steady pH throughout titration. For calcium/proton antiporters Ca^{2+} transport is likely driven by a pH gradient.

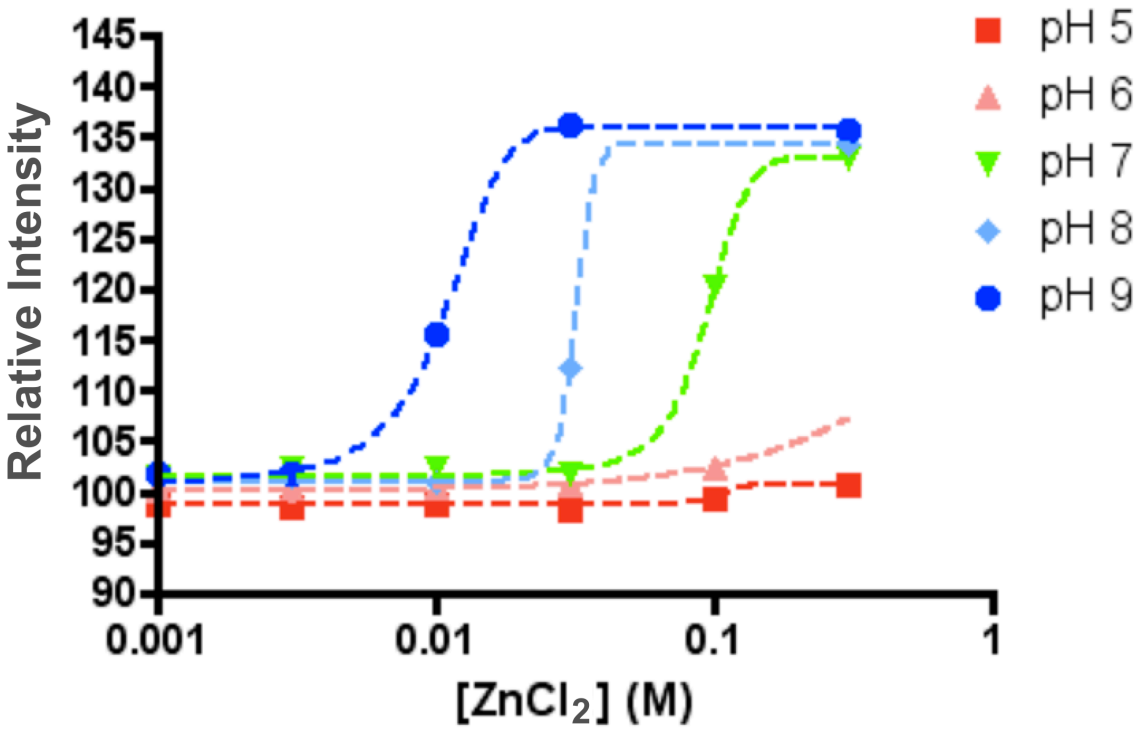

Figure 4-2. CAX^{CK31} intrinsic tryptophan fluorescence (emission intensity at 340 nm, excited at 295 nm) response to titration with $ZnCl_2$ beginning at various pHs. Data were normalized to indicate percentage changes to initial intensity and then fit to the model Y=BOTTOM + (TOP-BOTTOM)/(1+10^((KD-X)*HillSlope)) using GraphPad Prism software.

4.3 Divalent Cation Binding Analysis of CAX^{CK31} by CD

Changes in CAX^{CK31} secondary structure arising from changes to external pH or the presence of Ca^{2+} or Zn^{2+} were analyzed by circular dichroism spectroscopy as described in 3.3.5. Secondary structure was determined from CD spectra using K2D3 software (Perez-Iratxeta and Andrade-Navarro 2008). Divalent cations were present at 0, 0.01, 0.1, and 1.0 mM, each at pH 4.5, 6.0, and 6.8. CAX^{CK31} remained roughly 68 % helical under all conditions tested (Figure 4-3).

4.4 CAX^{CK31} Transport Activity

To test the ion transporting activity of CAX^{CK31} , it must be embedded in a membrane vesicle system separating two distinct environments at least one of whose contents can be monitored. Two types of vesicle systems were utilized: inverted membrane vesicles (IMVs) prepared from expression cells, in which every CAX^{CK31} molecule was expected to be in the same orientation and other *E. coli* proteins were present; and liposomes, containing exclusively CAX^{CK31} for experiments where purity was important or protein orientation was not.

4.4.1 Inverted Membrane Vesicles

The more robust IMV system enabled rapid screening of several divalent substrates and inhibitors as well as CAX^{CK31} point mutants. Inverted vesicles derived from *E. coli* expressing CAX^{CK31} were prepared with an outward proton gradient through exposure of inherent LADH to lactate, and acridine orange quenching inside the vesicles reported the resulting pH decrease.

Cells expressing CAX^{CK31}-GFP fusions were collected and resuspended in 10 mM Tris, pH 7.2, 140 mM choline chloride; 10% (v/v) glycerol, 6 mM β-meracaptoethanol (TCGB). Cells broken by Emulsiflex homogenization at 4000 psi were centrifuged at 15,000 × g and 4 ºC for 20 min to separate unbroken cells and debris. IMVs were collected by ultracentrifugation at 100,000 × g and 4 ºC for 1 h, resuspended in TCGB at 20 absorbance units at 280 nm/mL, and stored frozen in liquid nitrogen. For the assay, 200 µg vesicles were resuspended in 2.5 mL TCGB containing 1 µM Acridine Orange (AO) in a quartz cuvette containing a magnetic stirrer. IMVs were prepared with an outward proton gradient through exposure of existing LADH to lactate; AO quenching inside the vesicles reported the resulting pH decrease as protonated AO aggregated. Changes in AO fluorescence were monitored using excitation and emission wavelengths of 495 nm and 530 nm, respectively. Fluorescence dequenching of protonated AO in energized IMVs was monitored after addition of 100 µM free Ca^{2+} to promote Ca^{2+}/H^{+} exchange. Exposure of CAX^{CK31} to transportable divalent cations induced proton export and AO dequenching. Na^{+}/H^{+} exchange by NhaA served as a positive control.

Zn^{2+}, Ca^{2+} and Mg^{2+} transport was more than twice as efficient as transport of any other divalent cation tested, including Cd^{2+}, Co^{2+}, Ni^{2+}, Sr^{2+}, and Zn^{2+} (Figure 4-4A).

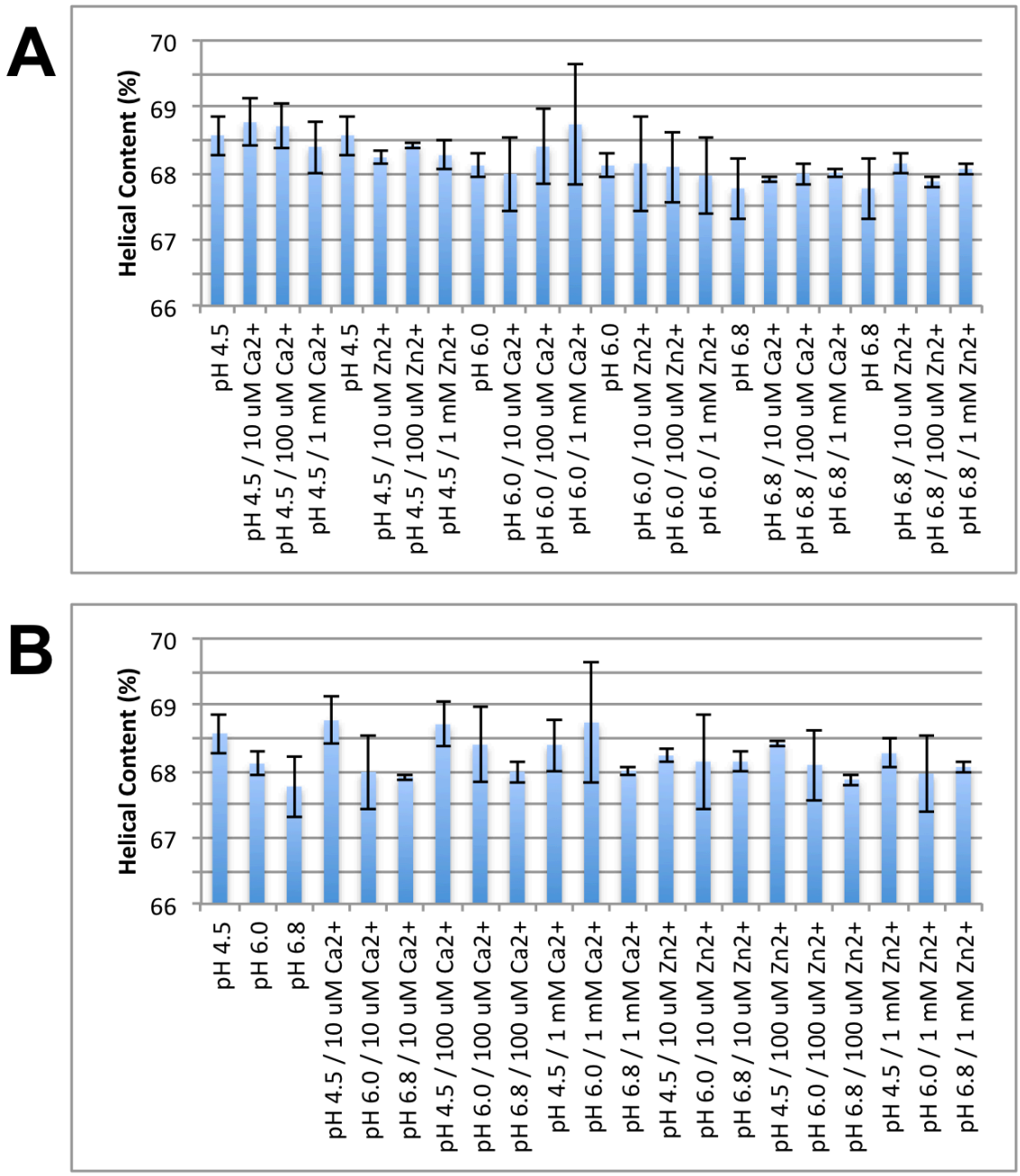

Figure 4-3. CAX^{CK31} secondary structure was stable across a range of pH and divalent cation conditions.

CAX^{CK31} activity after selective mutation of highly-conserved residues E83 and G112 was measured using IMVs. No E83 mutants were capable of efficient Ca^{2+}-induced H^+ transport, however mutations to G112 had no effect on activity (Figure 4-4B). Addition of 10 μM $LaCl_3$ blocked proton transport from inverted vesicles to lower-than-control levels (Figure 4-4C).

4.4.2 Liposomes

Preservation of protein function through purification was confirmed by liposome reconstitution of purified protein and a Ca^{2+}-transport assay reporting Ca^{2+} transport into liposomes through association with the Ca^{2+}-sensitive dye Fura-2. This assay was been used to demonstrate that transport of Ca^{2+} by CAX^{CK31} was proton-driven, and that higher pH stimulated Ca^{2+}/H^+ exchange (Figure 3-2C).

Transport of Ca^{2+} by reconstituted CAX^{CK31} was enhanced at higher pH and with opposing Na^+ gradients; and CAX^{CK31} was capable of transporting Ca^{2+} even in the absence of Na^+. In the absence of Na^+, Ca^{2+} transport remained sensitive to pH, with increased activity at higher pH. Additionally, Ca^{2+} transport was

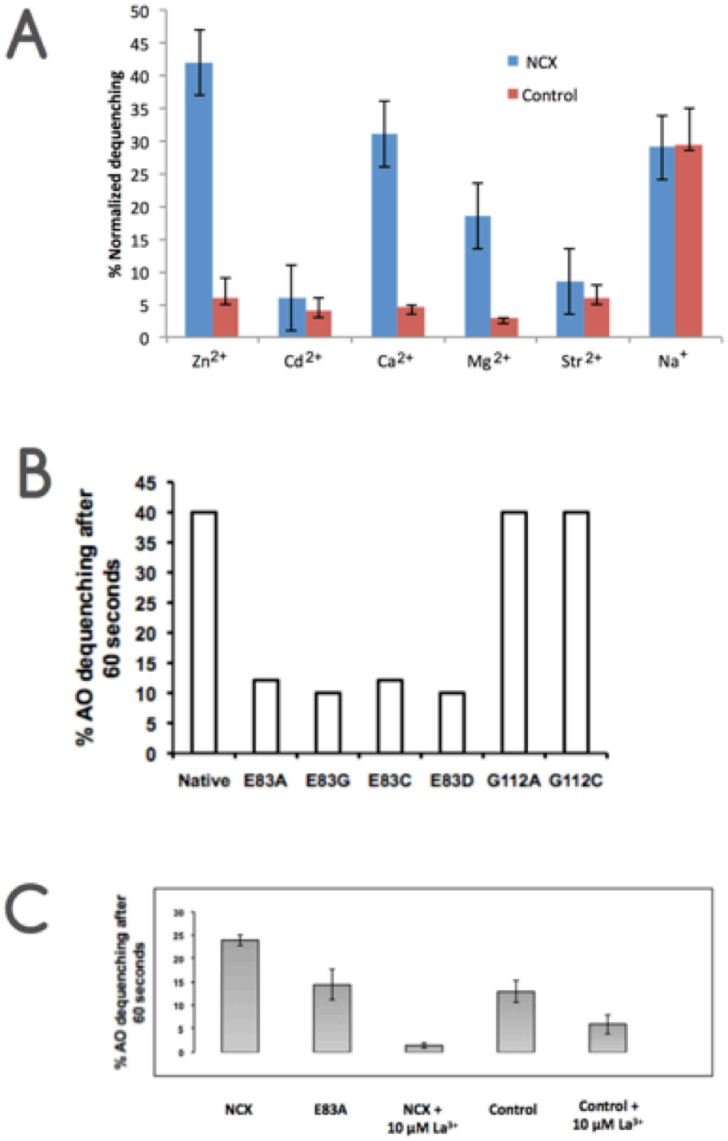

Figure 4-4. Exposure of CAX^{CK31} to transportable divalent cations induced proton export and Acridine Orange dequenching.
A. Potential divalent substrates were thus screened; sodium/proton exchange by NhaA served as a positive control. B. CAX^{CK31} activity after selective mutation of highly-conserved residues E83 and G112 was measured using *E. coli* inverted vesicles. No E83 mutants were capable of efficient Ca^{2+}-induced H^+ transport, however mutations to G112 did not have any effect on activity. C. Addition of 10 µM $LaCl_3$ blocked all proton transport from inverted vesicles to lower-than-control levels.

enhanced in the presence of opposing proton gradients, suggesting that protons may serve as the monovalent substrate under Na^+-limiting conditions.

A 6:6:3:3:1 mixture of POPC/POPE/POPS/SM/PI (1-palmitoyl-2-oleoyl-*sn*-glycero-3-phosphocholine, 1-palmitoyl-2-oleoyl-*sn*-glycero-3-phosphoethanolamine, 1-palmitoyl-2-oleoyl-*sn*-glycero-3-phospho-L-serine, sphingomyelin, and L-α-phosphatidylinositol) was prepared based on the composition of human neutrophil plasma membrane (S.-Y. Lee, Letts, and MacKinnon 2009). The mixture was dried by rotary-evaporation for 16 hours, then resuspended in 20 mM Tris, pH 8.0, 300 mM NaCl containing 100 μM Fura-2. The suspension was flash-frozen in liquid nitrogen and thawed ten times, then extruded through a 0.2 μm filter ten times. Purified CAX^{CK31} was added at a 1 % (w/w) ratio of protein to lipid, and lipid vesicles were destabilized with 3:16 (w/w) FC12 to allow protein incorporation. FC12 was removed by three two-hour treatments with 80 mg/mL Bio-Beads, then proteoliposomes were again extruded through a 0.2 μm filter ten times. Proteoliposomes were centrifuged and resuspended in 20 mM Tris, pH 8.0, 300 mM NaCl. Transport of Ca^{2+} was analyzed by addition of 300 μM $CaCl_2$ to a liposome suspension at 25 °C, and the changes in emission of Fura-2 at 510 nm upon excitation at 340 nm and 380 nm were continuously monitored. The ratio of emission intensities at the two excitation wavelengths was computed and normalized to the range between a baseline defined before addition of $CaCl_2$ and a systematic equilibrium obtained

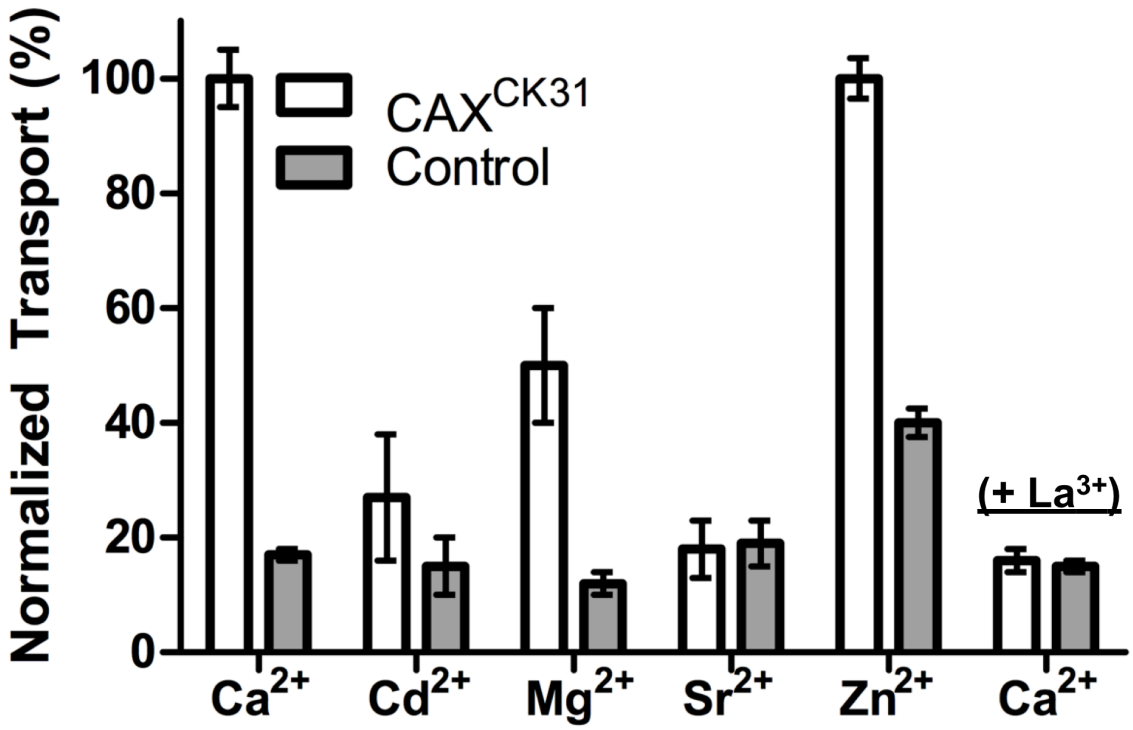

Figure 4-5. Fluorescence dequenching following addition of 100 μM free divalent cation to energized inverted membrane vesicles derived from BL21-AI cells expressing CAX^{CK31} containing quenched acridine orange.
Control vesicles lack CAX^{CK31}. 10 μM La^{3+} was added to reactions containing 100 μM Ca^{2+}. Data represent means of three measurements with error bars representing SEM.

at the end of each assay by disrupting the liposomes with 0.003 % (v/v) Triton X-100. Liposomes prepared without CAX^{CK31} served as a negative control.

4.5 Quantification of Protein and Lipid in Proteoliposomes

In order to optimize our CAX^{CK31} reconstitution in liposomes and measure transport rates with activity assays a sensitive protein assay to quantify protein:lipid ratios was needed. Several modifications were made to published methods of amido black staining of TCA-precipitated protein deposited on filter membranes, including use of PVDF and a dot-blotting apparatus and imaging with computational analysis instead of traditional extraction of dye from the membrane and spectrophotometric analysis. This method detected as little as 50 ng CAX^{CK31} in a lipid background, allowing these determinations without sacrifice of much proteoliposome sample.

The following quoted text and Figures 4-6 and 4-7 are from an unpublished manuscript by Marc Ridilla, Jeffrey T. Bolin, and Dinesh A. Yernool describing the method.

“Abstract: Amido black staining is commonly used for protein quantification, especially in cases with proteoliposomes or other samples with large lipid mass bias. Several improvements were demonstrated to previously-reported methods for quantifying amido black staining of blotted proteoliposomes that increase

protein sensitivity by forty fold, to below 50 ng. The procedure was at least two times faster for a single assay and readily-adaptable to 96-well format without requiring specialized equipment. The increased sensitivity reduced sample commitment, which facilitated research challenged by limited sample quantities.

With membrane proteins, basic methods for protein detection and quantification are often limited by low sample availability and interference by detergents or lipids required to maintain protein stability. For enzymes or transporters in proteoliposomes, accurate determination of protein quantity is essential for kinetic assays; and highly variable incorporation of protein and lipid into liposomes underscores the need to quantify protein after proteoliposome preparation. Herein a method is described for rapid and accurate quantification of protein and lipid in samples containing as little as fifty nanograms of protein in as much as four milligrams of lipid using the dye amido black. This constitutes a forty-fold increase in sensitivity of protein detection in the presence of lipid over previous reports (Kaplan and Pedersen 1985).

Ionic interactions between amido black and basic protein groups have been exploited to stain proteins in tissues, agarose and polyacrylamide gels, and membrane-supported assays (Kaplan and Pedersen 1985; JANSEN 1962; Kruski and Narayan 1974; Nakamura et al. 1985; Racusen 1973). A dominant method capable of detecting 2 μg protein in the presence of lipid involves: (1) excision of dyed spots from filter membranes used to capture trichloroacetic acid-

(TCA-) precipitated samples, (2) extraction of the dye, and (3) spectrophotometric detection of amido black (Kaplan and Pedersen 1985). *Via* densitometry, membrane-captured precipitates containing as little as 50 ng soluble protein are detectable; however, these methods require pre-treatment of the filter and specialized imaging equipment and have not been demonstrated with lipid-containing samples of membrane proteins (Nakamura et al. 1985; Gentile, Balì, and Pignalosa 1997).

The huge cost of producing purified membrane proteins coupled to inefficient reconstitution necessitates high-sensitivity protein quantification. For example, a typical reconstitution starting with 800 µg protein and 80 mg lipids yields 5 % protein incorporated into liposomes. Given a 2-µg lower detection limit for protein in the presence of lipid (Kaplan and Pedersen 1985), at least 5 % of a proteoliposome sample would be committed to protein quantification. It is desirable to use a smaller fraction to quantify protein, thus saving the rest for transport assays.

Increased sensitivity and reproducibility were achieved by (1) replacing large-diameter filtration discs with blotting membrane in a dot-blotting apparatus, and (2) replacing dye extraction and spectrophotometry with simple imaging and image analysis to quantify membrane staining. These advancements enabled detection of <50 ng protein in proteoliposome samples, less than 3 % of the 2 µg limit previously demonstrated (Kaplan and Pedersen 1985).

Sample preparation builds on previously-reported procedures (Kaplan and Pedersen 1985). Briefly, protein-containing samples were diluted to 2 mL with H_2O, followed by addition of 0.2 mL 10 % (w/v) SDS, 0.3 mL 1 M Tris pH 8.0 + 1 % (w/v) SDS, and 0.6 mL 104 % (w/v) TCA, with vortexing after each addition. Precipitate was deposited on polyvinylidene fluoride (PVDF) membrane (0.2 μm pore size) using a Bio-Dot apparatus (Bio-Rad Laboratories, Inc.; Hercules, CA, USA), then washed by filtration of 2 mL 6 % (w/v) TCA; simultaneous processing of up to 96 samples is thus possible per membrane. The membrane was immersed with stirring for three minutes in Amido Black Staining Solution (Sigma-Aldrich Corp.; St. Louis, MO, USA), then destained by immersion with stirring, once in water and thrice in 90 % (v/v) methanol, 2 % (v/v) glacial acetic acid, 8 % (v/v) H_2O, one minute per treatment, and once more in water for two minutes. The membrane was dried by blotting with paper towels; dried membranes can be stored indefinitely. The membrane was scanned at 600 dpi using a flatbed scanner (Hewlett-Packard Company; Palo Alto, CA, USA) connected to a computer. The resulting image (Figure 4-5A) was analyzed with open-source software ImageJ (Schneider, Rasband, and Eliceiri 2012) to measure integrated density of each dot (Figure 4-5B) as described in the ImageJ manual (http://rsbweb.nih.gov/ij/docs/examples/dot-blot/index.html). Linear regression in GraphPad Prism (La Jolla, CA, USA) established standard curves relating staining to quantity (Figure 4-5C).

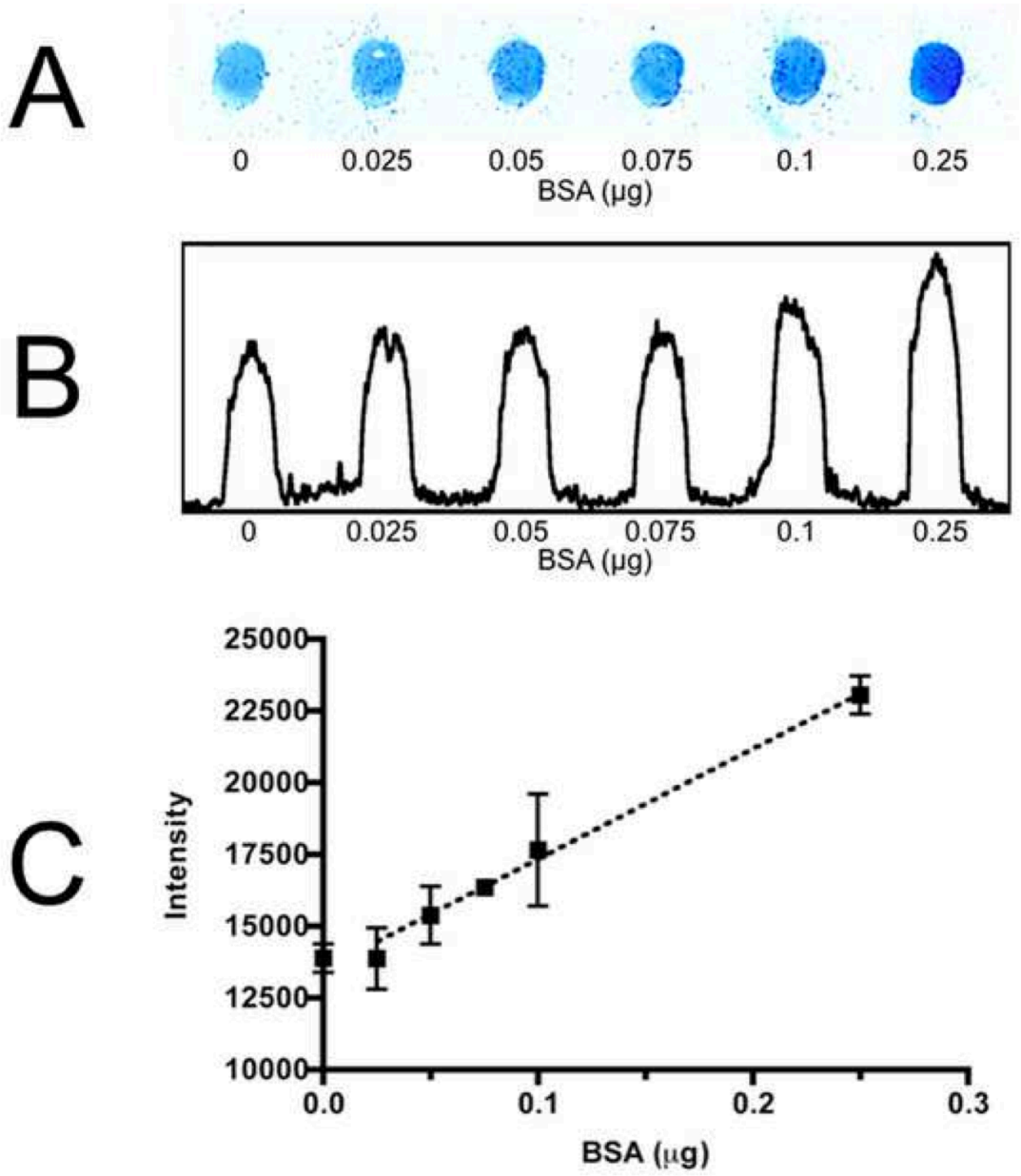

Figure 4-6. Scanned images of amido black stained blotting membranes enabled highly-sensitive protein quantification.
(A), scanned image of amido black-stained polyvinylidene fluoride membrane through which trichloroacetic acid-precipitated bovine serum albumin (BSA) in the indicated amounts has been filtered. (B), Integration of spot densities shown in (A) by ImageJ software. High signal-to-noise verified the suitability of the scanning/image analysis method. (C), linear regression of BSA standards. Points with error bars represent the mean and SE of triplicate measurements. Good linearity and reproducibility were seen across a wide range of BSA quantities, down to 25 nanograms.

The switch from excision/extraction using single-sample filtration discs to the dot-blot procedure increased not only sensitivity but also throughput by facilitating simultaneous processing of more independent and replicate samples. Typical estimates of error among replicate samples was 5.6 % - significantly lower than the 14.4 % achieved by the excision/extraction method (data not shown). PVDF is recommended over nitrocellulose membranes because of its mechanical properties and low background staining between blots (Figure 4-5A,B).

Using bovine serum albumin (BSA, fatty-acid-free; Sigma-Aldrich Corp.) as a standard, a linear response *vs.* protein quantity was demonstrated between 25 nanograms and one microgram (Figures 4-5C, 4-6A,B). Membrane pore size may be varied to access other ranges of protein quantity, with greater sensitivity achieved with smaller pore size. Increasing lipid content (*E. coli* total lipid extract; Avanti Polar Lipids, Inc., Alabaster, AL, USA) in the sample increased both the slope and y-intercept of protein response curves (Figure 4-6A), but the response remained linear. To account for lipid during protein quantification, protein-free liposomes were prepared in parallel with the proteoliposomes, and a volume matching that used for protein quantification was added to each sample used for the standard curve (Figure 4-6C). In routine practice, protein in proteoliposome samples at 0.05 mg/mL was quantified using only 10 µL sample volumes (≈500 ng protein).

In summary, this technique is of significant utility to the experimenter working with purified integral membrane proteins reconstituted in artificial liposomes or in studies of the association between lipids and membrane proteins. The methods introduced here offer significant improvements over previously-reported methods in terms of sensitivity, reproducibility, speed, and throughput. Moreover, dot- or slot-blot equipment, flatbed scanners, and personal computers are available in most laboratories; any or all can be used to improve upon the efficiency of the more traditional amido black staining methods."

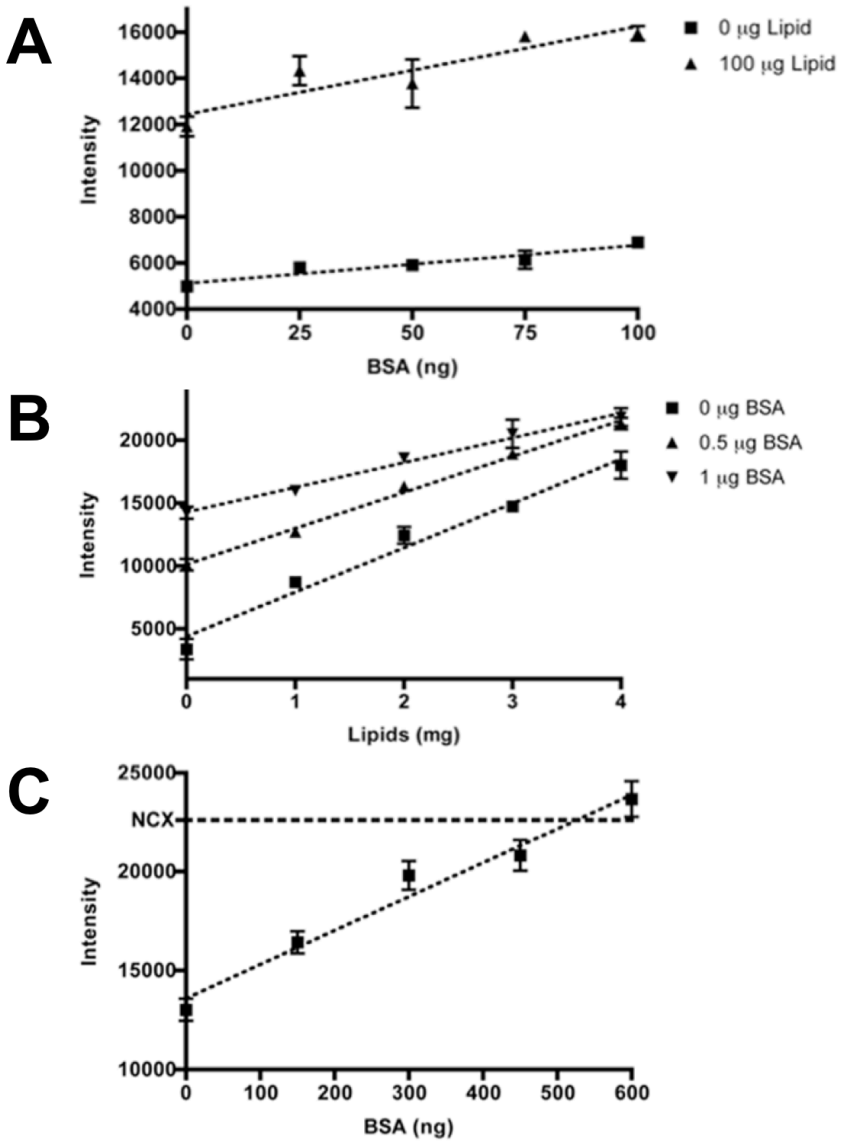

Figure 4-7. Linear response to amido black staining enabled quantification of either protein or lipid in proteoliposomes.
Mixtures of bovine serum albumin (BSA) and *E. coli* total lipid extract were prepared and assayed by the reported method. (A), response to BSA was linear in the presence of different amounts of lipid. (B), response to lipid was linear in the presence of different amounts of BSA, allowing accurate determination of lipid in protein-containing samples, given that protein concentration is known. (C), determination of a prokaryotic sodium-calcium exchanger homolog concentration in liposomes using a standard curve of BSA plus protein-free liposome sample. Points and error bars represent mean with SE of three replicates.

CHAPTER 5. FUTURE DIRECTIONS

5.1 Determination of the Molecular Structure of CAX^{CK31}

5.1.1 Crystallization

Ordered crystals of CAX^{CK31} are necessary for the determination of its atomic structure. Efforts were made to crystallize all purified CaCAs, utilizing robotic setup, commercially-available sparse-matrix reagent screens, and SONICC screening. No crystals were obtained from samples of CAX^{CK31} alone, and crystals grown using CAX^{CK31}-GFP samples produced crystals of GFP alone (unexpected degradation during incubation likely resulted in the release of crystallizable GFP monomers that formed the crystals observed).

CAX^{CK31}-GFP was used to test the possibility that crystallogenesis could be motivated by interactions among the soluble GFP molecules. Microcrystals were grown *in surfo* by the vapor-diffusion method with mother liquors containing Tris pH 8.5, MgCl2, and PEG 400. The crystals exhibited fluorescence due to the GFP, and they gave strong second-harmonic generation when imaged with second-order nonlinear imaging of chiral crystals (SONICC). Crystals diffracted X-rays to 2.5 Å resolution, and data indexing revealed a primitive orthorhombic spacegroup with unit cell dimensions of 51.6 Å × 67.4 Å × 60.0 Å (α=β=γ=90º),

however molecular replacement solutions revealed the presence of GFP alone in the crystals.

Further crystallization attempts conducted with stable CAX^{CK31} dimers isolated in the absence of GFP did not produce any promising leads.

Conditions verified to yield dimeric CAX^{CK31} should be applied to large-scale production, and dimeric CAX^{CK31} should be subjected to exhaustive crystallization screening. Increased protein:detergent ratio, polar surface area, and internal symmetry of dimeric CAX^{CK31} will result in a greater likelihood of success in crystallization compared to previous attempts using monomeric CAX^{CK31}.

Purified CaCAs were screened for crystallization by Hampton Research Crystal Screen, Crystal Screen 2, MembFac, Grid Screen MPD, and Grid Screen PEG/LiCl, Jena Biosciences JBScreen Classic 1, JBScreen Membrane 1, and JBScreen Membrane 2, and Molecular Dimensions MemStart and MemSys Crystallization Screens.

Additional parameters tested included protein concentration, incubation temperature, and protein buffer detergent.

Needle-shaped crystals grew in many conditions (unfortunately these crystals grew at 4 °C and disintegrated when moved to room temperature, so they could not be photographed). Attempts to optimize these conditions were unfruitful.

N21 and CAX^{CK31} were subjected to a multitude of vapor-diffusion crystallization experiments. No conditions tested reproducibly generated crystals of good quality. Efforts to utilize robotic equipment should be increased to maximize screening efficiency. Other methods such as batch (under oil) or lipid-cubic-phase crystallization should be tested. A collaboration with Vadim Cherezov at the Scripps Institute is directed toward crystallization of *via* lipid cubic phase. Dr. Cherezov has indicated that initial results were promising.

5.1.1.1 Antibody-Mediated Crystallization of NCX

Antibody-protein complexes are often used to promote crystallization of membrane proteins by increasing the relative polar protein surface available for crystal contacts (Laver 1990). High-quality antibodies to CAX^{CK31} may also simplify structure determination from X-ray diffraction data. Oregon Health & Science University was contracted to produce murine antibodies to both N21 and CAX^{CK31}. A number of hybridoma solutions were screened using size-exclusion chromatography (SEC), dot-blot, and Western-blot analyses to determine which contain antibodies that bind specific, tertiary structural epitopes on N21 or CAX^{CK31}. Promising results included earlier elution from the SEC column,

indicating increased size (complex as opposed to free antigen), and minimal staining of denatured protein on Western blot. Purification of CAX^{CK31}-Fab complexes has been demonstrated using fragments from the antibodies discussed above.

5.1.1.2 Surface Entropy Reduction

Replacement of surface residues to reduce entropy and increase the stability of proteins has been demonstrated to improve the likelihood of obtaining diffraction-quality protein crystals (Longenecker et al. 2001; Derewenda 2004).

Sequences were analyzed by the Surface Entropy Reduction prediction server (SERp) (Goldschmidt et al. 2007). For each CaCA, charged residues in intracellular loop 3 were recommended for mutation to alanine. These mutations, however, decreased the stability of the protein, evidenced by diminished shelf-life of purified protein solutions: mutants precipitated from solution within two days of purification when stored at 4 ºC.

Cysteines have been introduced into CAX^{CK31} reentrant loop regions α-1 and α-2 (see 3.4.4). Cross-linking of these regions is expected to reduce molecular flexibility and promote crystallization.

5.2 SEC-FRET

CAX^{CK31}-CFP, CAX^{CK31}-GFP, CAX^{CK31}-mCherry, a 1:1 mixture of CAX^{CK31}-CFP and CAX^{CK31}-mCherry, and a 1:1 mixture of CAX^{CK31}-GFP and CAX^{CK31}-mCherry were subjected to SEC at 1 mg/mL and 10 mg/mL as described above, and the peak shift indicating dimer formation was confirmed in each case. In-line fluorimetry of eluting protein confirms the presence of all expected colored fluorescent proteins at the expected elution positions. FRET is confirmed by acceptor emission intensity greater than expected from the sum of contributions of individual fluorophores due to spectral overlap.

All fluorescence chromatograms were normalized by simultaneously-measured absorbance (280 nm) data to provide “fluorescence per mg protein” data. Due to minimal spectral overlap, fluorescence is detected using the described FRET wavelength pairs even when testing individual fusions, however mixtures of CAX^{CK31}-CFP or CAX^{CK31}-GFP with CAX^{CK31}-mCherry produce more fluorescence per mg protein than expected from these contributions of the individual fluorophores. For the CFP/mCherry mixture fluorescence intensity at the elution peak increases on average by 7.5 %, and GFP/mCherry by 6.7 %. These data demonstrate the formation of stable dimers between CAX^{CK31}-CFP or CAX^{CK31}-GFP and CAX^{CK31}-mCherry. The relatively low FRET efficiencies reported here are likely due to an inability to select for heterodimers of differently-labeled CAX^{CK31} (*i.e.* no FRET would occur for homodimers of CAX^{CK31}-CFP, CAX^{CK31}-GFP, or CAX^{CK31}-mCherry).

5.3 Lipid Influence on CaCA Stability

During development of the purification scheme for CAX^{CK31} it was determined that CAX^{CK31} requires either lipids (i.e. lecithin) or lipid-like detergent (i.e. FosCholine-12 or LysoFos-Choline-12) for solubility, however there is not currently a suitable assay to elucidate the nature of this lipid requirement.

Quenching of tryptophan fluorescence by brominated lipids (Carney et al. 2006) may be utilized to study this further in the near future.

LIST OF REFERENCES

LIST OF REFERENCES

Arora, K K, and P L Pedersen. 1995. “Glucokinase of Escherichia Coli: Induction in Response to the Stress of Overexpressing Foreign Proteins.” *Archives of Biochemistry and Biophysics* 319 (2) (June 1): 574–578. doi:10.1006/abbi.1995.1333.

Baba, Tomoya, Takeshi Ara, Miki Hasegawa, Yuki Takai, Yoshiko Okumura, Miki Baba, Kirill A Datsenko, Masaru Tomita, Barry L Wanner, and Hirotada Mori. 2006. “Construction of Escherichia Coli K-12 In-frame, Single-gene Knockout Mutants: The Keio Collection.” *Molecular Systems Biology* 2: 2006.0008. doi:10.1038/msb4100050.

Beckwith, J R. 1967. “Regulation of the Lac Operon. Recent Studies on the Regulation of Lactose Metabolism in Escherichia Coli Support the Operon Model.” *Science (New York, N.Y.)* 156 (3775) (May 5): 597–604.

Beloin, Christophe, Jaione Valle, Patricia Latour-Lambert, Philippe Faure, Mickaël Kzreminski, Damien Balestrino, Janus A J Haagensen, et al. 2004. “Global Impact of Mature Biofilm Lifestyle on Escherichia Coli K-12 Gene Expression.” *Molecular Microbiology* 51 (3) (February): 659–674.

Berridge, Michael J., Martin D. Bootman, and H. Llewelyn Roderick. 2003. “Calcium Signalling: Dynamics, Homeostasis and Remodelling.” *Nat Rev Mol Cell Biol* 4 (7) (July): 517–529. doi:10.1038/nrm1155.

Blaustein, Mordecai P., and W. Jonathan Lederer. 1999. “Sodium/Calcium Exchange: Its Physiological Implications.” *Physiological Reviews* 79 (3) (July 1): 763 –854.

Bochkareva, Elena S, Alexander S Girshovich, and Eitan Bibi. 2002. “Identification and Characterization of the Escherichia Coli Stress Protein UP12, a Putative in Vivo Substrate of GroEL.” *European Journal of Biochemistry / FEBS* 269 (12) (June): 3032–3040.

Boulter, J M, and D N Wang. 2001. “Purification and Characterization of Human Erythrocyte Glucose Transporter in Decylmaltoside Detergent Solution.” *Protein Expression and Purification* 22 (2) (July): 337–348. doi:10.1006/prep.2001.1440.

Boyman, Liron, Brian M Hagen, Moshe Giladi, Reuben Hiller, W Jonathan Lederer, and Daniel Khananshvili. 2011. “Proton-sensing Ca2+ Binding Domains Regulate the Cardiac Na+/Ca2+ Exchanger.” *The Journal of Biological Chemistry* 286 (33) (August 19): 28811–28820. doi:10.1074/jbc.M110.214106.

Bruno-Bárcena, Jose M, M Andrea Azcárate-Peril, and Hosni M Hassan. 2010. “Role of Antioxidant Enzymes in Bacterial Resistance to Organic Acids.” *Applied and Environmental Microbiology* 76 (9) (May): 2747–2753. doi:10.1128/AEM.02718-09.

Cai, Xinjiang, and Jonathan Lytton. 2004. “The Cation/Ca2+ Exchanger Superfamily: Phylogenetic Analysis and Structural Implications.” *Molecular Biology and Evolution* 21 (9): 1692 –1703. doi:10.1093/molbev/msh177.

Cao, Yu, Xiangshu Jin, Hua Huang, Mehabaw Getahun Derebe, Elena J. Levin, Venkataraman Kabaleeswaran, Yaping Pan, et al. 2011. “Crystal Structure of a Potassium Ion Transporter, TrkH.” *Nature* 471 (7338) (March 17): 336–340. doi:10.1038/nature09731.

Carney, Joanne, J Malcolm East, Sanjay Mall, Phedra Marius, Andrew M Powl, J Neville Wright, and Anthony G Lee. 2006. “Fluorescence Quenching Methods to Study Lipid-protein Interactions.” *Current Protocols in Protein Science / Editorial Board, John E. Coligan ... [et Al.]* Chapter 19 (September): Unit 19.12. doi:10.1002/0471142301.ps1912s45.

Carpenter, Elisabeth P, Konstantinos Beis, Alexander D Cameron, and So Iwata. 2008. “Overcoming the Challenges of Membrane Protein Crystallography.” *Current Opinion in Structural Biology* 18 (5) (October): 581–586. doi:10.1016/j.sbi.2008.07.001.

Carruthers, Anthony, Julie DeZutter, Amit Ganguly, and Sherin U Devaskar. 2009. “Will the Original Glucose Transporter Isoform Please Stand Up!” *American Journal of Physiology. Endocrinology and Metabolism* 297 (4) (October): E836–848. doi:10.1152/ajpendo.00496.2009.

Chang, Dong-Eun, Darren J Smalley, and Tyrrell Conway. 2002. “Gene Expression Profiling of Escherichia Coli Growth Transitions: An Expanded Stringent Response Model.” *Molecular Microbiology* 45 (2) (July): 289–306.

Chang, Jia-Ming, Paolo Di Tommaso, Jean-François Taly, and Cedric Notredame. 2012. “Accurate Multiple Sequence Alignment of Transmembrane Proteins with PSI-Coffee.” *BMC Bioinformatics* 13 Suppl 4: S1. doi:10.1186/1471-2105-13-S4-S1.

Chang, S F, D Ng, L Baird, and C Georgopoulos. 1991. “Analysis of an Escherichia Coli dnaB Temperature-sensitive Insertion Mutation and Its Cold-sensitive Extragenic Suppressor.” *The Journal of Biological Chemistry* 266 (6) (February 25): 3654–3660.

Cho, Byung-Kwan, Eric M Knight, Christian L Barrett, and Bernhard Ø Palsson. 2008. “Genome-wide Analysis of Fis Binding in Escherichia Coli Indicates a Causative Role for A-/AT-tracts.” *Genome Research* 18 (6) (June): 900–910. doi:10.1101/gr.070276.107.

Craner, Matthew J., Bryan C. Hains, Albert C. Lo, Joel A. Black, and Stephen G. Waxman. 2004. “Co-localization of Sodium Channel Nav1.6 and the Sodium–calcium Exchanger at Sites of Axonal Injury in the Spinal Cord in EAE.” *Brain* 127 (2) (February 1): 294 –303. doi:10.1093/brain/awh032.

Cumming, Robert C., Nancy L. Andon, Paul A. Haynes, Minkyu Park, Wolfgang H. Fischer, and David Schubert. 2004. “Protein Disulfide Bond Formation in the Cytoplasm During Oxidative Stress.” *Journal of Biological Chemistry* 279 (21) (May 21): 21749–21758. doi:10.1074/jbc.M312267200.

Dalbey, Ross E, Peng Wang, and Andreas Kuhn. 2011. “Assembly of Bacterial Inner Membrane Proteins.” *Annual Review of Biochemistry* 80 (1): 161–187.

Danese, P N, and T J Silhavy. 1998. “CpxP, a Stress-combative Member of the Cpx Regulon.” *Journal of Bacteriology* 180 (4) (February): 831–839.

Derewenda, Zygmunt S. 2004. “Rational Protein Crystallization by Mutational Surface Engineering.” *Structure (London, England: 1993)* 12 (4) (April): 529–535. doi:10.1016/j.str.2004.03.008.

Doering, A E, and W J Lederer. 1993. “The Mechanism by Which Cytoplasmic Protons Inhibit the Sodium-calcium Exchanger in Guinea-pig Heart Cells.” *The Journal of Physiology* 466 (1) (July 1): 481–499.

Domka, Joanna, Jintae Lee, and Thomas K Wood. 2006. “YliH (BssR) and YceP (BssS) Regulate Escherichia Coli K-12 Biofilm Formation by Influencing Cell Signaling.” *Applied and Environmental Microbiology* 72 (4) (April): 2449–2459. doi:10.1128/AEM.72.4.2449-2459.2006.

Dong, H, L Nilsson, and CG Kurland. 1995. “Gratuitous Overexpression of Genes in Escherichia Coli Leads to Growth Inhibition and Ribosome Destruction.” *The Journal of Bacteriology* 177 (6) (March 1): 1497–1504.

Dutzler, Raimund, Ernest B. Campbell, Martine Cadene, Brian T. Chait, and Roderick MacKinnon. 2002. “X-ray Structure of a ClC Chloride Channel at 3.0[thinsp][angst] Reveals the Molecular Basis of Anion Selectivity.” *Nature* 415 (6869) (January 17): 287–294. doi:10.1038/415287a.

Edmond, Clare, Toshiro Shigaki, Sophie Ewert, Matthew D Nelson, James M Connorton, Vesela Chalova, Zeenat Noordally, and Jon K Pittman. 2009. “Comparative Analysis of CAX2-like Cation Transporters Indicates Functional and Regulatory Diversity.” *The Biochemical Journal* 418 (1) (February 15): 145–154. doi:10.1042/BJ20081814.

Folta-Stogniew, E, and K R Williams. 1999. “Determination of Molecular Masses of Proteins in Solution: Implementation of an HPLC Size Exclusion Chromatography and Laser Light Scattering Service in a Core Laboratory.” *Journal of Biomolecular Techniques: JBT* 10 (2) (June): 51–63.

Fontaine, Fanette, Ryan T Fuchs, and Gisela Storz. 2011. “Membrane Localization of Small Proteins in Escherichia Coli.” *The Journal of Biological Chemistry* 286 (37) (September 16): 32464–32474. doi:10.1074/jbc.M111.245696.

Gaillard, I, D J Slotboom, J Knol, J S Lolkema, and W N Konings. 1996. “Purification and Reconstitution of the Glutamate Carrier GltT of the Thermophilic Bacterium Bacillus Stearothermophilus.” *Biochemistry* 35 (19) (May 14): 6150–6156. doi:10.1021/bi953005v.

Gallant, J A. 1979. “Stringent Control in E. Coli.” *Annual Review of Genetics* 13: 393–415. doi:10.1146/annurev.ge.13.120179.002141.

Garavito, R M, D Picot, and P J Loll. 1996. “Strategies for Crystallizing Membrane Proteins.” *Journal of Bioenergetics and Biomembranes* 28 (1) (February): 13–27.

Gärtner, Rebecca M, Camilo Perez, Caroline Koshy, and Christine Ziegler. 2011. "Role of Bundle Helices in a Regulatory Crosstalk in the Trimeric Betaine Transporter BetP." *Journal of Molecular Biology* 414 (3) (December 2): 327–336. doi:10.1016/j.jmb.2011.10.013.

Gentile, F, E Balì, and G Pignalosa. 1997. "Sensitivity and Applications of the Nondenaturing Staining of Proteins on Polyvinylidene Difluoride Membranes with Amido Black 10B in Water Followed by Destaining in Water." *Analytical Biochemistry* 245 (2) (February 15): 260–262.

George, H A, A L Powell, M E Dahlgren, W K Herber, R Z Maigetter, B W Burgess, S M Stirdivant, and R L Greasham. 1992. "Physiological Effects of TGF(alpha)-PE40 Expression in Recombinant Escherichia Coli JM109." *Biotechnology and Bioengineering* 40 (3) (July): 437–445. doi:10.1002/bit.260400314.

Gill, R T, J J Valdes, and W E Bentley. 2000. "A Comparative Study of Global Stress Gene Regulation in Response to Overexpression of Recombinant Proteins in Escherichia Coli." *Metabolic Engineering* 2 (3) (July): 178–189. doi:10.1006/mben.2000.0148.

Goldschmidt, Lukasz, David R Cooper, Zygmunt S Derewenda, and David Eisenberg. 2007. "Toward Rational Protein Crystallization: A Web Server for the Design of Crystallizable Protein Variants." *Protein Science: a Publication of the Protein Society* 16 (8) (August): 1569–1576. doi:10.1110/ps.072914007.

Hammon, Justus, Dinesh V Palanivelu, Joy Chen, Chintan Patel, and Daniel L Minor Jr. 2009. “A Green Fluorescent Protein Screen for Identification of Well-expressed Membrane Proteins from a Cohort of Extremophilic Organisms.” *Protein Science: a Publication of the Protein Society* 18 (1) (January): 121–133. doi:10.1002/pro.18.

Harcum, S W, and W E Bentley. 1993. “Response Dynamics of 26-, 34-, 39-, 54-, and 80-kDa Proteases in Induced Cultures of Recombinant Escherichia Coli.” *Biotechnology and Bioengineering* 42 (6) (September 5): 675–685. doi:10.1002/bit.260420602.

Harold, Franklin M., and Peter C. Maloney. 1996. “Energy Transduction by Ion Currents.” In *Escherichia Coli and Salmonella: Cellular and Molecular Biology*, 1:283–306. Washington, D.C.: ASM Press.

Hayashi, Yutaro, Hideo Matsui, and Toshio Takagi. 1989. “Membrane Protein Molecular Weight Determined by Low-angle Laser Light-scattering Photometry Coupled with High-performance Gel Chromatography.” In *Biomembranes Part S*, Volume 172:514–528. Academic Press.

Henderson, Scott A., Joshua I. Goldhaber, Jessica M. So, Tieyan Han, Christi Motter, An Ngo, Chana Chantawansri, et al. 2004. “Functional Adult Myocardium in the Absence of Na+-Ca2+ Exchange.” *Circulation Research* 95 (6): 604 –611. doi:10.1161/01.RES.0000142316.08250.68.

Herz, Katia, Abraham Rimon, Gunnar Jeschke, and Etana Padan. 2009. “β-Sheet-dependent Dimerization Is Essential for the Stability of NhaA Na+/H+ Antiporter.” *Journal of Biological Chemistry* 284 (10) (March 6): 6337 –6347. doi:10.1074/jbc.M807720200.

Hilge, Mark, Jan Aelen, and Geerten W. Vuister. 2006. “Ca2+ Regulation in the Na+/Ca2+ Exchanger Involves Two Markedly Different Ca2+ Sensors.” *Molecular Cell* 22 (1) (April 7): 15–25. doi:10.1016/j.molcel.2006.03.008.

Hilgemann, D W. 1990. “Regulation and Deregulation of Cardiac Na(+)-Ca2+ Exchange in Giant Excised Sarcolemmal Membrane Patches.” *Nature* 344 (6263) (March 15): 242–245. doi:10.1038/344242a0.

Hoffmann, Frank, and Ursula Rinas. 2004. “Stress Induced by Recombinant Protein Production in Escherichia Coli.” *Advances in Biochemical Engineering/biotechnology* 89: 73–92.

Hunte, Carola, Emanuela Screpanti, Miro Venturi, Abraham Rimon, Etana Padan, and Hartmut Michel. 2005. “Structure of a Na+/H+ Antiporter and Insights into Mechanism of Action and Regulation by pH.” *Nature* 435 (7046) (June 30): 1197–1202. doi:10.1038/nature03692.

Ilbert, Marianne, Vincent Méjean, and Chantal Iobbi-Nivol. 2004. “Functional and Structural Analysis of Members of the TorD Family, a Large Chaperone Family Dedicated to Molybdoproteins.” *Microbiology (Reading, England)* 150 (Pt 4) (April): 935–943.

JANSEN, M T. 1962. “On the Quantitative Amido Black B Staining of Protein Spots in Agar Gel at Low Local Protein Concentrations.” *Biochimica et Biophysica Acta* 60 (June 18): 121–125.

Jeon, Daejong, Yu-Mi Yang, Myung-Jin Jeong, Kenneth D Philipson, Hyewhon Rhim, and Hee-Sup Shin. 2003. “Enhanced Learning and Memory in Mice Lacking Na+/Ca2+ Exchanger 2.” *Neuron* 38 (6) (June 19): 965–976. doi:10.1016/S0896-6273(03)00334-9.

John, Scott A., Bernard Ribalet, James N. Weiss, Kenneth D. Philipson, and Michela Ottolia. 2011. “Ca2+-dependent Structural Rearrangements Within Na+–Ca2+ Exchanger Dimers.” *Proceedings of the National Academy of Sciences* 108 (4) (January 25): 1699 –1704. doi:10.1073/pnas.1016114108.

Kalamorz, Falk, Birte Reichenbach, Walter März, Bodo Rak, and Boris Görke. 2007. “Feedback Control of Glucosamine-6-phosphate Synthase GlmS Expression Depends on the Small RNA GlmZ and Involves the Novel Protein YhbJ in Escherichia Coli.” *Molecular Microbiology* 65 (6) (September): 1518–1533. doi:10.1111/j.1365-2958.2007.05888.x.

Kamiya, Takehiro, and Masayoshi Maeshima. 2004. “Residues in Internal Repeats of the Rice cation/H+ Exchanger Are Involved in the Transport and Selection of Cations.” *The Journal of Biological Chemistry* 279 (1) (January 2): 812–819. doi:10.1074/jbc.M309726200.

Kannan, Geetha, Jessica C Wilks, Devon M Fitzgerald, Brian D Jones, Sandra S Bondurant, and Joan L Slonczewski. 2008. “Rapid Acid Treatment of Escherichia Coli: Transcriptomic Response and Recovery.” *BMC Microbiology* 8: 37. doi:10.1186/1471-2180-8-37.

Kaplan, R S, and P L Pedersen. 1985. “Determination of Microgram Quantities of Protein in the Presence of Milligram Levels of Lipid with Amido Black 10B.” *Analytical Biochemistry* 150 (1) (October): 97–104.

Kawate, Toshimitsu, and Eric Gouaux. 2006. “Fluorescence-Detection Size-Exclusion Chromatography for Precrystallization Screening of Integral Membrane Proteins.” *Structure* 14 (4) (April): 673–681. doi:doi: 10.1016/j.str.2006.01.013.

Khananshvili, Daniel. 2013. “The SLC8 Gene Family of Sodium-calcium Exchangers (NCX) - Structure, Function, and Regulation in Health and Disease.” *Molecular Aspects of Medicine* 34 (2-3) (April): 220–235. doi:10.1016/j.mam.2012.07.003.

Kruski, A W, and K A Narayan. 1974. “Some Quantitative Aspects of the Disc Electrophoresis of Ovalbumin Using Amido Black 10B Stain.” *Analytical Biochemistry* 60 (2) (August): 431–440.

Laffend, L, and M L Shuler. 1994. “Ribosomal Protein Limitations in Escherichia Coli Under Conditions of High Translational Activity.” *Biotechnology and Bioengineering* 43 (5) (March 5): 388–398. doi:10.1002/bit.260430507.

Laskowska, E, A Wawrzynów, and A Taylor. 1996. “IbpA and IbpB, the New Heat-shock Proteins, Bind to Endogenous Escherichia Coli Proteins Aggregated Intracellularly by Heat Shock.” *Biochimie* 78 (2): 117–122.

Laver, W. Graeme. 1990. “Crystallization of Antibody-protein Complexes.” *Methods* 1 (1) (August): 70–74. doi:10.1016/S1046-2023(05)80148-3.

Lee, J, S R Hiibel, K F Reardon, and T K Wood. 2010. “Identification of Stress-related Proteins in Escherichia Coli Using the Pollutant Cis-dichloroethylene.” *Journal of Applied Microbiology* 108 (6) (June): 2088–2102. doi:10.1111/j.1365-2672.2009.04611.x.

Lee, Seok-Yong, James A Letts, and Roderick MacKinnon. 2009. “Functional Reconstitution of Purified Human Hv1 H+ Channels.” *Journal of Molecular Biology* 387 (5) (April 17): 1055–1060. doi:10.1016/j.jmb.2009.02.034.

Lewinson, Oded, Allen T Lee, and Douglas C Rees. 2008. “The Funnel Approach to the Precrystallization Production of Membrane Proteins.” *Journal of Molecular Biology* 377 (1) (March 14): 62–73. doi:10.1016/j.jmb.2007.12.059.

Liao, Jun, Hua Li, Weizhong Zeng, David B. Sauer, Ricardo Belmares, and Youxing Jiang. 2012. “Structural Insight into the Ion-Exchange Mechanism of the Sodium/Calcium Exchanger.” *Science* 335 (6069) (February 10): 686 –690. doi:10.1126/science.1215759.

Libby, Elizabeth A, Manuela Roggiani, and Mark Goulian. 2012. “Membrane Protein Expression Triggers Chromosomal Locus Repositioning in Bacteria.” *Proceedings of the National Academy of Sciences of the United States of America* 109 (19) (May 8): 7445–7450. doi:10.1073/pnas.1109479109.

Longenecker, K L, M E Lewis, H Chikumi, J S Gutkind, and Z S Derewenda. 2001. “Structure of the RGS-like Domain from PDZ-RhoGEF: Linking Heterotrimeric g Protein-coupled Signaling to Rho GTPases.” *Structure (London, England: 1993)* 9 (7) (July 3): 559–569.

Lytton, Jonathan. 2007. “Na+/Ca2+ Exchangers: Three Mammalian Gene Families Control Ca2+ Transport.” *Biochem J* 406 (3): 365–382.

Matsuoka, S, D A Nicoll, L V Hryshko, D O Levitsky, J N Weiss, and K D Philipson. 1995. “Regulation of the Cardiac Na(+)-Ca2+ Exchanger by Ca2+. Mutational Analysis of the Ca(2+)-binding Domain.” *The Journal of General Physiology* 105 (3) (March): 403–420.

Mercado Besserer, Gabriel, Debora A. Nicoll, Jeff Abramson, and Kenneth D. Philipson. 2012. “Characterization and Purification of a Na+/Ca2+ Exchanger from an Archaebacterium.” *Journal of Biological Chemistry* (January 27). doi:10.1074/jbc.M111.331280. http://www.jbc.org/content/early/2012/01/27/jbc.M111.331280.abstract.

Merten, O.-W. 2001. *Recombinant Protein Production with Prokaryotic and Eukaryotic Cells: A Comparative View on Host Physiology : Selected Articles from the Meeting of the EFB Section on Microbial Physiology, Semmering, Austria, 5th-8th October 2000*. Springer.

Minagawa, Shu, Hiroshi Ogasawara, Akinori Kato, Kaneyoshi Yamamoto, Yoko Eguchi, Taku Oshima, Hirotada Mori, Akira Ishihama, and Ryutaro Utsumi. 2003. “Identification and Molecular Characterization of the Mg2+ Stimulon of Escherichia Coli.” *Journal of Bacteriology* 185 (13) (July): 3696–3702.

Mogk, Axel, Elke Deuerling, Sonja Vorderwülbecke, Elizabeth Vierling, and Bernd Bukau. 2003. “Small Heat Shock Proteins, ClpB and the DnaK System Form a Functional Triade in Reversing Protein Aggregation.” *Molecular Microbiology* 50 (2) (October): 585–595.

Nakamura, K, T Tanaka, A Kuwahara, and K Takeo. 1985. “Microassay for Proteins on Nitrocellulose Filter Using Protein Dye-staining Procedure.” *Analytical Biochemistry* 148 (2) (August 1): 311–319.

Nannenga, Brent L, and François Baneyx. 2011. “Enhanced Expression of Membrane Proteins in E. Coli with a P(BAD) Promoter Mutant: Synergies with Chaperone Pathway Engineering Strategies.” *Microbial Cell Factories* 10: 105. doi:10.1186/1475-2859-10-105.

Narayanan, Anoop, Marc Ridilla, and Dinesh A. Yernool. 2011. “Restrained Expression, a Method to Overproduce Toxic Membrane Proteins by Exploiting Operator–repressor Interactions.” *Protein Science* 20 (1): 51–61. doi:10.1002/pro.535.

Nicoll, Debora A, Michael R Sawaya, Seunghyug Kwon, Duilio Cascio, Kenneth D Philipson, and Jeff Abramson. 2006. “The Crystal Structure of the Primary Ca2+ Sensor of the Na+/Ca2+ Exchanger Reveals a Novel Ca2+ Binding Motif.” *The Journal of Biological Chemistry* 281 (31) (August 4): 21577–21581. doi:10.1074/jbc.C600117200.

Nury, H, C Dahout-Gonzalez, V Trézéguet, G Lauquin, G Brandolin, and E Pebay-Peyroula. 2005. “Structural Basis for Lipid-mediated Interactions Between Mitochondrial ADP/ATP Carrier Monomers.” *FEBS Letters* 579 (27) (November 7): 6031–6036. doi:10.1016/j.febslet.2005.09.061.

Oh, M K, and J C Liao. 2000. “DNA Microarray Detection of Metabolic Responses to Protein Overproduction in Escherichia Coli.” *Metabolic Engineering* 2 (3) (July): 201–209. doi:10.1006/mben.2000.0149.

Park, K, S Choi, M Ko, and C Park. 2001. “Novel sigmaF-dependent Genes of Escherichia Coli Found Using a Specified Promoter Consensus.” *FEMS Microbiology Letters* 202 (2) (August 21): 243–250.

Pebay-Peyroula, Eva, Cécile Dahout-Gonzalez, Richard Kahn, Véronique Trézéguet, Guy J-M Lauquin, and Gérard Brandolin. 2003. “Structure of Mitochondrial ADP/ATP Carrier in Complex with Carboxyatractyloside.” *Nature* 426 (6962) (November 6): 39–44. doi:10.1038/nature02056.

Perez-Iratxeta, Carolina, and Miguel Andrade-Navarro. 2008. “K2D2: Estimation of Protein Secondary Structure from Circular Dichroism Spectra.” *BMC Structural Biology* 8 (1): 25.

Petersen, Thomas Nordahl, Søren Brunak, Gunnar von Heijne, and Henrik Nielsen. 2011. “SignalP 4.0: Discriminating Signal Peptides from Transmembrane Regions.” *Nature Methods* 8 (10): 785–786. doi:10.1038/nmeth.1701.

Philipson, K D, and D A Nicoll. 2000. “Sodium-calcium Exchange: a Molecular Perspective.” *Annual Review of Physiology* 62: 111–133. doi:10.1146/annurev.physiol.62.1.111.

Pott, Christian, Joshua I. Goldhaber, and Kenneth D. Philipson. 2004. “Genetic Manipulation of Cardiac Na+/Ca2+ Exchange Expression.” *Biochemical and Biophysical Research Communications* 322 (4) (October 1): 1336–1340. doi:doi: 10.1016/j.bbrc.2004.08.038.

Racusen, D. 1973. “Stoichiometry of the Amido Black Reaction with Proteins.” *Analytical Biochemistry* 52 (1) (March): 96–101.

Reed, Jennifer L, Trina R Patel, Keri H Chen, Andrew R Joyce, Margaret K Applebee, Christopher D Herring, Olivia T Bui, Eric M Knight, Stephen S Fong, and Bernhard O Palsson. 2006. “Systems Approach to Refining Genome Annotation.” *Proceedings of the National Academy of Sciences of the United States of America* 103 (46) (November 14): 17480–17484. doi:10.1073/pnas.0603364103.

Ren, Xiaoyan, Debora A. Nicoll, Giselle Galang, and Kenneth D. Philipson. 2008. “Intermolecular Cross-Linking of Na+−Ca2+ Exchanger Proteins: Evidence for Dimer Formation.” *Biochemistry* 47 (22) (June 1): 6081–6087. doi:doi: 10.1021/bi800177t.

Ridilla, Marc, Anoop Narayanan, Jeffrey T Bolin, and Dinesh A Yernool. 2012. “Identification of the Dimer Interface of a Bacterial Ca(2+)/H(+) Antiporter.” *Biochemistry* 51 (48) (December 4): 9603–9611. doi:10.1021/bi3012109.

Rimon, Abraham, Tzvi Tzubery, and Etana Padan. 2007. “Monomers of the NhaA Na+/H+ Antiporter of Escherichia Coli Are Fully Functional yet Dimers Are Beneficial Under Extreme Stress Conditions at Alkaline pH in the Presence of Na+ or Li+.” *The Journal of Biological Chemistry* 282 (37) (September 14): 26810–26821. doi:10.1074/jbc.M704469200.

Robertson, Janice L, Ludmila Kolmakova-Partensky, and Christopher Miller. 2010. “Design, Function and Structure of a Monomeric ClC Transporter.” *Nature* 468 (7325) (December 9): 844–847. doi:10.1038/nature09556.

Rost, Burkhard, Guy Yachdav, and Jinfeng Liu. 2004. “The PredictProtein Server.” *Nucleic Acids Research* 32 (suppl 2) (July 1): W321 –W326. doi:10.1093/nar/gkh377.

Saier Jr., Milton H, Brian H Eng, Sharouz Fard, Joy Garg, David A Haggerty, William J Hutchinson, Donald L Jack, et al. 1999. “Phylogenetic Characterization of Novel Transport Protein Families Revealed by Genome Analyses.” *Biochimica et Biophysica Acta (BBA) - Reviews on Biomembranes* 1422 (1) (February 25): 1–56. doi:10.1016/S0304-4157(98)00023-9.

Saier, Milton H, Jr, Can V Tran, and Ravi D Barabote. 2006. “TCDB: The Transporter Classification Database for Membrane Transport Protein Analyses and Information.” *Nucleic Acids Research* 34 (Database issue) (January 1): D181–186. doi:10.1093/nar/gkj001.

Sali, A, and T L Blundell. 1993. “Comparative Protein Modelling by Satisfaction of Spatial Restraints.” *Journal of Molecular Biology* 234 (3) (December 5): 779–815. doi:10.1006/jmbi.1993.1626.

Santacruz-Toloza, Lucia, Michela Ottolia, Debora A. Nicoll, and Kenneth D. Philipson. 2000. “Functional Analysis of a Disulfide Bond in the Cardiac Na+-Ca2+ Exchanger.” *Journal of Biological Chemistry* 275 (1) (January 7): 182–188. doi:10.1074/jbc.275.1.182.

Scheu, Patrick D., Yun-Feng Liao, Julia Bauer, Holger Kneuper, Thomas Basche, Gottfried Unden, and Wolfgang Erker. 2010. “Oligomeric Sensor Kinase DcuS in the Membrane of Escherichia Coli and in Proteoliposomes: Chemical Cross-linking and FRET Spectroscopy.” *The Journal of Bacteriology* 192 (13) (July 1): 3474–3483. doi:10.1128/JB.00082-10.

Schneider, Caroline A, Wayne S Rasband, and Kevin W Eliceiri. 2012. “NIH Image to ImageJ: 25 Years of Image Analysis.” *Nature Methods* 9 (7) (July): 671–675.

Schwarz, E M, and S Benzer. 1997. “Calx, a Na-Ca Exchanger Gene of Drosophila Melanogaster.” *Proceedings of the National Academy of Sciences of the United States of America* 94 (19) (September 16): 10249–10254.

Schwarzer, Andreas, Tom S. Y. Kim, Volker Hagen, Robert S. Molday, and Paul J. Bauer. 1997. “The Na/Ca-K Exchanger of Rod Photoreceptor Exists as Dimer in the Plasma Membrane†.” *Biochemistry* 36 (44): 13667–13676. doi:10.1021/bi9710232.

Shiba, K, K Ito, and T Yura. 1984. “Mutation That Suppresses the Protein Export Defect of the secY Mutation and Causes Cold-sensitive Growth of Escherichia Coli.” *Journal of Bacteriology* 160 (2) (November): 696–701.

Shigaki, T, I Rees, L Nakhleh, and K D Hirschi. 2006. “Identification of Three Distinct Phylogenetic Groups of CAX Cation/proton Antiporters.” *Journal of Molecular Evolution* 63 (6) (December): 815–825. doi:10.1007/s00239-006-0048-4.

Shigekawa, Munekazu, and Takahiro Iwamoto. 2001. “Cardiac Na+-Ca2+ Exchange : Molecular and Pharmacological Aspects.” *Circulation Research* 88 (9) (May 11): 864 –876. doi:10.1161/hh0901.090298.

Shigekawa, Munekazu, Takahiro Iwamoto, Akira Uehara, and Satomi Kita. 2002. “Probing Ion Binding Sites in the Na+/Ca2+ Exchanger.” *Annals of the New York Academy of Sciences* 976 (November): 19–30.

Sohlenkamp, Christian, Isabel M López-Lara, and Otto Geiger. 2003. “Biosynthesis of Phosphatidylcholine in Bacteria.” *Progress in Lipid Research* 42 (2) (March): 115–162.

Teich, A, H Y Lin, L Andersson, S Meyer, and P Neubauer. 1998. “Amplification of ColE1 Related Plasmids in Recombinant Cultures of Escherichia Coli after IPTG Induction.” *Journal of Biotechnology* 64 (2-3) (October 8): 197–210.

Vagin, Alexei A, Roberto A Steiner, Andrey A Lebedev, Liz Potterton, Stuart McNicholas, Fei Long, and Garib N Murshudov. 2004. “REFMAC5 Dictionary: Organization of Prior Chemical Knowledge and Guidelines for Its Use.” *Acta Crystallographica. Section D, Biological Crystallography* 60 (Pt 12 Pt 1) (December): 2184–2195. doi:10.1107/S0907444904023510.

Veenhoff, Liesbeth M, Esther H.M.L Heuberger, and Bert Poolman. 2002. “Quaternary Structure and Function of Transport Proteins.” *Trends in Biochemical Sciences* 27 (5) (May 1): 242–249. doi:10.1016/S0968-0004(02)02077-7.

Vind, J, M A Sørensen, M D Rasmussen, and S Pedersen. 1993. “Synthesis of Proteins in Escherichia Coli Is Limited by the Concentration of Free Ribosomes. Expression from Reporter Genes Does Not Always Reflect Functional mRNA Levels.” *Journal of Molecular Biology* 231 (3) (June 5): 678–688. doi:10.1006/jmbi.1993.1319.

Von Heijne, G, and Y Gavel. 1988. “Topogenic Signals in Integral Membrane Proteins.” *European Journal of Biochemistry / FEBS* 174 (4) (July 1): 671–678.

Wagner, Samuel, Louise Baars, A Jimmy Ytterberg, Anja Klussmeier, Claudia S Wagner, Olof Nord, Per-Ake Nygren, Klaas J van Wijk, and Jan-Willem de Gier. 2007. “Consequences of Membrane Protein Overexpression in Escherichia Coli.” *Molecular & Cellular Proteomics: MCP* 6 (9) (September): 1527–1550. doi:10.1074/mcp.M600431-MCP200.

Wang, Zhong, Mark Gerstein, and Michael Snyder. 2009. “RNA-Seq: a Revolutionary Tool for Transcriptomics.” *Nature Reviews Genetics* 10 (1) (January): 57–63. doi:10.1038/nrg2484.

Weber, Jan, Frank Hoffmann, and Ursula Rinas. 2002. “Metabolic Adaptation of Escherichia Coli During Temperature-induced Recombinant Protein Production: 2. Redirection of Metabolic Fluxes.” *Biotechnology and Bioengineering* 80 (3) (November 5): 320–330. doi:10.1002/bit.10380.

Weber, Mary M, Christa L French, Mary B Barnes, Deborah A Siegele, and Robert J C McLean. 2010. “A Previously Uncharacterized Gene, yjfO (bsmA), Influences Escherichia Coli Biofilm Formation and Stress Response.” *Microbiology (Reading, England)* 156 (Pt 1) (January): 139–147. doi:10.1099/mic.0.031468-0.

Weltzien, H U, G Richter, and E Ferber. 1979. “Detergent Properties of Water-soluble Choline Phosphatides. Selective Solubilization of acyl-CoA:lysolecithin Acyltransferase from Thymocyte Plasma Membranes.” *The Journal of Biological Chemistry* 254 (9) (May 10): 3652–3657.

Wen, Jie, Tsutomu Arakawa, and John S. Philo. 1996. “Size-Exclusion Chromatography with On-Line Light-Scattering, Absorbance, and Refractive Index Detectors for Studying Proteins and Their Interactions.” *Analytical Biochemistry* 240 (2) (September 5): 155–166. doi:doi: 10.1006/abio.1996.0345.

Wilkins, M R, E Gasteiger, A Bairoch, J C Sanchez, K L Williams, R D Appel, and D F Hochstrasser. 1999. “Protein Identification and Analysis Tools in the ExPASy Server.” *Methods in Molecular Biology (Clifton, N.J.)* 112: 531–552.

Winn, Martyn D, Charles C Ballard, Kevin D Cowtan, Eleanor J Dodson, Paul Emsley, Phil R Evans, Ronan M Keegan, et al. 2011. “Overview of the CCP4 Suite and Current Developments.” *Acta Crystallographica. Section D, Biological Crystallography* 67 (Pt 4) (April): 235–242. doi:10.1107/S0907444910045749.

Woldringh, Conrad L. 2002. “The Role of Co-transcriptional Translation and Protein Translocation (transertion) in Bacterial Chromosome Segregation.” *Molecular Microbiology* 45 (1) (July): 17–29.

Yamada, M, A A Talukder, and T Nitta. 1999. “Characterization of the ssnA Gene, Which Is Involved in the Decline of Cell Viability at the Beginning of Stationary Phase in Escherichia Coli.” *Journal of Bacteriology* 181 (6) (March): 1838–1846.

Yano, R, H Nagai, K Shiba, and T Yura. 1990. “A Mutation That Enhances Synthesis of Sigma 32 and Suppresses Temperature-sensitive Growth of the rpoH15 Mutant of Escherichia Coli.” *Journal of Bacteriology* 172 (4) (April): 2124–2130.

Yernool, Dinesh, Olga Boudker, Ewa Folta-Stogniew, and Eric Gouaux. 2003. “Trimeric Subunit Stoichiometry of the Glutamate Transporters from Bacillus Caldotenax and Bacillus Stearothermophilus†.” *Biochemistry* 42 (44) (November 1): 12981–12988. doi:doi: 10.1021/bi030161q.

Zottola, R J, E K Cloherty, P E Coderre, A Hansen, D N Hebert, and A Carruthers. 1995. “Glucose Transporter Function Is Controlled by Transporter Oligomeric Structure. A Single, Intramolecular Disulfide Promotes GLUT1 Tetramerization.” *Biochemistry* 34 (30) (August 1): 9734–9747.

VITA

VITA

Marc Robert Ridilla was born in Latrobe, Pennsylvania where he was a student of the Greater Latrobe School District through high school. He earned a Bachelor of Science degree in Biochemistry and Cell Biology from Rice University in 2005, then worked as a technician at the University of Michigan for one year before entering the Ph.D. program at Purdue in 2006.

In 2013 Marc accepted a National Research Service Award as a Trainee in the UNC Lineberger Comprehensive Cancer Center Postdoctoral Training Program in North Carolina. He will study the dynamic nanoscale architecture of C-type lectin receptor microdomains during pathogen uptake by dendritic cells with Dr. Ken Jacobson.

PUBLICATIONS

PUBLICATIONS

Ridilla M, Narayanan A, Bolin JT, Yernool DA. Identification of the Dimer Interface of a Bacterial Ca(2+)/H(+) Antiporter. Biochemistry. 2012 Dec 4;51(48):9603-11.

Narayanan A, Ridilla M, Yernool DA. Restrained expression, a method to overproduce toxic membrane proteins by exploiting operator-repressor interactions. Protein Sci. 2011 Jan;20(1):51-61.

Lutz S, Shankaranarayanan A, Coco C, Ridilla M, Nance MR, Vettel C, Baltus D, Evelyn CR, Neubig RR, Wieland T, Tesmer JJ. Structure of Galphaq-p63RhoGEF-RhoA complex reveals a pathway for the activation of RhoA by GPCRs. Science. 2007 Dec 21;318(5858):1923-7.